Experimental Bifurcation Analysis Using Control-Based Continuation

Bureau, Emil; Santos, Ilmar; Thomsen, Jon Juel; Starke, Jens

Publication date:
2014

Document Version
Publisher's PDF, also known as Version of record

Experimental Bifurcation Analysis Using Control-Based Continuation

PhD Thesis

$$(EIv'')''=q-\rho A\ddot{v}$$

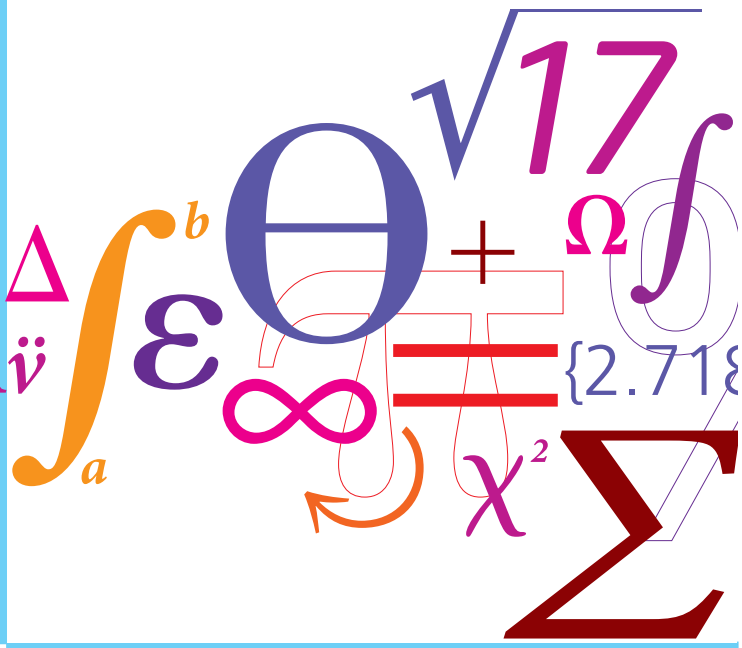

Emil Bureau
DCAMM Special Report No. S163
January 2014

DTU Mechanical Engineering
Department of Mechanical Engineering

Experimental Bifurcation Analysis Using Control-Based Continuation

by

Emil Bureau

Preface

This thesis is submitted as partial fulfilment of the requirements for awarding the Danish ph.d. degree. The work has been carried out from January 2010 to January 2014 at the Department of Mechanical Engineering and the Department of Mathematics at the Technical University of Denmark. The project has been under main supervision of professor Dr.-Ing. dr. techn. Livre-Docente Ilmar Ferreira Santos and co-supervision of associate professor dr.techn. Jon Juel Thomsen and associate professor Dr.rer.nat. Jens Starke. The research has been carried out in close collaboration with postdoc Frank Schilder. I wish to show my biggest gratitude to these people. I have worked with Ilmar for almost 10 years, and every single project, meeting and conversation has been a pleasure both professionally and personally. I would like to thank Jon for some very inspiring meetings, both on and off topic, for his rigorous feedback on my work and for teaching me good scientific practice and attention to details. Thanks to Jens for keeping the whole research project together and introducing me to the mathematical community. I would also like to thank Frank for good collaboration, making the countless hours in the laboratory enjoyable and helping me take my research to another level. Finally, I would like to thank Michael Elmegård for many constructive discussions during the project.

During my Ph.d. studies I had the pleasure of visting professor Marcelo Savi and his research team in the Federal University of Rio de Janeiro, Brazil. I wish to gratefully thank Marcelo and all of his team for an inspiring and pleasant stay.

On behalf of our research group I wish to thank Jan Sieber, David Barton, Harry Dankowicz and Bernd Krauskopf for helpful comments and discussions when setting up the experiments.

Finally, I would like to thank all my co-workers and friends at the department, which are too many to mention by name, for contributing to a nice atmosphere and for fruitful discussions. I also wish to thank my friends and family for their support and love.

This work was supported by the Danish Research Council FTP under the project number 09-065890/FTP.

Kgs. Lyngby, January 31. 2014

Emil Bureau

Abstract

The focus of this thesis is developing and implementing techniques for performing experimental bifurcation analysis on nonlinear mechanical systems. The research centers around the newly developed control-based continuation method, which allows to systematically track branches of stable and unstable equilibria under variation of parameters. As a test case we demonstrate that it is possible to track the complete frequency response, including the unstable branches, for a harmonically forced impact oscillator with hardening spring nonlinearity, controlled by electromagnetic actuators. The method requires the constitution of a non-invasive and locally stabilizing control scheme, which must be tuned without a-priori study of a model. We propose a sequence of experiments that allows to choose optimal control-gains, filter parameters and settings for a continuation method. This experimental tuning procedure is applied to our test rig, resulting in a reliable non-invasive, locally stabilizing control. The use of stabilizing control makes it difficult to determine the stability of the underlying uncontrolled equilibrium. Based on the idea of momentarily modifying or disabling the control and study the resulting behavior, we propose and test three different methods for assessing stability of equilibrium states during experimental continuation. We show that it is possible to determine the stability without allowing unbounded divergence, and that it is under certain circumstances possible to quantify instability in terms of finite-time Lyapunov exponents. A software toolbox for the Matlab continuation platform COCO has been developed and will be made freely available. This toolbox implements functions necessary for interfacing a numerical continuation code with a real experiment, as well as provide means for simulating control-based continuation experiments. Finally, the feasibility of implementing the method for rotating machinery is discussed.

Resumé

Fokus i denne afhandling er på udvikling og implementering af teknikker til at udføre eksperimentel bifurkations analyse på ikke-lineære mekaniske systemer. Forskningen tager udgangspunkt i den ny-udviklede 'control-based continuation' metode, som gør det muligt at systematisk følge grene af stabile og ustabile dynamiske ligevægts tilstande under variation af parametre. For at teste metoden viser vi at det er muligt at måle det komplette frekevensrespons, inklusiv den ustabile del, for en ikke-linær mekanisk oscillator som er påvirket af en ekstern harmonisk kraft, og reguleret med elektromagnetiske aktuatorer. Metoden kræver en ikke-invasiv og lokalt stabiliserende regulering, som er nødt til at blive justeret uden brug af en model af systemet. Vi introducerer en serie af eksperimenter, som gør det muligt at vælge optimale parametre for regulatoren og continuation-algoritmen. Dette testes på vores forsøgsopstilling, resulterende i en pålidelig ikke-invasiv og lokalt stabiliserende regulering. Anvendelsen af reguleringen gør det svært at afgøre stabiliteten af underliggende dynamiske ligevægtstilstand. Baseret på en grundlæggende ide om momentant at slukke eller modificere regulatoren og observere systemets respons, introducerer vi tre forskellige metoder til at afgøre stabiliteten af dynamiske ligevægtsstililnger, som kan benyttes under continuation. Vi viser at det er muligt at bestemme stabiliteten uden at tillade systemet at divergerer ubegrænset, samt at det under visse omstændigheder er muligt at kvantificere ustabiliteten i form af finite-time Lyapunov eksponenter. En software værktøjskasse til Matlab continuation platformen COCO er blevet udviklet, og vil blive gjort frit tilgængelig. Denne værktøjskasse implementerer de funktioner som er nødvendige for at kunne benytte en numerisk contination algoritme i et fysisk eksperiment, samt giver mulighed for at simulere control-based continuation eksperimenter. Afslutningsvis bliver muligheden for at anvende metoden til roterende maskineri diskuteret.

List of Publications

The following publications are part of this thesis:

[P1] E. Bureau, F. Schilder, I. F. Santos, J. J. Thomsen, and J. Starke. Experimental bifurcation analysis for a driven nonlinear flexible pendulum using control-based continuation. In *7th European Nonlinear Dynamics Conference*, 2011. (Can be found on page 67)

[P2] E. Bureau, I. F. Santos, J. J. Thomsen, F. Schilder, and J. Starke. Experimental bifurcation analysis of an impact oscillator - tuning a non-invasive control scheme. *Journal of Sound and Vibration*, 332(22):5883–5897, 2013. (Can be found on page 75)

[P3] E. Bureau, I. F. Santos, J. J. Thomsen, F. Schilder, and J. Starke. Experimental Bifurcation Analysis By Control-based Continuation - Determining Stability. In *Proceedings of the ASME 2012 International Design Engineering Technical Conferences & Computers and Information in Engineering Conference*, 2012. (Can be found on page 91)

[P4] E. Bureau, F. Schilder, M. Elmegård, I. F. Santos, J. J. Thomsen, and J. Starke. Experimental bifurcation analysis of an impact oscillator - determining stability. *Accepted for publication in: Journal of Sound and Vibration*, January 2014. (Can be found on page 101)

[P5] E. Bureau, F. Schilder, I. F. Santos, J. J. Thomsen, and J. Starke. Experiments in nonlinear dynamics using control-based continuation: Tracking stable and unstable response curves. In *8th European Nonlinear Dynamics Conference*, 2014. (Can be found on page 117)

[**P6**] F. Schilder, E. Bureau, J. Starke, H. Dankowicz, and J. Sieber. A Matlab Continuation Toolbox for Response Tracking in Experiments. In *7th European Nonlinear Dynamics Conference*, 2011. (Can be found on page 121)

[**P7**] F. Schilder, E. Bureau, I. F. Santos, J. J. Thomsen, and J. Starke. Continex: A toolbox for continuation in experiments. In *8th European Nonlinear Dynamics Conference*, 2014. (Can be found on page 125)

Contents

1 Introduction

Experimental investigations of nonlinear mechanical vibrations are interesting and relevant both from an academic and practical engineering perspective. Real systems are inherently nonlinear, but nevertheless we often attempt to describe them using linear models. This is because the linear theory is well established and relatively straightforward. Similarly, many of the well established experimental methods use estimation and identification techniques that are based on the assumption that the system under test is linear or close to linear. Applying such techniques to strongly nonlinear systems can lead to wrong measurements and hence wrong model-assumptions, poor designs and failure of mechanical components.

Nonlinear dynamical systems are difficult to deal with experimentally due to the fact that they might have multiple coexisting stable and unstable equilibrium states, super/sub harmonic resonances, quasi-periodic and chaotic behaviour. Furthermore, nonlinear systems can undergo bifurcations, where a small change of a system parameter cause a sudden qualitative change of the response. Figure 1.1a shows examples of a theoretical frequency response for a linear and a nonlinear harmonically forced oscillator. The linear response is characterised by only having one possible equilibrium state for each forcing frequency, while the nonlinear response has a region in which multiple stable and unstable equilibrium states coexist. Bifurcations occur at two points along the curve, namely where the stability changes. At these points a small change of the forcing frequency will qualitatively change the response of the system, as the system will not settle on an unstable equilibrium in absence of control.

Despite not being directly observable in experiments, unstable equilibrium states hold important information about the dynamics of a system. As illustrated in

Figure 1.1b, the unstable equilibria act as seperatrices between the stable attractors, dividing the phase plane into bassins of attraction. With information about the unstable states, one can predict which steady state the system progresses towards given a set of initial conditions. Furthermore, branches of stable equilibria might be connected through the unstable equilibria branches, which means that following an unstable branch can help in uncovering a more complete bifurcation diagram. Lastly, if stabilized by control, the unstable equilibria might hold useful dynamical proporties.

This underlines the usefulness and need for a method that can perform systematic experimental bifurcation analysis, by tracking both stable and unstable time periodic equilibrium states of nonlinear mechanical systems under variation of parameters. The aim and contribution of this thesis is to show how this can be achieved using the control-based continuation method. As a test case for the method and its implementation, non-trivial responses of a harmonically forced impact oscillator are investigated. Special focus is put on developing and implementing methods for determining stability during continuation and tuning a non-invasive control necessary for applying the method.

1.1 Experiments in nonlinear dynamics

Figure 1.1a and b underlines the complication of dealing with strongly nonlinear dynamical systems: There might be multiple possible equilibrium states coexisting for a certain set of parameters and a perturbation can cause the system to diverge from one equilibrium state and settle onto another. Therefore, classical experimental techniques, such as experimental modal analysis, where the system is excited by an impulse or broadband noise signal while the response is recorded, does not ensure that the correct state is measured. The conventional experimental method used with strongly nonlinear systems is a parameter sweep, where a parameter, e.g. the forcing frequency, is ramped smoothly up and down while the response is recorded. If the perturbations are sufficiently small compared to the separation of coexisting equilibrium states, it is possible to trace a path or branch of equilibrium states as it is done in Figure 1.1c (marked by + and ∘). By varying the parameter smoothly, the system stays on the equilibrium path on which it is initiated until that path seize to exist, at which point the system jumps and settles onto another nearby stable equilibrium state. This means that multiple coexisting equilibrium paths can be measured by careful initialisation and sweeping in different directions, as it is done in Figure 1.1c. Unfortunately, the method is not very robust with respect to perturbations and does not provide any information about the unstable equilibrium states.

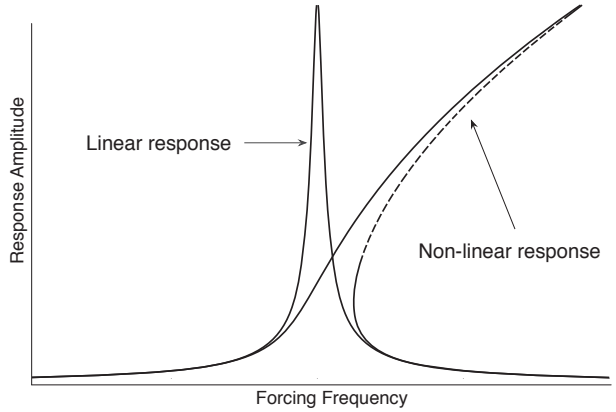

(a) Examples of a linear and a nonlinear frequency response. Stable branches are denoted by (—) and unstable by (- - -). Taken from [P2].

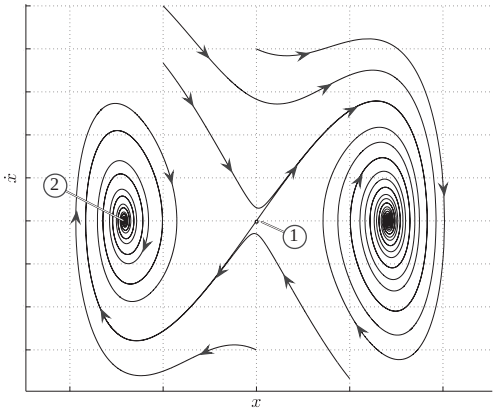

(b) Example of flow in a phase plane for a nonlinear dynamical system. (1) An unstable equilibrium point. (2) A stable equilibrium point.

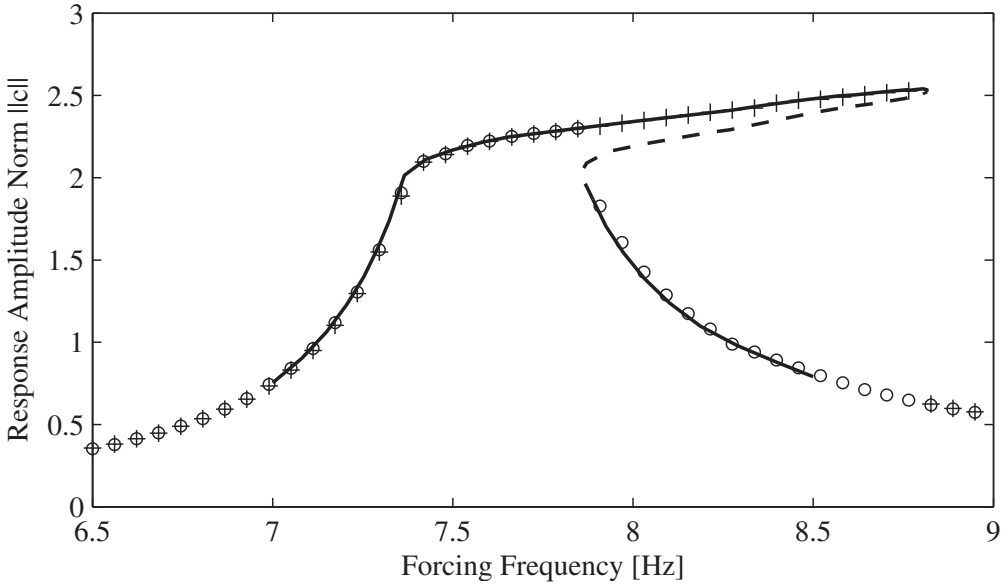

(c) Experimental frequency response of a harmonically forced nonlinear impact oscillator obtained by parameter sweep and control-based continuation. Response from traditional frequency sweeps is denoted by (+) for increasing and (∘) for decreasing frequency. Response obtained by control-based continuation is denoted by (—) for stable part and (− − −) for unstable part. Taken from [P4].

Figure 1.1: Examples of difficulties encountered in experiments with nonlinear dynamical systems.

Experimental techniques for stabilizing unstable periodic orbits (UPOs) in chaotic systems, such as Delayed Feedback Control [8] and OGY-control [9], are emerging (see [10] for an overview). They enable unstable periodic orbits to be stabilized, but does generally not work at saddle-node bifurcations, which makes them unfit for bifurcation analysis [11]. For nonlinear mechanical systems with periodic or quasi-periodic behaviour, the parameter-sweep remains the most widely used experimental method. The control-based continuation method requires the constitution of a non-invasive real-time control and the use of a predictor-corrector type path following algorithm. In turn the method can provide information about how both stable and unstable equilibrium states change when system parameters are varied. Furthermore, the stability can be determined, and in some cases the instability can be quantified in terms of finite-time Lyapunov exponents [P4]. The metod works for linear, weakly nonlinear and strongly nonlinear systems and can handle multiple coexisting equilibrium states, quasi-periodic behavior and the occurrence of bifurcations. An example of applying the method to an experiment is presented in Figure 1.1c. Note that in addition to the information obtained by the parameter sweep, using control-based continuation it is possible to track around the two fold-points and obtain also the unstable part of the response diagram along with the information about its stability.

1.2 Literature review

The subject of control-based continuation is young and only few key articles exist, with even fewer examples of the method tested on real experiments. The method is essentially based on numerical continuation and extended time-delayed feedback. Numerical continuation employs a path-following algorithm to investigate sets of equations describing dynamical systems and makes it possible to trace stable and unstable solution branches as well as detect and continue bifurcations in multiple parameters. For a thorough description of numerical continuation we refer the reader to [12, 13]. Extended time-delayed feedback is a control technique that enables stabilization of unstable periodic orbits without the use of a model. The technique was introduced in [8] and [10] gives an overview of the development of this method.

Sieber and Krauskopf 2008 [11] were the first authors to present the control-based continuation method. They test the method using a simulation of a dry-friction oscillator experiment, and demonstrate that the method makes it possible to perform continuation of periodic orbits with only the output of a simulation or experiment available.

Sieber and Krauskopf 2007 [14] explain how the control-based continuation method can be used as a framework for hybrid testing. Hybrid testing (also referred to as real-time dynamic sub structured testing) is an experimental technique that couples physical experiments and computer simulations in real-time. A complex structure is split into components for which a reliable model is available and the mechanical part that needs to be tested, e.g. a finite element model of an aircraft and a physical landing gear. Loads and displacements are transferred between the simulation and the experiment using actuators and sensors, making it possible to test the mechanical part as if it was part of the full (simulated) structure. A fundamental problem of this technique is delays in the coupling between simulation and experiment. In [14] the authors show how this problem can be overcome by using control-based continuation and a uni-directional coupling between the simulation and experiment. In conclusion they simulate an experimental nonlinear pendulum connected to a mass-spring-damper model, and show that it is possible to perform bifurcation analysis of the combined system using the method.

Sieber et al. 2008 [15] report on the first application of control-based continuation in an experiment. Periodic orbits consisting of stable and unstable rotations of a vertically forced pendulum were tracked, and it was shown how it is possible to track through a fold bifurcation, at which the stability changes. The non-invasive control is obtained by overlaying the control force onto the harmonic forcing, and the control signal is constituted by using a modification of the time-delayed feedback scheme [8]. In Krauskopf et al. 2011 [16] the authors present more technical details and the complete set of results of the experiments from [15]. Furthermore, the paper presents a model-based analysis of the convergence of the control-based continuation over a large parameter range.

Barton and Burrow 2011 [17] successfully apply the method to track experimental bifurcation diagrams for a nonlinear energy harvester. Barton et al. 2012 [18] follow in the lines of [17] by tracking bifurcation diagrams for two different nonlinear energy harvesters and comparing with theoretical results. Both [17] and [18] report that their choice of globally stabilizing control gains failed to stabilise the system at an upper fold point of the bifurcation diagram.

Barton and Sieber 2013 [19] present a simplification of the control-based continuation scheme which is possible whenever feedback control is obtained by varying the bifurcation parameter, e.g. when super-imposing the control-signal onto the harmonic forcing signal. The simplification reduces the correction step to a simple fixed-point iteration and gives rise to a substantial speed-up of the experiment-time, but only works for a limited type of dynamical systems.

1.3 Contribution of this work

Building on the findings of the above papers, the original contributions of this work can be outlined as following: In [P2] we present a formalisation and alternative description of the control-based continuation method minded specifically at the mechanical engineering community. We present the first implementation of the robust non-invasive control using projection onto multiple Fourier modes in an experiment, as it was originally suggested in [11]. In the previous works, the control was established by using a modification of the extended time-delayed feedback combined with the first Fourier mode of the reference-signal. In our work however, the higher order Fourier modes are important, because the system we investigate has impacts which excites higher-order modes. Furthermore, we implement and test the experimental evaluation of the Jacobian using both finite differences and Broyden updates.

We split the harmonic forcing and the control using electromagnetic actuators instead of superimposing the control signal on the harmonic forcing. This is important for many types of machinery, where control cannot be obtained through the system parameters, e.g. nonlinear rotors. In [P1, P2] we present and implement a systematic method for tuning a non-invasive control constituted by nonlinear actuators. We find that for our test rig it is possible, by careful investigation and choice, to find sets of control gains that can stabilise all equilibrium states along the full bifurcation diagram, overcoming the types of problems reported in [17, 18].

In [P3, P4] we present and implement methods for detecting stability and in some cases estimating finite-time Lyapunov exponents without allowing unbounded divergence from equilibrium states. Determining changes in stability is a mean to detect bifurcation points and necessary if one wishes to trace out stability boundaries.

Finally, a software toolbox for enabling control-based continuation in experiments using an existing continuation algorithm has been developed. This also includes functionality to run simulated experiments both synchronously and asynchronously.

1.4 Structure of this thesis

At The Technical University of Denmark there are two accepted ways to write a PhD thesis. One is a self contained thesis in which the author presents all the work done throughout the PhD-study. The other option is to publish scientific papers about the research during the PhD-study, and then summarise the contributions of these

papers in the thesis. This is an article based thesis, which means that its main part is the appended journal and conference articles. The remaining thesis summarises and extends on the findings of these articles, but also reports on additional research that did not make it into the papers. The reader is encouraged to read the appended papers before reading this thesis.

Articles [P1, P2] focus on tuning a non-invasive control and their main contributions are summarised in Chapter 4. Articles [P3, P4] focus on methods for determining and quantifying stability during control-based continuation and are summarised in Chapter 5. Publication [P5] is an extended abstract submitted for the European Nonlinear Dynamics (ENOC) conference 2014. It gives an overview of the current state of our research and is meant to promote the method and the developed Continex-toolbox. Finally, publications [P6, P7] are co-authored extended abstracts already presented or to be presented at ENOC. They treat the details of implementing the control-based continuation method.

Chapter 3 gives a detailed supplementary description of the experimental test rig, equipment and implementation and is written for anyone who wants to continue work on the test rig, or is interested in setting up a similar experiment. Chapter 6 focus on simulating experiments using the developed Continex-toolbox and use this to investigating and discuss the feasibility of applying the control-based continuation method in the field of rotor dynamics. Chapter 7 concludes on the presented work and discusses future aspects of the method and problems to be tackled.

2 Method background

Control-based continuation can be thought of as a guided experiment where one investigates how a dynamical system responds to changes in parameters, such as the frequency or amplitude of an external forcing. Starting at a stable equilibrium state of an uncontrolled experiment, a path-following algorithm makes a prediction of a new equilibrium state for a new set of system parameters. This predicted state might not be natural for the dynamical system nor stable, but can be realised by an active control. A correction algorithm then seeks to modify this prediction such that it again matches with an actual equilibrium state of the uncontrolled experiment. It is important that the active control is non-invasive, by which we mean a control that vanishes whenever the state of the system is an equilibrium of the underlying uncontrolled system. Iterating a series of such prediction and correction steps while constantly applying a stabilizing control allows to trace a so-called path of equilibrium states irrespective of their stability.

Let us illustrate the basic principle with a simplified example: Figure 2.1 shows a ball in a topological landscape of peaks and valleys, representing respectively stable and unstable equilibria for the ball. We wish to roll the ball along the center ridge using a simple control based continuation-algorithm: Move the ball a small distance in the direction tangential to the center ridge (prediction) followed an orthogonal correction step onto the nearest equilibrium position. Since several stable and unstable steady states coexist, the prediction step-length must be small enough not to move the ball onto one of the other equilibria. In case this happens, the continuation algorithm might follow the equilibrium path on which the new equilibrium resides. The control is necessary for realising the state requested by the prediction and the stable state created by the control might be thought of as artificial as the system would never settle there in the absence of control. Furthermore, a

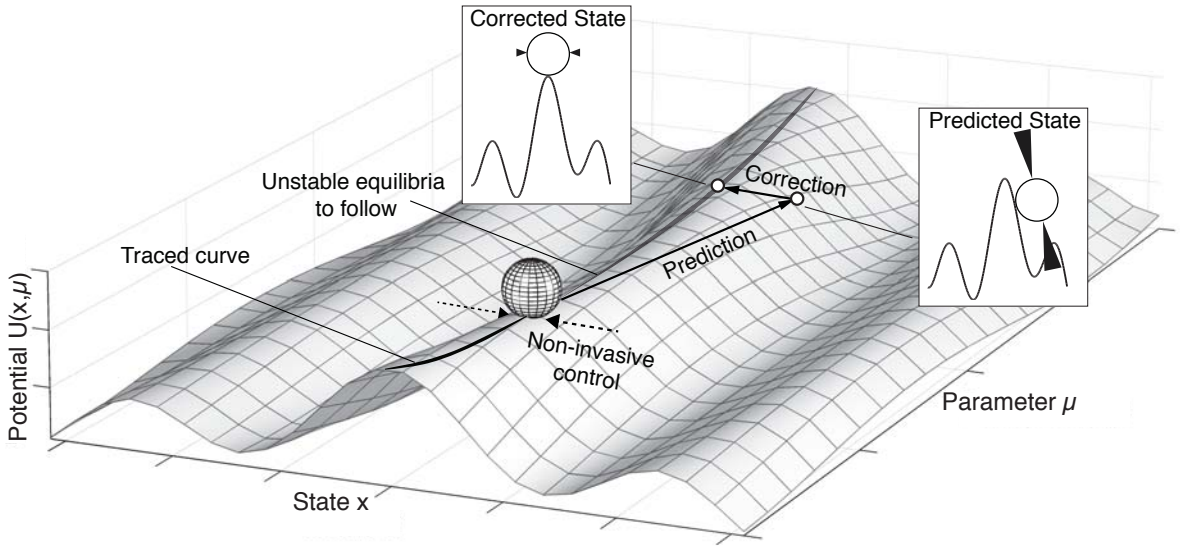

Figure 2.1: Simplified illustrative example: Non-invasive control and control-based continuation for a ball in a landscape of peaks and valleys. The branch of unstable equilibria created by the center ridge is followed as μ is varied. When the correction step converges to an equilibrium state for the uncontrolled system, the control force vanishes.

non-invasive control-scheme will make the control effort vanish once the ball is exactly on an equilibrium state for the uncontrolled system. This means that the control is only enabled when the ball starts to roll off the ridge. This keeps the ball on the ridge without altering the equilibrium states.

To employ the method in an actual experiment presents a number of challenges: Many dynamical systems of interest will have time periodic equilibrium states, i.e. the steady state vibration approached when transients due to initial conditions has decayed, rather than static equilibrium states as in the ball-example. Therefore we sample several periods of experimental data and compute the Fourier-transform of the equilibrium-state. Similarly, the predicted state is formulated in terms of its Fourier coefficients and a reference trajectory is generated by inverse Fourier-transformation. A zero-problem is formulated as:

$$F(c, \mu; N) := \mathcal{F}_Q \left(Z_{u_c}(\mu, N, \mathcal{F}_\infty^{-1}(c)) \right) - c = 0, \tag{2.1}$$

where Z_{u_c} is the measurement of the controlled experiment (after transients have settled), N is a number of sampled points, μ is parameters, Q is the number of modes used in the Fourier transformation $\mathcal{F}$ and c is the predicted state expressed in terms of its Fourier modes. The continuation algorithm makes a predicted step in parameters μ based on an experimentally estimated Jacobian, and a corrector algorithm (typically a Newton-method) seeks to corrects the predicted state c until

the prediction and measurement match, taking into account that the transient behavior must be given time to settle before each new measurement.

Creating and tuning a non-invasive control also presents challenges: To avoid that the controller affects the measured dynamics, the control-actuators must not add any inertia, stiffness, damping or extra degrees of freedom to the system when the control signal tends to zero. This makes many types of control-actuators unfit for non-invasive control. As the control-based continuation method is mostly relevant for nonlinear systems for which we do not want to make any prior model-assumptions, tuning the control must be a completely experimental procedure. In many cases, such as with electromagnetic actuators, the control-force also has a nonlinear dependency on system parameters, further complicating the tuning procedure. A non-invasive control can be constituted as a PD control, G, with appropriately chosen gains K_p and K_d. The control signal $u_c(t)$ is thus expressed as

$$u_c(t) = G(x(t), z(t)) := K_p(x(t) - z(t)) + K_d(\dot{x}(t) - \dot{z}(t)), \tag{2.2}$$

where $z(t)$ is the measurement of the state of the controlled system at time t, $(\dot{})$ denotes differentiation w.r.t. time and $x(t) = \mathcal{F}_\infty^{-1}(c)$ is the reference trajectory produced by the continuation. When $x(t) - z(t) \approx 0$ and $\dot{x}(t) - \dot{z}(t) \approx 0$ the control tends to zero, meaning that one does in fact measure the local dynamics of the underlying uncontrolled system when the correction converges.

A number of precautions must be taken when applying a numerical continuation algorithm to an experiment. Measured states are subject to noise contamination, which makes statistical weighting and interpolation of the equilibrium-path necessary. The correction algorithm however ensures the measured equilibrium states to be correct to the tolerance of the convergence criteria, which can typically be chosen to be of the same order as the measurement noise. Furthermore, the experimental evaluation of a Jacobian is slow because the transient settling time for each parameter-perturbation might be long. This problem is addressed by using mainly Broyden-updates [20] and only few complete measurements of a Jacobian.

Publication [P2] contains a detailed description of the control-based continuation method and how to implement it in our experimental test rig using the computational continuation core COCO [21, 22, 23]. The developed COCO software toolbox Continex (Continuation in experiments) will be made freely available online (as a part of COCO [21]) together with examples of a simulated experiment in the near future, in the hope that the method will become widely used in the field of experimental nonlinear dynamics.

3 Experimental Setup

The experimental test rig used to implement and test experimental bifurcation analysis using the control-based continuation method is depicted in Figures 3.1 and 3.2. It comprises a harmonically forced impact oscillator with a hardening nonlinearity controlled by electromagnetic actuators. This type of control actuators is chosen because they do not add any damping, stiffness or inertia to the system when the control is inactive, making them able to fulfil the requirement of non-invasiveness. Additionally, they function as a prototype for electromagnetic bearings and similar, making the method readily available for rotor systems. The impactor system is relative simple, but it has a strongly nonlinear dynamic behavior. It serves as a good test case for the method as it represents a class of systems that are difficult to deal with experimentally as well as theoretically, i.e. impacting systems. Furthermore, it mimics dynamic behavior that occurs in many real applications.

A thorough description of the test rig and implementation of control-based continuation is presented in publication P2. The following sections provide supplementary details that could be of interest to anyone who continues work on the test rig, or attempt setting up a similar experiment. Table 3.1 presents a complete list of the experimental equipment used.

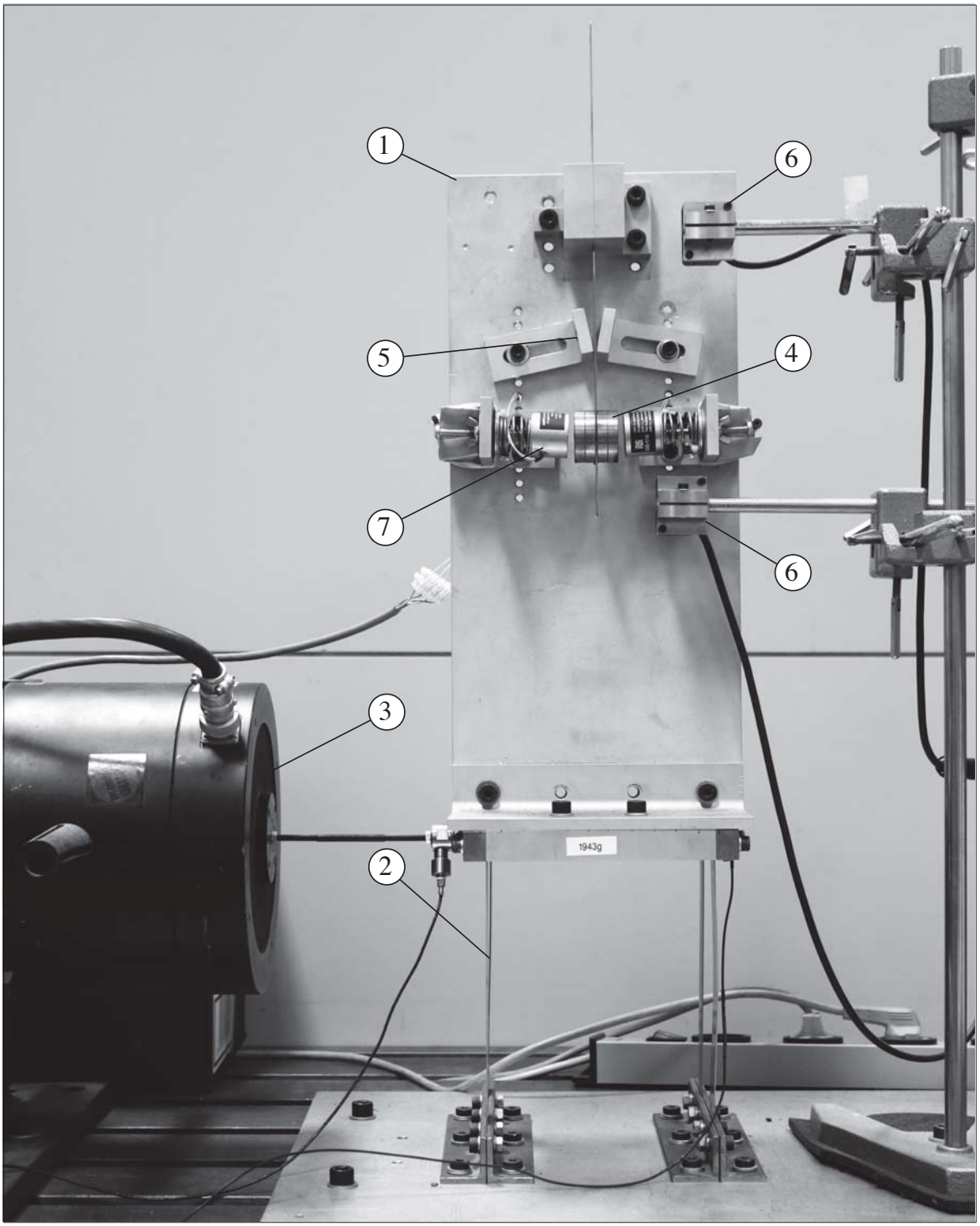

Figure 3.1: The experimental test rig: A platform (1) with flexible legs (2) allowing only in-plane translation. An electromagnetic shaker (3) that can exert a harmonic force on the platform. A flexible impactor with a tip mass (4) moves along with the platform. Vibration amplitudes of the impactor exceeding the gap-size between the mechanical stops (5) causes an impact and a stiffening of the spring (hardening nonlinearity). Displacement of the platform and impactor are measured by laser displacement sensors (6). A control force can be exerted directly on the impactor mass by electromagnetic actuators (7).

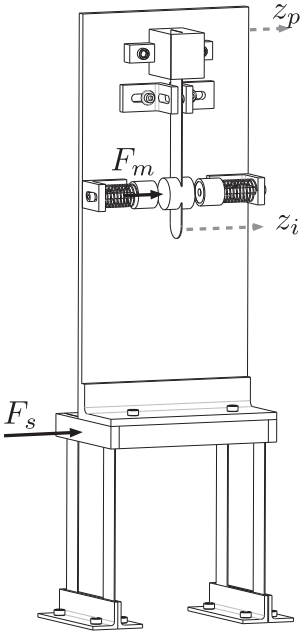

Figure 3.2: Sketch of the harmonically forced impact oscillator. The harmonic force from the electromagnetic shaker is ideally $F_s = A\cos\Omega t$, but as we will show the dynamics of the shaker and the impactor are coupled to create a two degree of freedom system. The control force from the electromagnetic actuators $F_m = f(u(t)$ is a nonlinear function of the control-signal $u(t)$ generated in the real-time application. The relative displacement of the impactor is calculated as the difference between the the displacement of the impactor and platform $z = z_i - z_p$.

Item	Model	Description
Electromagnetic shaker	B&K 4809	Open loop shaker used to produce a harmonic excitation of the base structure.
Shaker power amplifier	B&K 2712	Power supply and amplifier for the shaker.
2 × Position sensors	Omron ZX-LD40	Laser positions sensors with a range of ±10 mm.
Analog lowpass filter	Wavetek/Rockland 752A	Two channel analog tuneable lowpass filter used for filtering position sensor signals before AD-conversion.
Magnet power supply	Danica TPS21	2 channel 30V DC power supply unit for the electromagnetic actuators.
2 × Control signal amplifier		Two simple transistor circuit to regulate the voltage sent to the electro magnets (see section 3.1.3).
2 × Electro magnets	Magnet-Schultz GMH030	Two DC holding magnets.
Controller board	dSpace DS1104	Board used for data-acquisition, generation for the forcing signal and the real-time control.
Computer	Dell Optiplex 960	A standard PC running Matlab, Simulink and dSpace Control Desk.

Table 3.1: List of experimental equipment.

3.1 Hardware

3.1.1 Impactor and platform

The impactor, mechanical stops and control actuators are mounted on the platform, which is connected to the electromagnetic shaker through a stinger. The platform has four flexible legs that are designed to only allows in-plane translation by having a much larger stiffness in torsion and out-of-plane bending. Vertical displacement and rotation of the platform are also negligible due to the small displacements created by the shaker.

The impactor is depicted in Figure 3.3 and consists of a clamped beam with a concatenated mass, which moves together with the platform. When the amplitude of the impactor exceeds the gap-size between the mechanical stops (cf. Figure 3.3a) it starts to impact and bend around the stop, effectively changing its boundary conditions and characteristic length. As a result the spring stiffness suddenly increases, creating a hardening nonlinearity. The stops are angled to ensure that only one part of the beam impacts. The gap-size and angle can be adjusted, but it is difficult to get it to be exactly symmetrical. This asymmetry can create additional nonlinear phenomena by changing the type of bifurcations observed.

3.1.2 Electromagnetic shaker

The electromagnetic shaker used for creating the harmonic excitation is not feedback controlled. This adds to the complexity of the system, since its dynamics are coupled with the impactor and platform effectively adding an extra degree of freedom. The shaker produces a harmonic force, but not with constant amplitude. Figure 3.4 presents frequency responses for the impactor and base structure obtained by sweeping the forcing frequency up and down while recording the responses. Note that at the primary resonance of the impactor, the platform and impactor are in anti-resonance, causing the amplitude of the platform to become small. To keep the forcing amplitude constant over the whole sweep would require control of the shaker. The design of such a control using adaptive filtering together with a simple model for a similar shaker is proposed in [24], but it requires knowledge about physical parameters that the company producing the shaker would not provide. Fortunately, the added complexity is not problematic for the experimental investigations. In fact it creates a scaling of the impactor amplitudes which shows to be advantageous for the measurement equipment: The large amplitudes at the impactor resonance are attenuated making better use of the measurement range of the laser displacement sensors. It turns out to only be a problem when comparing with model-investigations

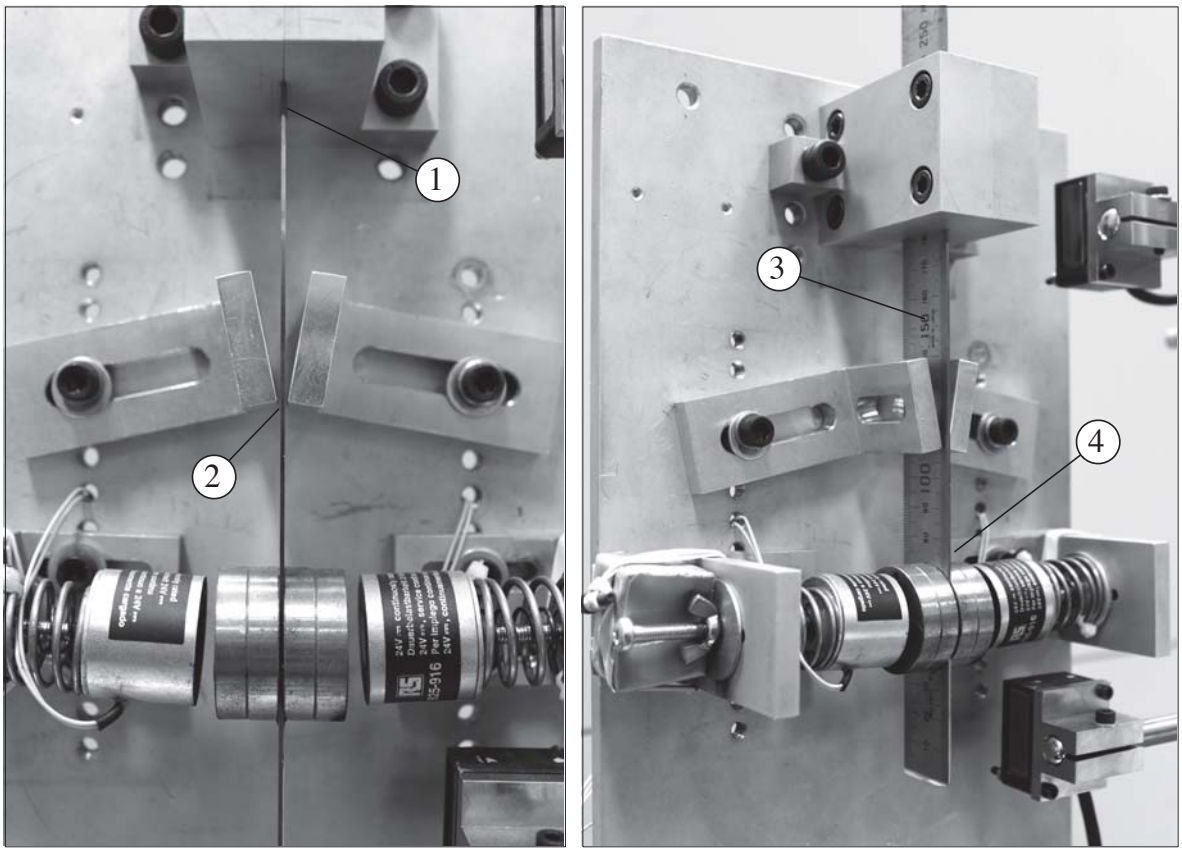

(a) Impactor front close-up

(b) Impactor side view

Figure 3.3: The harmonically forced impact oscillator viewed from (a) the front and (b) the side. (1) Impactor beam has one end clamped and one end free. (2) Gap between mechanical stops. (3) Impactor-beam is flexible in the forcing direction, but much stiffer out of plane and in vertical direction. (4) Impactor steel mass with much higher weight than the impactor beam.

or if one wish to add the control-signal to the harmonic shaker signal, as it was done in [15, 16, 17, 18, 19].

3.1.3 Electromagnetic actuators

The electromagnetic actuators are shown in Figure 3.5. They are placed in a pair on each side of the impactor mass. This is necessary because each magnet can only exert a pulling force on the impactor steel mass. The control-signal is split in the real-time application so that positive values of the signal is sent to one actuator and negative values are sent to another, making it possible to change the direction of the force that is exerted on the impactor mass. For each magnet a simple circuit is used to amplify the control signal from the dSpace boards maximal possible output

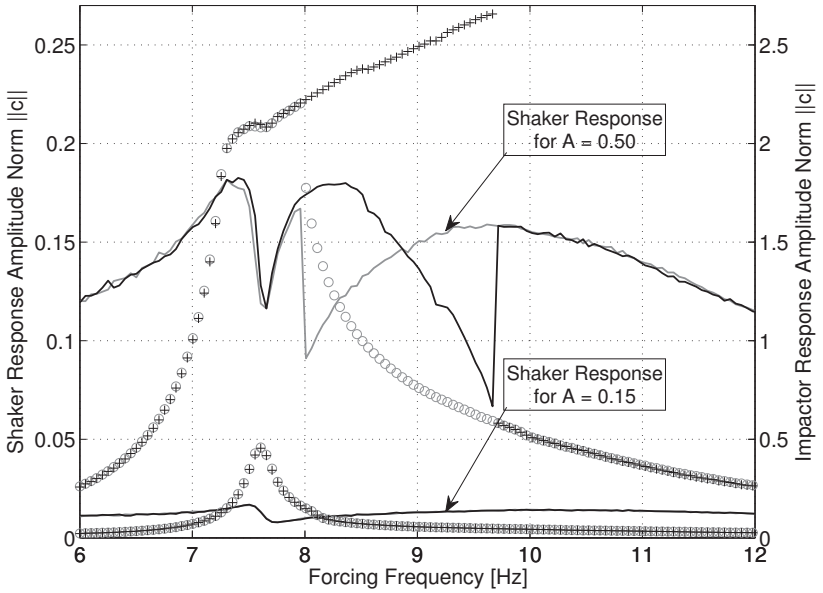

Figure 3.4: Displacement of the base produced by the shaker for two different fixed amplitudes of the shaker signal. The lower set of curves (A=0.15) has been scaled down by a factor of 75% to make the figure less cluttered. The upwards sweep is denoted by the black curves (——) and the downwards by gray (——). For the overlaid frequency response curves of the impactor (+) marks the upwards while (o) marks the downwards sweep. Taken from [P2]

of 10V (DC) to the maximal permitted supply voltage of 24V (DC). One such circuit is illustrated in Figure 3.6. By varying the size of the control-signal it is possible to smoothly vary the magnitude of the exerted force.

The force generated by each electromagnetic actuator depends nonlinearly on the control voltage and the air gap between the impactor mass and the active magnet. Figure 3.7 presents an experimental characterisation of these relationships. The measurements were made using a single magnet and the impactor mass, and do not include the restoring force from the flexible beam. Furthermore, each measurement was made by supplying a constant voltage to the electromagnet, meaning that the results do not take the electromagnet and amplifiers dynamical proporties into account. The generated force is observed to be proportional to the square of the control signal voltage and inversely proportional to the cube of the air gap, which agrees well with theory. In addition, the electromagnets have been measured to have a real pole at 31 Hz causing a reduction of the generated force for higher frequencies. During operation the air gap is often quite large causing smaller forces with a close to linear dependency on voltage and air gap. Note that only small control forces are necessary for stabilizing the dynamical equilibrium states of the system.

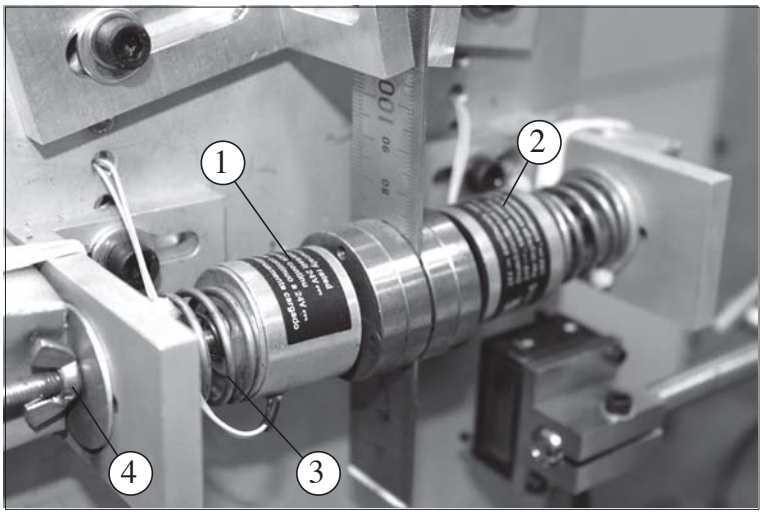

Figure 3.5: Close-up of the electromagnetic actuators: (1) and (2) electromagnets mounted on each side of the impactor mass; (3) and (4) spring, screw and wing nut assembly allowing to vary distance between actuator and the impactor mass.

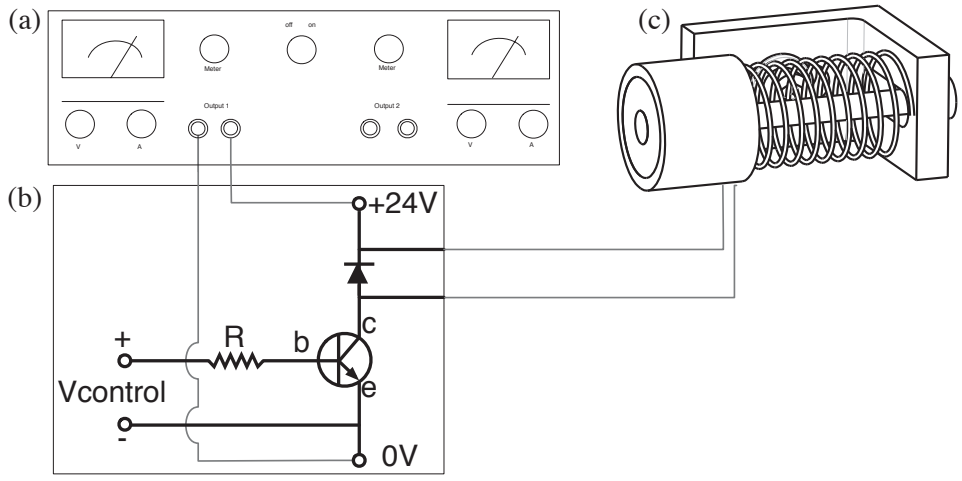

Figure 3.6: Diagram for one of the two electromagnetic actuators. (a) Power Supply Unit (PSU) supplying a constant voltage of 24V (DC). (b) A very simple amplifier circuit consisting of a resistor, a transistor and a diode amplifying a control-signal for the electromagnet. (c) An electromagnet generating a pulling force on impactor steel mass.

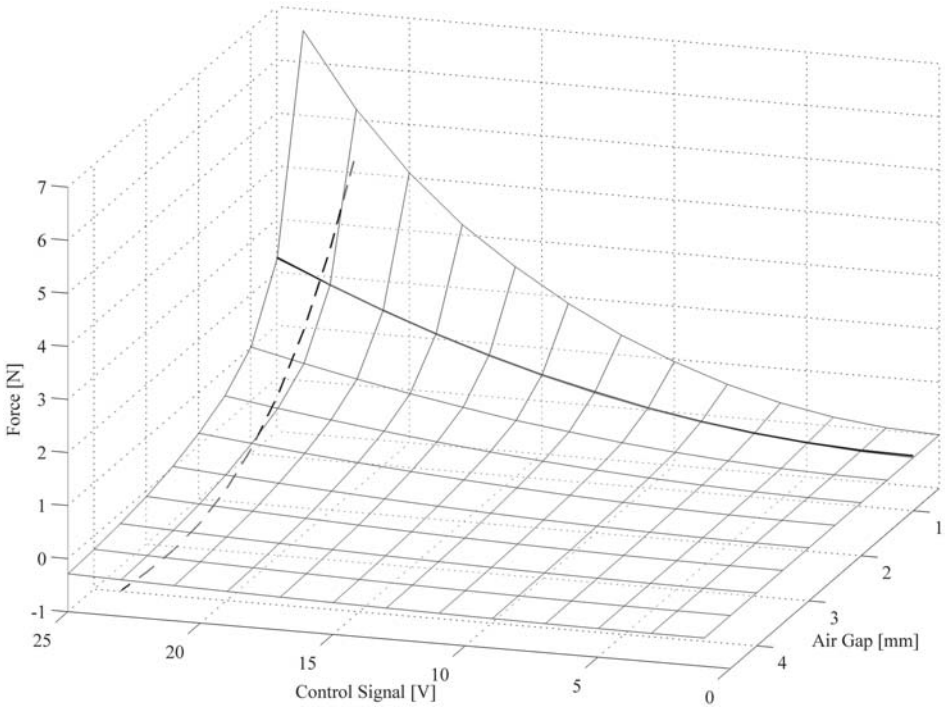

Figure 3.7: Experimentally measured (static) pulling-force produced by one of the electromagnets as a function of (constant) supply-voltage and the air gap between magnet and impactor mass. The thick black line (——) is a second order approximation to the experimental data and the dashed line (- - -) is a third order approximation.

3.2 Implementation

The implementation of control-based continuation to the test rig is done using a dSpace DS1104 real-time control board and a computer running Matlab, Simulink and dSpace Control Desk. Figure 3.8 gives an overview of the real-time application which is programmed in Simulink and then compiled and uploaded to run on the DSpace board. The real-time application on the board and the continuation code on the computer runs asynchronously, and only communicates to change parameters, set a new reference trajectory, read Fourier coefficients of the current state etc.

Fourier transformation and inverse transformation is done in real-time on the board. This is not necessary for continuation, but it makes it easy monitor the settling of transient behavior and reduces the amount of data that is transferred between the computer and the dSpace board. How to compute the Fourier-modes online is explained in [P2].

3.2.1 Real-time control and harmonic forcing

The control signal is generated in real-time on the board using a PD-controller according to Equation (2.2). The control target in Figure 3.8 is the state predicted by the continuation algorithm expressed in terms of its Fourier modes. A reference trajectory in constructed from this by inverse Fourier transform. The measured state and the reference trajectory are fed into the Simulink Proportional Derivative (PD) control block, which constructs and outputs the control signal. A suitable control requires tuning of the proportional and derivative gain K_p and K_d as well as a coefficient for a lowpass filter implemented in the derivative term of the PD-controller. Chapter 4 explains how to tune these parameters when both the

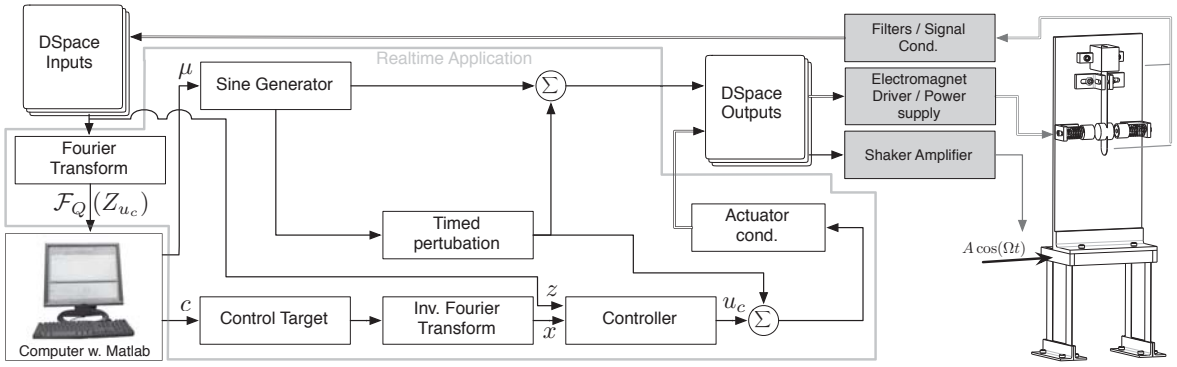

Figure 3.8: Simplified Simulink model and its interaction with the continuation code and experiment. Taken from [P2].

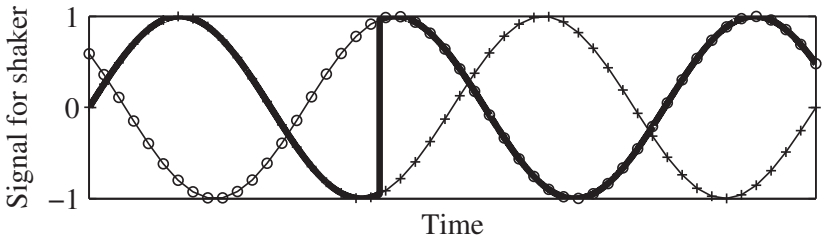

Figure 3.9: Illustration of phase jumps when changing excitation frequency. Time-series of a 1 Hz (+) and 1.01 Hz sine-wave (o) slowly drifting in and out of phase: A small change in frequency can result in the non-smooth signal (▬) being sent to the shaker. Taken from [P2].

experiment and actuators has nonlinear unknown dynamics. The output of the PD controller is sent to the actuator conditioner block which splits the signal and sends positive values to one electromagnetic actuator and negative to the other.

It is important that the forcing parameters (amplitude and frequency) can be changed by the continuation code. This is done by constructing the harmonic signal sent to the shaker in the real-time application, cf. sine generator in Fig. 3.8. The shaker signal must change smoothly in response to a change in forcing parameters in order to avoid unwanted perturbations of the system. Changing the amplitude is not problematic if done in small steps, but even a very small change in frequency can give rise to a large unwanted perturbation of the system. This is because two sine-waves with very close frequencies will slowly drift in and out of phase as experiment time elapses. Sending the signal depicted in Fig. 3.9 to the shaker would cause a perturbation that could result in the system settling onto a different steady state. This can be avoided by using a scaled time defined by $\dot{\tau} = \omega(t) \Rightarrow \tau = \int_0^t \omega(s)ds$ to calculate the harmonic forcing signal, since the integration will smoothen out any discontinuous changes to the frequency ω.

3.2.2 The Continex toolbox

Continuation is applied to the controlled experiment using the Matlab pseudo arc-length continuation-platform COCO [22]. A toolbox named Continex (Continuation in experiments) has been specifically developed to handle the communication between COCO and the real-time application running on the DSpace board. It constructs and experimentally evaluates a zero-problem (2.1) and its Jacobian as well as applying statistical and interpolation methods to minimize the influence of measurement noise. It consists of the real-time application shown in Figure 3.8 and a set of functions which makes it possible for the continuation algorithm to evaluate the experiment as if it was a set of differential equations. The real-time application

constructs the forcing signal, the non-invasive locally stabilizing control signal and performs Fourier transform and its inverse. Using the developed set of function it is possible to change many parameters during run-time. Continex also implements the stability tests as well as features for automating experiments, managing and plotting recorded data, resuming previous continuation-runs etc. Continex is included as a toolbox in the COCO continuation platform, which is freely available from [21].

3.3 Frequency and amplitude responses

Figure 3.10 presents parameter sweeps for the impact oscillator performed with the electromagnetic shaker. Note that the dynamics of the impactor, platform and shaker is coupled, and the response of full system is measured as the relative displacement of the impactor. Figure 3.10a presents series of frequency responses obtained by sweeping the forcing frequency while keeping the amplitude constant. In Figure 3.10b the forcing amplitude is swept while keeping fixed values of the frequency. For small non-impacting response amplitudes, the response is linear, while for increasing (impacting) responses, a large hysteresis loop develops.

3.4 Further remarks

In conclusion the constructed test rig serves as a good test case for the method. It has a strongly non-linear response well within the measurement range of the sensors. The setup is simple but it reproduces dynamics found in real life applications. The actuators have a complicated non-linear dependence on system parameters that vary, but in turn they allow to add a non-invasive control to many types of complicated systems, such as rotating machinery. In [P2] frequency sweeps similar to those in Figure 3.10a are performed using the control-actuators to confirm that the actuators are able to provide sufficient control-energy for the intended application.

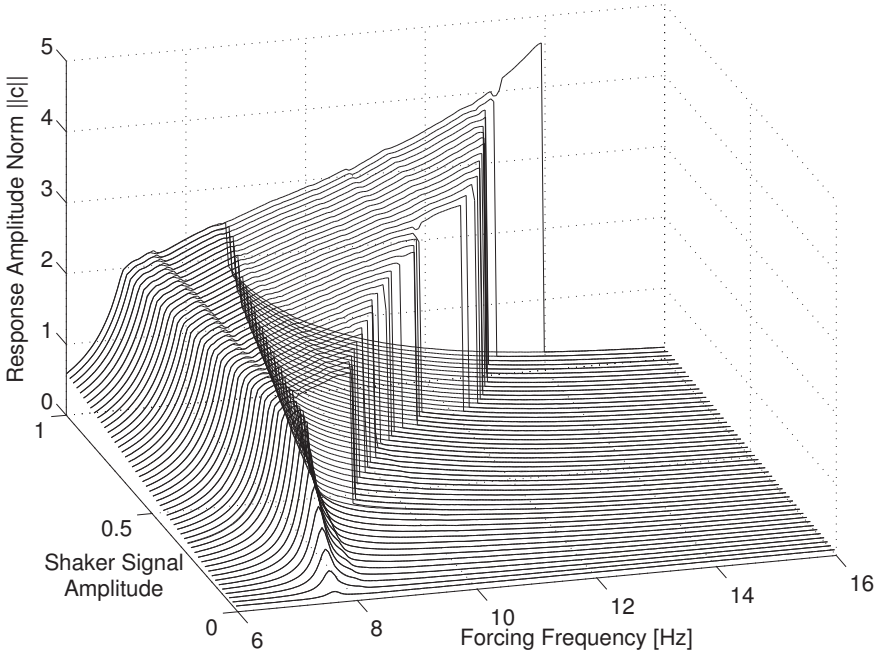

(a) Frequency response of the mechanical system obtained by sweeping the frequency of the external forcing for fixed values of shaker signal amplitude.

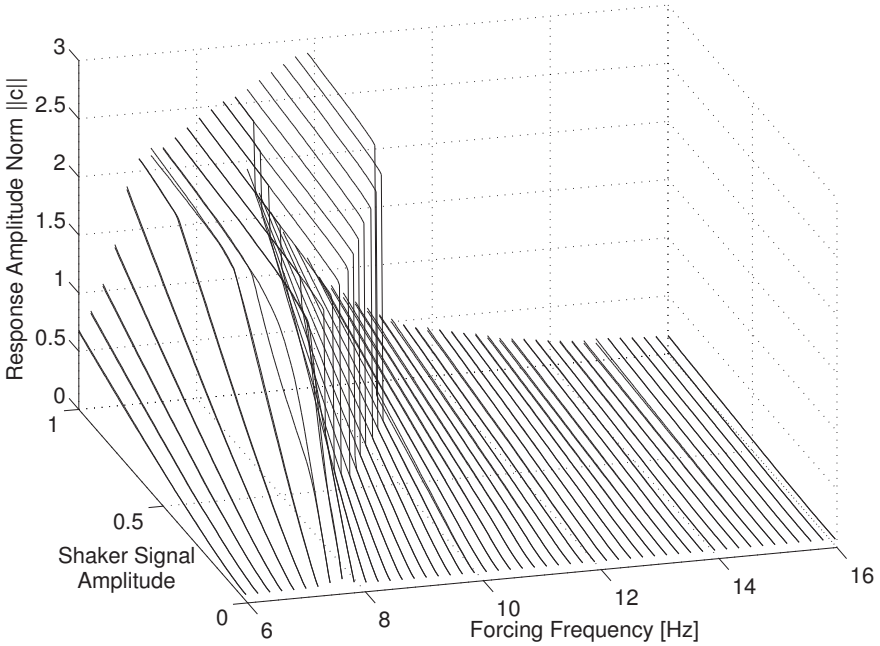

(b) Amplitude response of the mechanical system obtained by sweeping the amplitude of the shaker signal for fixed values of the forcing frequency.

Figure 3.10: Results of frequency and amplitude sweeps performed on the experimental test rig (Fig. 3.1). The response amplitude is given as the Euclidean norm of the Fourier-coefficients ||c||. Taken from [P2].

4 Control tuning

Constituting a stabilizing and non-invasive control is a prerequisite for control-based continuation. Such a control can be realised using a PD-controller (2.2) with properly chosen gains and filtering. Selection of proper gains and filtering is referred to as control tuning and is normally done using mathematical models of the system and actuators. However, since the control-based continuation method intends to investigate properties of dynamical systems without models, this approach cannot be used. Purely experimental methods for tuning PD-controllers, such as Ziegler-Nichols methods [25] or the Good Gain method [26], exist but cannot be used since we wish to stabilize periodic orbits rather than static equilibrium states. Furthermore, we wish to control a strongly nonlinear mechanical system with unknown dynamics using nonlinear actuators. This causes hysteresis in the control, making it impossible to use gradient based adaptive control methods.

In Publications [P1] and [P2] we propose a sequence of experiments that allows to choose optimal control gains, filter parameters and settings for a continuation method without a-priori study of a model. The gains are adjusted to constitute a control that is effective in stabilizing the states predicted by the continuation and minimizing effects of disturbances. Additionally, the control must become non-invasive whenever the predicted state matches an equilibrium-state of the underlying uncontrolled system. This constitutes two competing targets and the goal of the tuning process is to find a suitable compromise between control effectiveness/aggressiveness and non-invasiveness. The tuning method is developed and tested for the harmonically forced impact oscillator, but the experimental procedure can be generalized and used with other similar setups. Furthermore, the actuators serve as a prototype for electromagnetic bearings and similar actuators which can be used with rotating machinery.

4.1 Non-invasive, locally stabilizing control

Consider a sampled measurement of an uncontrolled experiment Y running over time t and depending on a parameter μ. This can be expressed as

$$Y(\mu, N) = \{y_0, \ldots, y_{N-1}\}, \tag{4.1}$$

where N denotes the number of sampled points. For control-based continuation, we construct a suitable controlled experiment of which a measurement is denoted

$$Z_{u_c}(\mu, N, x) = \{z_0, \ldots, z_{N-1}\}. \tag{4.2}$$

Here $u_c = u_c(t)$ denotes a control signal, and $x = x(t)$ is the reference trajectory provided by the continuation algorithm. In order to apply a continuation algorithm to the experiment, the controller and the controlled experiment must satisfy a number of conditions:

1. The controlled experiment must be *consistent*, that is, for zero control $Z_0 \equiv Y$ holds and the controlled experiment Z_{u_c} converges uniformly to the *un*-controlled experiment as $u_c \to 0$.
2. The control must be *locally stabilizing*, meaning that any equilibrium state of Y (stable or unstable) must become an asymptotically stable equilibrium state of Z_{u_c}.
3. The control must be *non-invasive*, that is, the control-signal u_c must vanish whenever the requested state x is a equilibrium state of the uncontrolled experiment.

Condition 1 requires the control actuator not to alter the dynamics of the system when the control signal is zero. Actuators such as servo-motors and hydraulic actuators add inertia, stiffness and damping to the system, and hence are likely to violate this requirement. A workaround is to add the control force to the external excitation force, as done in for example [15]. Condition 2 makes it possible to observe unstable equilibrium states and distinguish coexisting steady states as long as they are sufficiently well separated in phase-space compared to the accuracy of measurements and control. Condition 3 is satisfied if the control signal is bounded by the difference between the reference trajectory and the measurement of the controlled experiment:

$$||u_c|| \leq \delta ||x - z||, \tag{4.3}$$

where $z = z(t)$ is the measurement of the controlled experiment taken at time t. The inequality (4.3) can be satisfied by many types of controllers. For our

implementation we chose a PD-controller because of its simple implementation and in general good performance. The control strategy described by Equation (2.2) is implemented in the model using the standard Simulink PD-block. As shown in Figure 3.8 the controller is designed to minimize the difference between reference trajectory $x(t)$, set in the code as the inverse Fourier transform of the control target c, and the current measured trajectory $z(t)$. In addition to the proportional and derivative gains (K_p,K_d), a low-pass filter must be applied in the differential term of the controller to avoid amplification of high-frequency noise. This is necessary to ensure that the control signal (2.2) to satisfies (4.3). This filter must balance the two competing targets of removing high-frequency noise while not making the control too slow. The output of the controller is scaled by an overall gain, CFGain, which can also be varied.

4.2 Experimental control tuning

4.2.1 The initial idea

Two simple experiments are developed to determine the influence of different control gains on effectiveness and non-invasiveness of the control:

1. Measure the response of a stable (impacting) equilibrium state for the uncontrolled system, and set this as reference trajectory for the control while retaining the forcing parameters. For a properly tuned non-invasive control-scheme this produces a vanishing control signal, although in an experiment we must expect a smal residual control signal due to noise in measurements and control. This experiment is performed for different sets of control gains, and the resulting control signal is used as a measure for the non-invasiveness of the control.

2. Set the reference trajectory to zero, corresponding to the static equilibrium state of the impactor, while applying a harmonic perturbation using the shaker. Varying the control gains while recording the response of the impactor gives an inverse measure of the effectiveness of the control.

Figure 4.1 shows a number of such parameter sweeps in the control gains. The top row illustrates the level of invasiveness (experiment 1) of the control and the bottom row the effectiveness (experiment 2). For both invasiveness and effectiveness, high and low plateaus are observed depending on the overall gain G[1]. A good set of gains

[1]Except for a scaling factor, G is equivalent to the CFGain.

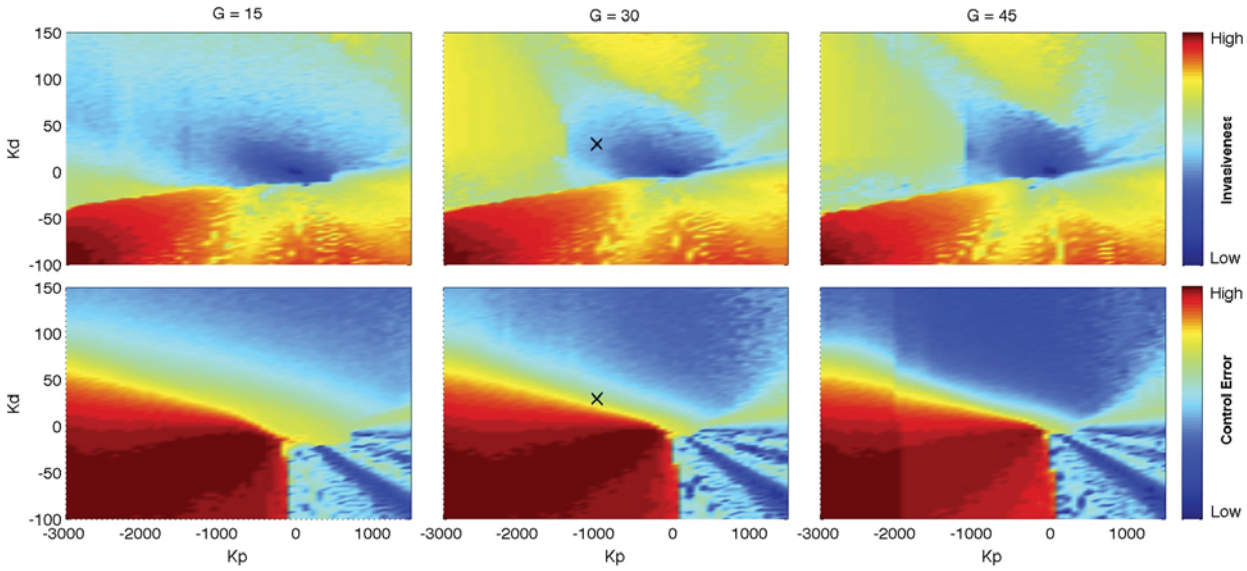

Figure 4.1: Experimentally obtained parameter sweeps of gains for the PD-Controller for different overall gains G applied to the controller output. K_p denotes proportional gain and K_d denotes differential gain. The top row illustrates the level of invasiveness of the control while the bottom row illustrates the effectiveness (inverse proportional to the control error). $\times$ denotes the chosen gain combination for continuation. Taken from [P1].

constitute an appropriate compromise between non-invasiveness and effectiveness, which means that one should aim at a low plateau for both conditions.

Subsequent analysis of continuation runs using the gains obtained using this tuning procedure led to some important conclusions: Firstly, in both experiments, hysteresis is observed in the control and in order to have a conservative estimate, the maximum value was plotted. It was found that seemingly appropriate sets of gains in some cases could give rise to bi-stable control or control which was not robust to perturbations. As a solution to this problem an in-phase perturbation is included in the sweep-procedure, as will be described in the next section. A second important conclusion was that the problem of tuning the control proved to be more complex than first presumed: Sets of gains that could successfully stabilize the stable equilibrium states sometimes would fail when tracking the unstable part of the bifurcation diagram. Furthermore, the stabilization of the unstable equilibrium states showed a strong dependency on the filter coefficient determining the pole location, and hence the cut-off frequency, of the low-pass filter in the derivative term of the controller. Finally, internal scaling-gains were introduced in the real-time model in order to get a proper balance between the measured trajectory and parameters in the residuum used to determine convergence of the correction-algorithm. This makes it impossible to quantitatively compare Figure 4.1 with the following results.

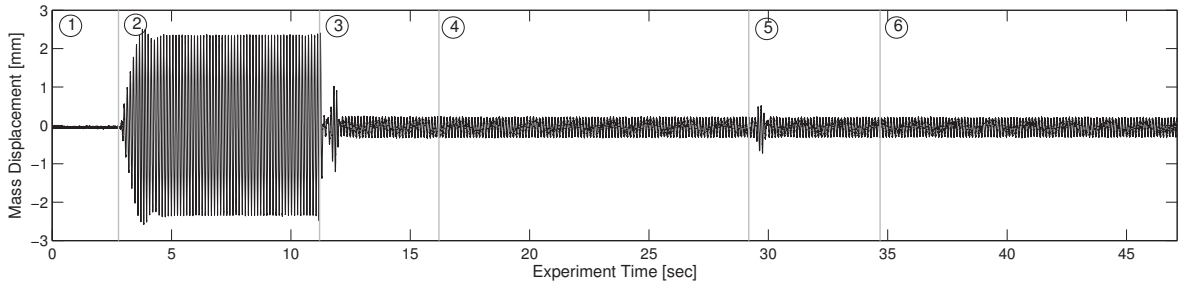

Figure 4.2: Time series for the impactor mass during one measurement cycle for the experiment of stabilizing the static equilibrium. (1) No harmonic forcing is applied, (2) Harmonic forcing is applied and transients are allowed to settle, (3) Stabilizing control is enabled and the system is allowed to settle, (4) Extra wait-time to allow for a possible instability of the control to grow, (5) An in-phase perturbation is added to shaker and control-signal to test the controls' robustness against large perturbations, and transients are allowed to settle, (6) The response is measured and Fourier-transformed. Taken from [P2].

4.2.2 Timed perturbation

A timed in-phase perturbation is introduced during control gain sweeps to ensure that the control is robust with respect to perturbations and that it is not bi-stable. This is necessary since the continuation will frequently change parameters and the reference trajectory, which can cause large perturbations to the system. The perturbation signal is constructed from a sine-wave multiplied with an envelope function, ensuring that the signal sent to the shaker is continuous. After changing control parameters, the perturbation-signal is applied to the control and forcing signal in order to verify that the control is stabilizing, even under large perturbations. The proces of measuring a set of control gains effectiveness including an in-phase perturbation is shown in Figure 4.2.

4.2.3 Stabilizing the static equilibrium state

Using the timed perturbation and internal scalings we repeat Experiment 2. The reference trajectory is set to $x(t) = 0$ and a harmonic forcing with amplitude $A_{\text{shaker}} = 0.5$ and frequency $\omega = 7.75$ Hz is applied. The control parameters are varied and we use the resulting amplitude of the impactor as a measure of control effectiveness. Figure 4.3 shows the result of three such investigations for different values of the overall scaling gain CFGain. Note that the results are much simpler in comparison with what was found in Figure 4.1, supporting the observation that seemingly stabilizing control gains would sometimes lead to bi-stable or a non-robust control. The results in Figure 4.3 suggest a more effective control for increasing

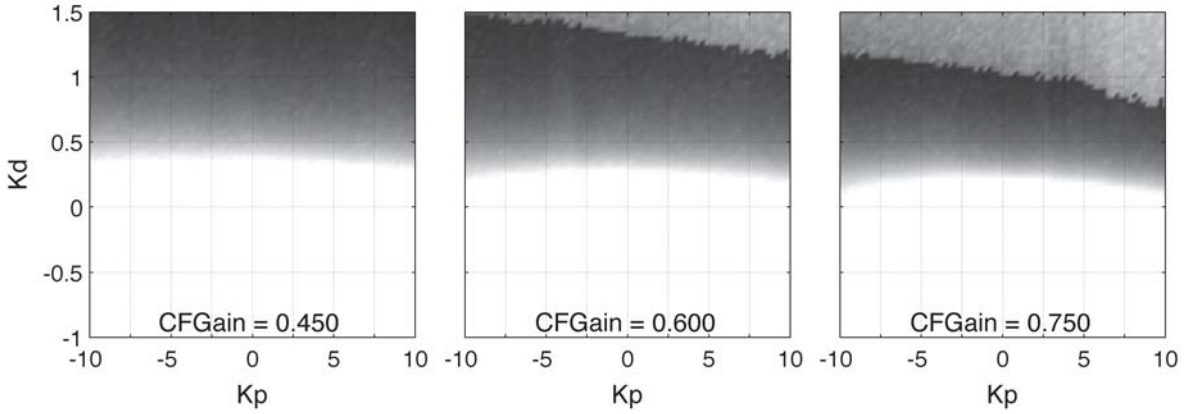

Figure 4.3: Stabilization of the static equilibrium state of the impactor as the control-gains K_p and K_d are varied for different but fixed values of the scaling gain CFGain and a fixed filter coefficient PDFC = 180. The gray scale indicates the amplitude of the response, where a darker shade corresponds to smaller amplitude and, hence, to more effective control. We observe an improvement of the control for increasing K_d, but also an onset of inefficient control indicated by the light-gray area appearing at the top-right corner of the diagram for increasing overall gain. Taken from [P2].

derivative gains K_d while for increasing values of the overall gain CFGain, a region of inefficient control appears in the top-right corner. Somewhat counter-intuitive is the observation that negative proportional gain K_p seems to improve the control. In conclusion, these results suggest to use a pair of gains that is close to the boundary of effective control as the control strength increases with increasing gains.

4.2.4 Stabilizing a stable impacting equilibrium state

We repeat Experiment 1 using the modified real-time model and the timed perturbation. The forcing parameters are chosen to be the same as in the previous experiment, and these parameters ensure that the impact oscillator has a unique impacting equilibrium state. This equilibrium state is particularly interesting because it has a strongly nonlinear response. The reference trajectory is set to the measured trajectory and the difference between reference trajectory and observed response is used as a measure for the controls ability to non-invasively stabilize the equilibrium state. Figure 4.4 shows the result for the corresponding values of the overall scaling gain CFGain. Again we observe a simpler result than what was found in Figure 4.1. A strip of control gains resulting in non-invasive control, bounded from below and above is observed. Figure 4.3 and 4.4 indicate that, for CFGain = 0.6 a good choice of gains is $K_p \approx 2$ and $K_d \in [0.5, 0.75]$, resulting in stabilizing and non-invasive control. Subsequent continuation runs showed that these gains made it possible

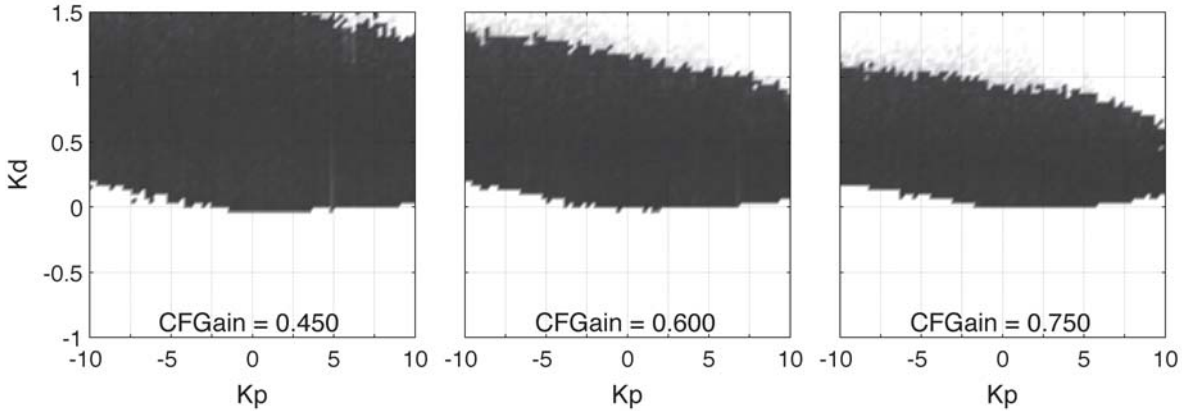

Figure 4.4: Stabilization of an impacting stable equilibrium state as the control gains K_p and K_d are varied for different but fixed values of the scaling-gain CFGain and a fixed filter coefficient PDFC = 180. The gray scale indicates the deviation of the measured response from the reference trajectory, which is generated from the Fourier-coefficients of the stable equilibrium state. Darker shade corresponds to smaller deviation and, hence, to less invasive control. We observe that proportional control increases invasiveness as the region of low invasiveness is further away from the line $\mathrm{K_d} = 0$ as stronger proportional control is applied. A good choice is $K_p \approx 2$. We also observe high invasiveness for control gains that led to inefficient control in the previous experiment; cf. Fig. 4.3. Taken from [P2].

to apply control-based continuation to the test rig, but that the continuation ran quite unreliably and often would fail while tracking along the branch of unstable equilibrium states.

4.2.5 Stabilizing an unstable impacting equilibrium state

Experiment 2 is now modified to stabilize an unstable impacting equilibrium state. The state is obtained by a successful continuation run, and using the corrector algorithm it is possible to resume and correct the state before each set of gains is tested. This ensures that any effects of drift due to changes in the environment are minimized. During experiments it was noted that the cut-off frequency of the lowpass filter implemented in the derivative term of the PD-controller had a significant impact on the control performance. Therefore, for this experiment we fix the overall gain at CFGain = 0.65, restrict the control gains to the strip $(K_p, K_d) \in [1, 3] \times [0, 1.5]$ and sweep for different but fixed values of the filter-coefficient PDFC. The results are presented in Figure 4.5. We observe the emergence of a strip of efficient and non-invasive control around $K_d = 0.5$ as well as a dramatic improvement for PDFC up to 150, with seemingly little improvement for larger values. The proportional gain K_p is seen to have very little influence on the control for PDFC > 140.

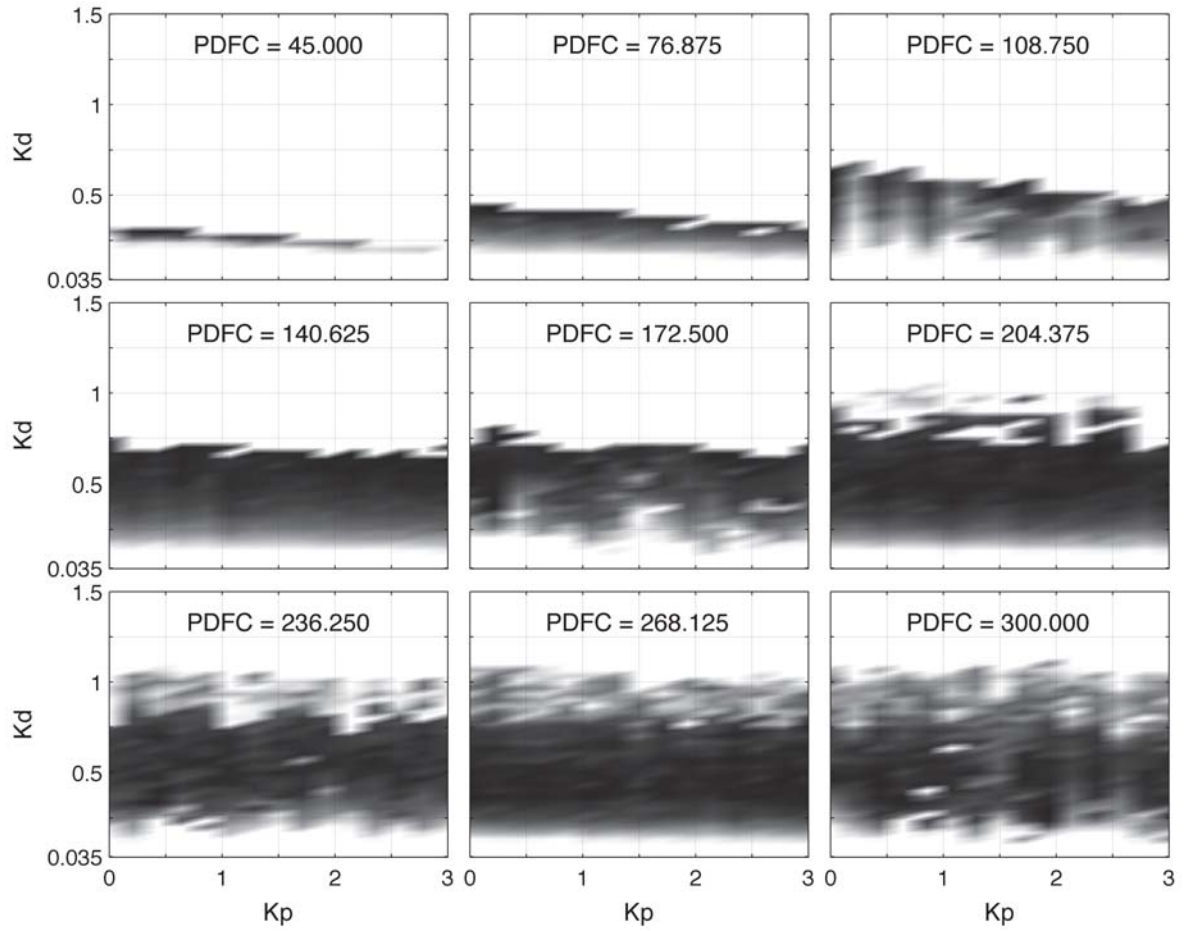

Figure 4.5: Stabilization of an impacting unstable equilibrium state as the control-gains K_p and K_d are varied for different but fixed values of the filter coefficient PDFC and a fixed scaling-gain CFGain = 0.65. The grayscale indicates the deviation of the measured response from the reference trajectory, which is set to the Fourier-coefficients of an unstable equilibrium state. Darker shade corresponds to smaller deviation and, hence, to both, more effective and less invasive control. We observe the emergence of a strip of effective control parameters around $K_d = 0.5$. Taken from [P2].

4.2.6 Optimizing performance of Newton's method

In addition to examine how different sets of control parameters are able to non-invasively and effectively stabilize stable and unstable equilibrium states, an interesting question to consider is: How do they influence the performance of the Newton corrector-algorithm? For some sets of parameters giving stable and efficient control, the Newton-method would converge very slowly or even fail to converge. This usually happened while tracking a branch of unstable equilibria or while tracking around a fold point. Furthermore, the use of complete recomputations of the Jacobian in addition to Broyden-updates seemed to improve the convergence, at the cost of increased experiment time. A reasons for this might be the noise contamination of the measurements resulting in Broyden updates that are sometimes not accurate enough to ensure convergence. As in the previous experiments, the proportional gain K_p had little influence on the convergence of the Newtons-method.

An experiment is set up in which an unstable equilibrium state is restored and the number of iterations necessary for convergence of the Newtons-method is measured as a function of the derivative gain K_d and filter coefficient PDFC. The experiment is performed using Broyden-updates only as well as full recomputations of the Jacobian every 45 steps. The result is presented in Figure 4.6 and it is interesting to note that a frequent recomputation of the Jacobian seems to stabilize the convergence of Newtons method for a larger set of gains, at the expense of experiment time. Equally interesting is that, for the case of Broyden updates only, there exist a triangular island of low iteration numbers and short convergence time for PDCF $= [109; 236]$ and $K_d = [0.2; 0.3]$, where the correction succeeds reliably. In conclusion, the choice of parameters should depend on how one computes the Jacobian matrix. For testing the method a frequent re-computation makes it easier to tune a proper control, while an substantial speed up of the overall runtime is possible by carefully selecting gains and parameters that allow for the use of Broyden updates only. For our subsequent continuation runs we used $K_p = 2, K_d = 0.35, \text{PDFC} = 180$ and CFGain $= 0.65$, which is noted to work well in both cases.

4.3 Continuation results

To verify the result of the tuning process, we apply control-based continuation to the test rig with the obtained control parameters. The results are presented in Figure 4.7. It is noted that there is good agreement between results obtained with the parameter sweep and continuation (cf. Figure 4.7a), and that the continuation is able to reliably reproduce the results (cf. Figure 4.7b). The continuation also performs well in following the unstable part of the diagram and tracking around the

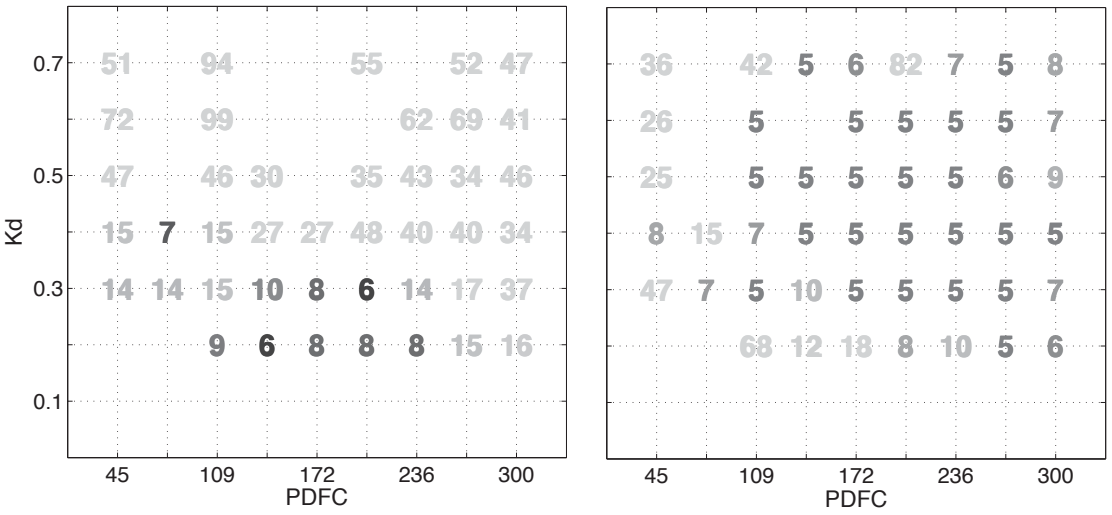

(a) Broyden updates only.

(b) Finite difference updates every 45 steps.

Figure 4.6: Number of corrector-iterations required for one correction-step to converge depending on control parameters K_d and PDFC. In panel (a) only Broyden updates are used to calculate the Jacobian whereas in panel (b) the Jacobian is re-computed initially and every $\mathrm{N_{Jac}} = 45$ steps using finite difference approximations. The integers indicate the number of iterations necessary for convergence, and are shaded according to computation time with black corresponding to low computation time and grey high. Note that computation time and number of iterations do not correlate, as re-computing the Jacobian using finite differences is expensive. Also a minimum of 5 steps are used in order to provide statistical evidence that the correction did not satisfy the convergence criteria by chance. Non-converging parameter sets are removed leaving empty spaces. The sweeps were made using a fixed proportional gain of $K_p = 2$ and CFGain = 0.650. Taken from [P2].

two fold points. The upper fold point (cf. Figure 4.7d) of the bifurcation diagram presents a challenge for the algorithm, since the quasi-periodic vibrations exist in this region. Nevertheless, the continuation produces robust and consistent results. The small hysteresis bubble observed in Figure 4.7c often causes the continuation to terminate, since the braches at this point cannot be distinguished due to insufficient measurement and actuation precision.

4.4 Further remarks

The results of the tuning method presented here are specific for our test rig and actuators, but the experiments and many of the conclusions can be generalized. The sequence of experiments presented throughout Section 4.2 can be applied to other experiments and the important parameters are expected to be the same. An important aspect is that with this specially designed test rig is possible to make the control unstable without causing damage to the system, which cannot always be expected. In case the control cannot be made unstable, the sweep method can be modified to trace out the stability boundary without making the control unstable. The control sweeps presented here has been performed with a high resolution for presentation purposes and amounts to approximately one month of consecutive experiments, but an estimate of good control parameters can be obtained with coarser sweeps and a more restricted sweep range.

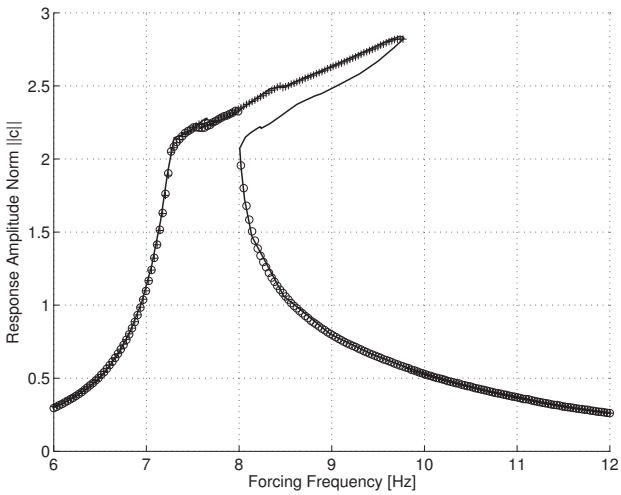

(a) Continuation run

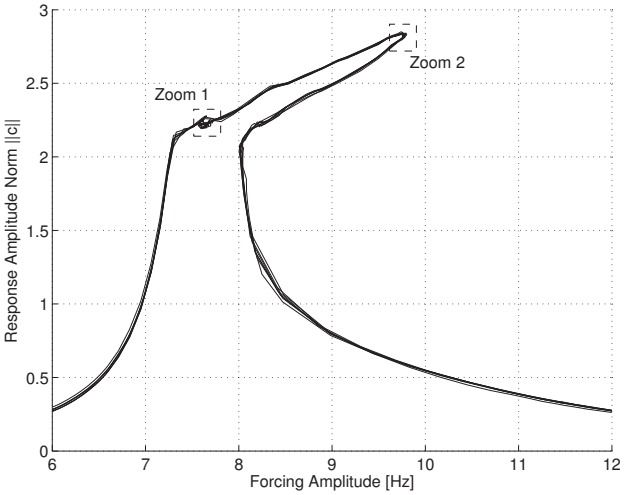

(b) Multiple continuation runs

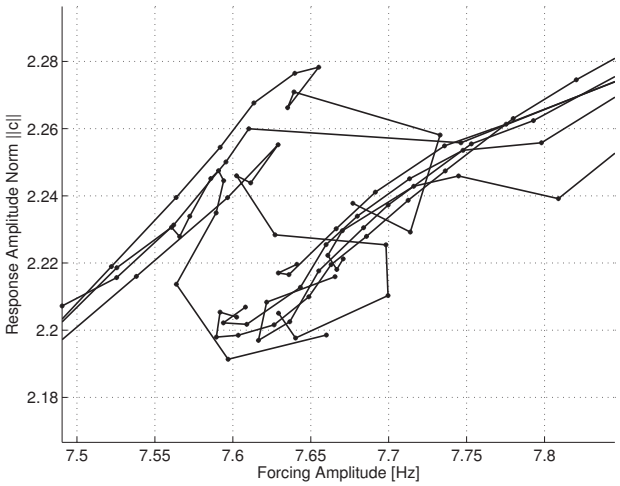

(c) Zoom 1

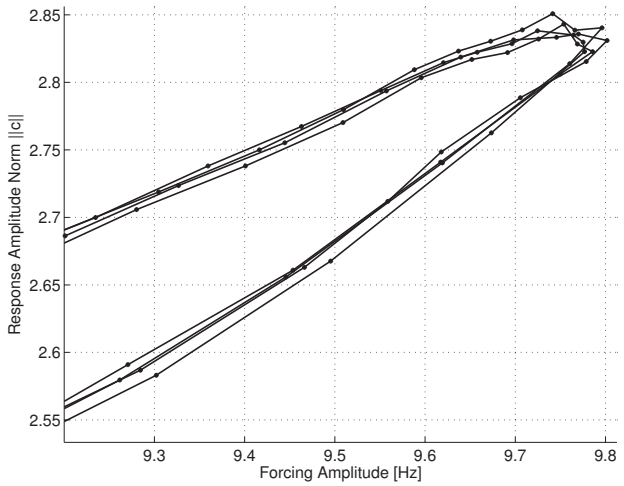

(d) Zoom 2

Figure 4.7: Frequency responses for the impact oscillator obtained by control-based continuation. Panel (a) compares the result of the continuation method with those of a parameter-sweep. Panel (b) shows several consecutive continuation-runs overlaid, and confirms that the method provides consistent results. Panel (c) shows the occurrence of a small hysteresis bubble. Continuation runs often terminate at this point because the accuracy of measurements and actuation is insufficient to distinguish the coexisting states. Panel (d) shows a zoom of the upper part of the frequency-response, and confirms that the continuation method is able to track around the fold point. Taken from [P2].

5 Determining Stability

The control-based continuation method utilizes a non-invasive stabilizing control which locally turns both stable and unstable equilibrium states into asymptotically stable ones. This in turn makes it difficult to determine if an equilibrium state of the underlying uncontrolled system is stable or unstable. The information about the systems' stability is important for tracing out stability boundaries, detecting bifurcations and predicting the transient behavior. Three different methods for determining the stability of an equilibrium during control-based continuation are presented in Publication [P3] and [P4]. In [P3] the basic concepts are introduced along with divergence tests from stable and unstable equilibrium states. The methods are implemented and tested in [P4] and make it possible to produce bifurcation diagrams with indication of stability, like the one show in Figure 1.1c. The methods for determining stability are developed, based on the principal idea of modifying momentarily turning off the control while observing the resulting behavior. Each of the methods has its advantages and drawbacks and they are useful in different situations. Two of the methods allows to determine stability without generating unbounded divergence from an equilibrium state. In some cases it is possible to quantify the level of instability in terms of the finite-time Lyapunov exponent (FTLE).

5.1 Disabling control at an equilibrium state

In the following we investigate what happens if the the control is disabled at a stabilized equilibrium state. Figure 5.1 presents a frequency response with three different coexisting dynamical equilibrium states (1)-(3) marked at the same forcing frequency. Figure 5.2a shows time series at a stable equilibrium state (1). After

some time the control is turned off and, as expected the state does not diverge. This verifies that the state is a stable equilibrium state of the underlying uncontrolled system, and that the control is non-invasive. Note that, since the continuation algorithm accepts a state as an equilibrium to a certain tolerance, there will always be some small residual drift upon disabling the control. We define an equilibrium state as stable, in the classical Lyapunov sense, if the periodic orbits stay close in phase space. If they however diverge, we define the equilibrium as unstable and the rate with which they separate is used as a quantitative measure of the instability. Figure 5.2b shows time series with the system initiated on the unstable equilibrium (2). The control is turned off, and the system diverges until it finally settles on a higher amplitude stable equilibrium (1). The divergence of the measured state from the reference (target) state is noted to occur mainly in the phase. In Figure 5.2c the system is again initiated on the unstable state (2). After the control is disabled, the state diverges and settles onto the lower amplitude equilibrium (3). The divergence is here predominantly in the amplitude. Finally, the control is re-enabled and the unstable equilibrium state is restored. Note that if the noise in the system is very low, it might be necessary to introduce a perturbation to initiate the divergence, but in our case this is not necessary.

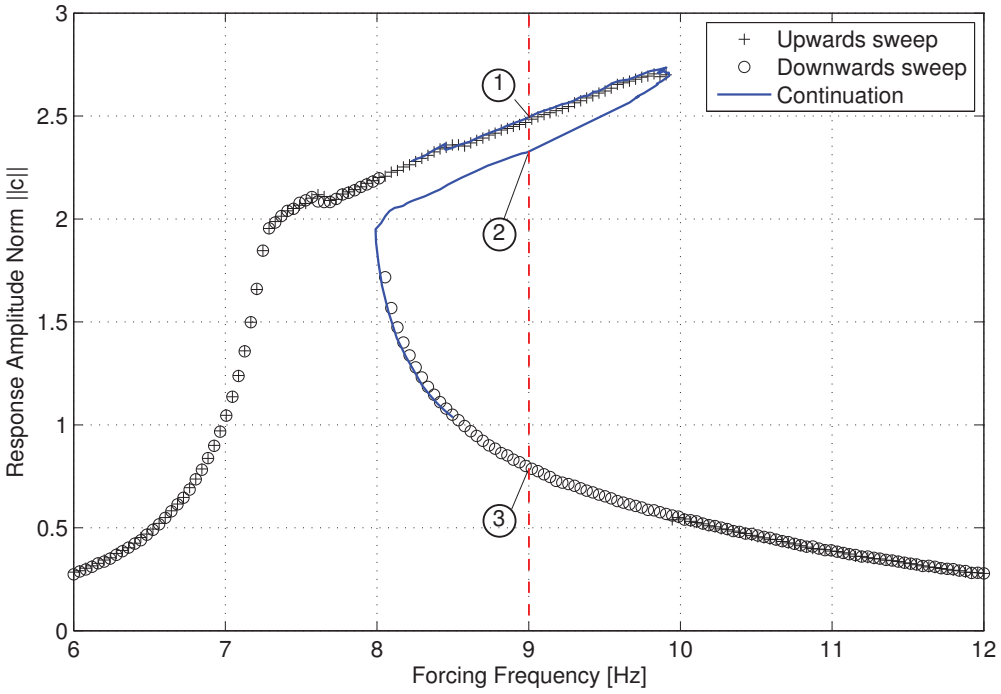

Figure 5.1: Experimentally obtained frequency response for the harmonically forced impact oscillator showing multiple coexisting equilibrium states: (1) High amplitude stable equilibrium state, (2) unstable equilibrium, (3) low amplitude stable equilibrium. Taken from [P3].

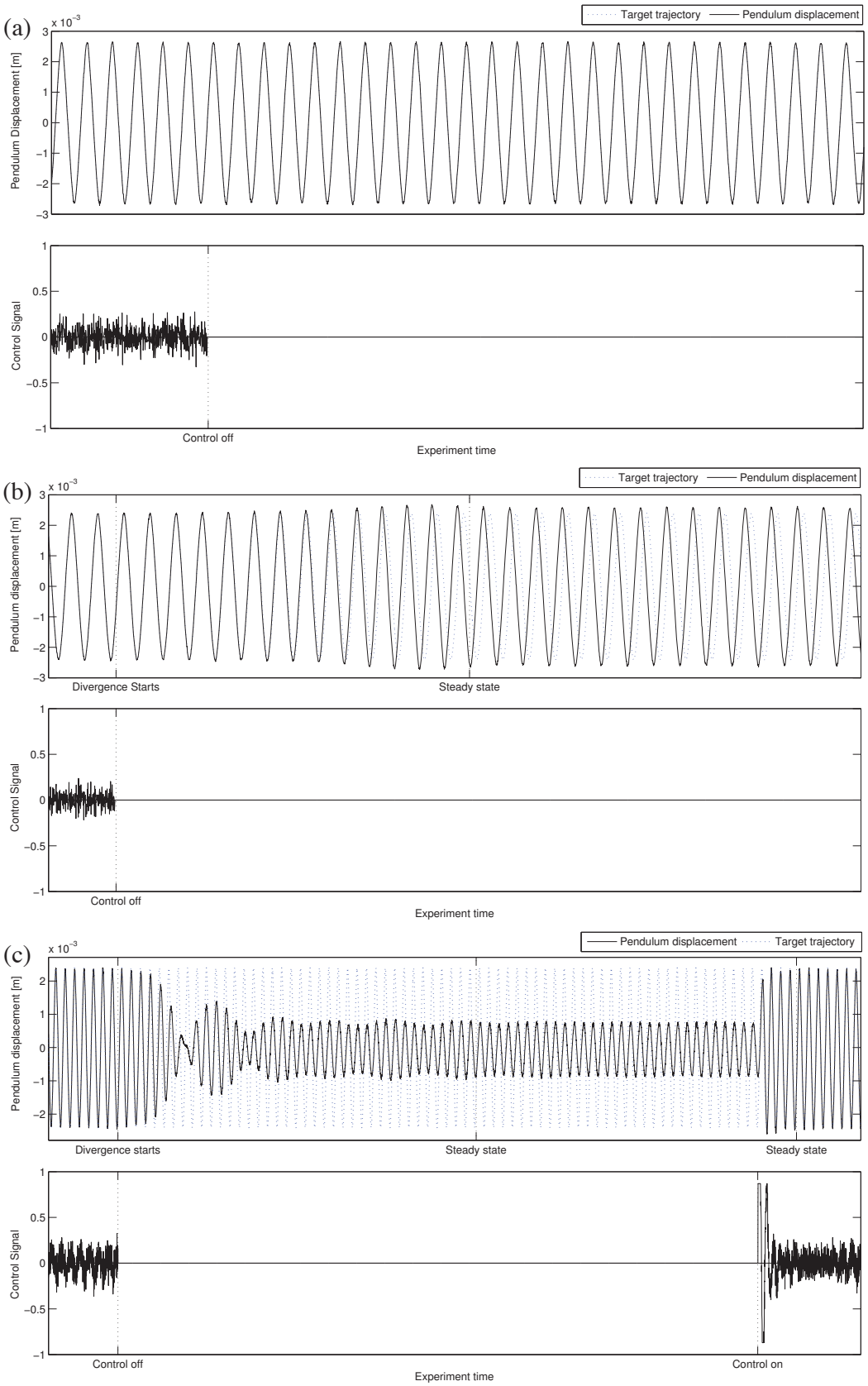

Figure 5.2: Time series for disabling the control at a stable and an unstable equilibrium state. (a) High amplitude stable equilibrium state, (b) unstable equilibrium to high amplitude stable equilibrium, (c) Unstable equilibrium to low amplitude stable equilibrium. Taken from [P3].

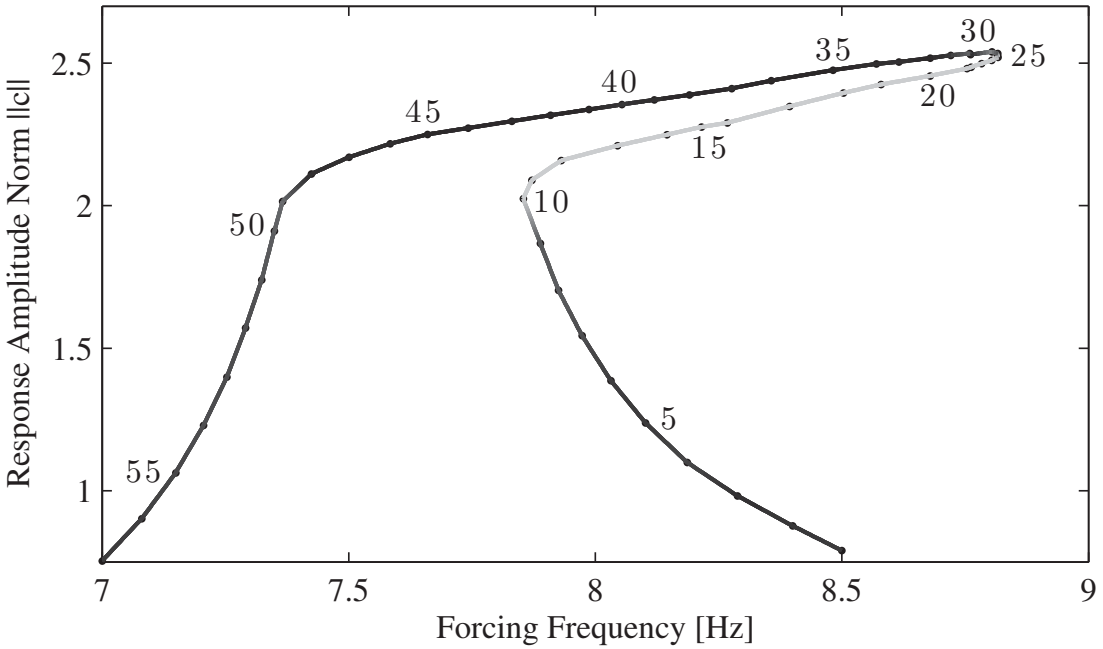

Figure 5.3: Bifurcation diagram with a continuous measure of stability plotted in grayscale (interpolated in between measurement points): Dark tones denote a small stability estimator and hence a stable state. Lighter tones denote a large stability estimator and hence an unstable state. All measurement points are marked with $(\cdot)$ and consecutively number labeled (shown for every fifth point). These labels will be used to identify different equilibrium states and will be referred to with # and label number throughout the this chapter. Taken from [P4].

5.2 Methods for determining stability

The following will present three methods for determining stability: Free-flight stability check, deadband control and deadband limited free-flight. The methods are developed for use during control-based continuation. The control-based continuation method tracks bifurcation diagrams, as the one in Figure 5.3, by repeating a series of prediction and correction steps. When the correction algorithm converges, the state is accepted as a equilibrium state of the underlying uncontrolled system. The bifurcation diagram in Figure 5.3 consists of a number of such accepted states, and at each such state we wish to test, determine and in some cases quantify the stability during continuation.

Note that in this Chapter we will use a different nomenclature for the measured state and reference or target trajectory. This is to make it consistent with the nomenclature used in Publication [P4]. The measured state is now denoted x (in the previous this was z) and the reference trajectory is denoted y (in the previous this was x).

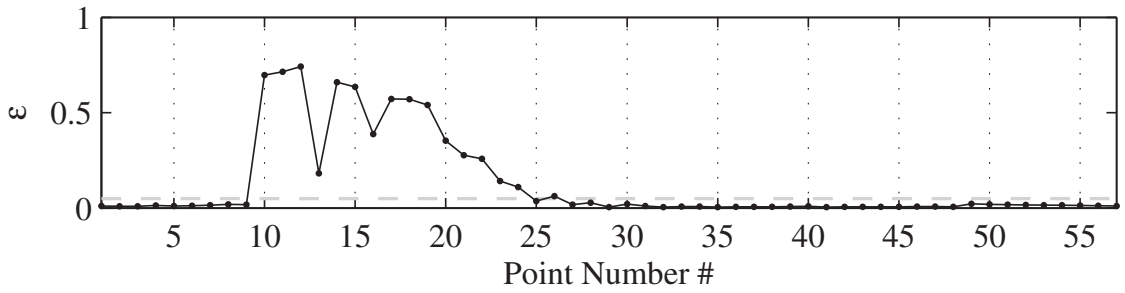

Figure 5.4: Stability indicator ε for the bifurcation diagram in Figure 5.3. Numbers on the x-axis correspond to label numbers along the bifurcation branch. The chosen threshold, which indicates the limit of instability $\varepsilon_t = 0.05$, is marked by (- - -). Taken from [P4].

5.2.1 Free-flight stability check

The free-flight stability check is based on the same experiment as the initial tests presented in Figure 5.2: Turn off control and observe if the current state x diverges from the reference state y, implying that the equilibrium state is unstable. As it was noted the divergence can be in both amplitude and phase, and it is therefore helpful to study the difference $x - y$ rather than x. We define a normalized root mean square error by

$$\varepsilon = \frac{\mathrm{RMS}(x - y)}{1 + \mathrm{RMS}(y)} \tag{5.1}$$

where RMS denotes the root mean square value of a sampled signal defined as

$$\mathrm{RMS}(x) = \sqrt{\frac{1}{n}\left(x_1^2 + x_2^2 + \cdots + x_n^2\right)}. \tag{5.2}$$

This seems to provide a robust measure of instability, but it does not provide a quantitative measure of the instability. Since ε is a continuous measure, it is necessary to chose a threshold for instability. Figure 5.4 shows the estimator for each point of the bifurcation diagram in Figure 5.3 along with the chosen threshold for instability. The onset of instability occurs in good agreement with theory and parameter sweeps. Furthermore, the estimator shows a considerable difference between stable and unstable equilibria, meaning that the coexisting equilibria are sufficiently separated in phase space, compared to the measurement and control accuracy. Note that the control must be able to restore the equilibrium state in order to resume continuation after a stability test. This generally requires more control power than necessary for continuation and cannot always be expected. It also requires that the divergence does not alter the equilibrium state.

The initial part of the divergence from an unstable equilibrium state is noted to be

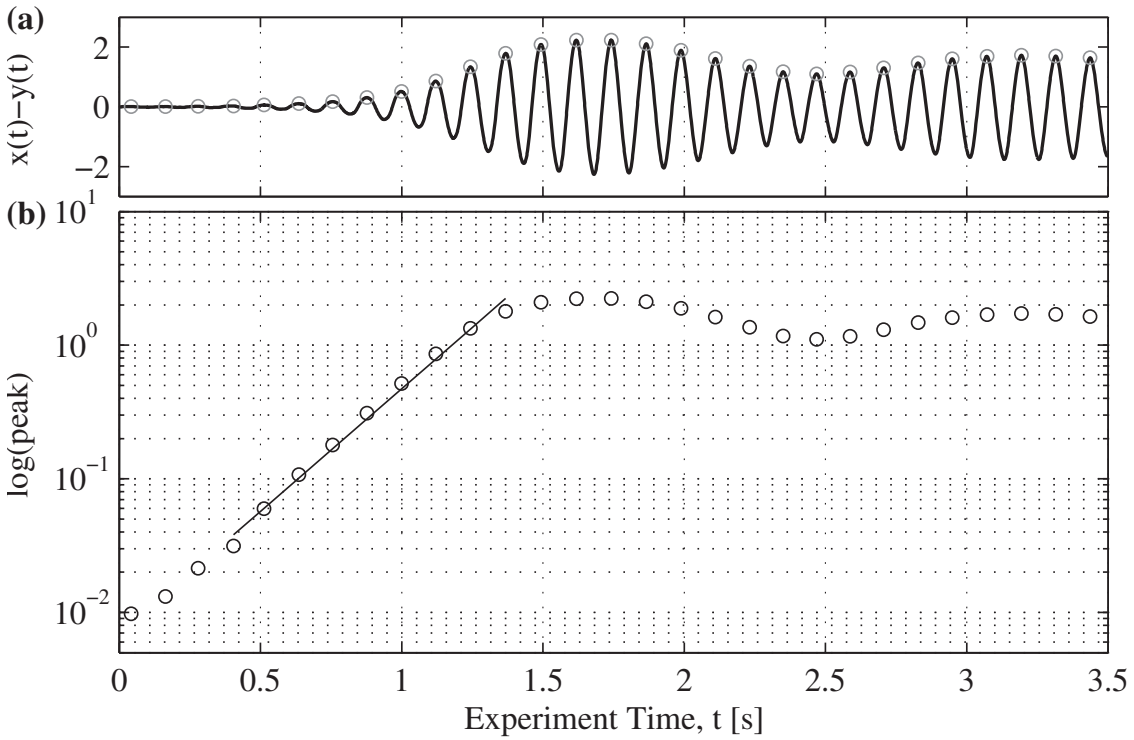

Figure 5.5: Retrieving stability information for an unstable state (#16) by using a linear fit to the logarithm of the peaks. (a) Smoothened difference $x - y$ with detected peaks (using the Matlab functions: Smooth (moving average filter from the Curve Fitting Toolbox) with a 20 points window and Findpeaks (Signal Processing Toolbox)). (b) Logarithmic plot of the detected peaks ($\circ$) along with linear fit (—) in the time-interval $t \in [0.4; 1.2]$. Taken from [P4].

close to exponential. This means that it is possible to estimate the rate of divergence by doing a linear fit to the logarithm of the peaks, as shown in Figure 5.5. The slope of this fit will yield the finite-time Lyapunov exponent (FLTE) λ.

5.2.2 Stability check using deadband control

We introduce a deadband Π in the non-invasive control signal (2.2). Using our current nomenclature the control signal becomes

$$u(t) = \begin{cases} 0 & \text{for } ||PD(x(t) - y(t))|| \leq \Pi \\ PD(x(t) - y(t)) & \text{for } ||PD(x(t) - y(t))|| > \Pi. \end{cases} \tag{5.3}$$

In effect the control is only enabled when the deadband is exceeded. A properly adjusted deadband allows the stability to be determined without letting the system diverge unbounded: Upon enabling the deadband in the control, an unstable state

will start to diverge until the deadband is exceeded, while a stable equilibrium will not be affected. The stability is determined by noting if the control is enabled or not. If the deadband is kept narrow in order to allow minimal divergence, the number of control-bursts can be used as a measure of stability, distinguishing between a few peaks due to noise and repeated enabling of the control due to instability.

The results of a stability test using deadband control is shown in Figure 5.6. Note that here a wide deadband has been used for visualization purposes. In conclusion the method allows for performing stability tests during continuation, without allowing the system to diverge. It is not possible to properly quantify the instability, although the number of control bursts might be proportional to the finite-time Lyapunov exponent λ. Note that the time window for the stability test must be sufficient to allow for divergence to develop at any of the unstable equilibrium states along the equilibrium branch.

5.2.3 Deadband limited free-flight

The deadband limited free flight stability check attempts to combine the two previous methods, in order to estimate finite-time Lyapunov exponents without allowing the system unbounded divergence. This is done by adjusting the deadband such that it allows some divergence, essentially capturing the initial (exponential) part. The control is modified such that whenever the deadband is exceeded, the control is kept active for enough time to completely restore the equilibrium state. At unstable equilibrium states this results in a series of divergence measurements. Our observations suggest that the estimated Lyapunov exponent is not dependent on which side of the equilibrium-branch the state diverges to, as long as we only study the local behavior. For each stability check (at every point of the bifurcation curve) the following steps of postprocessing are performed:

1. Center the data set $x - y$ by subtracting its mean value.

2. Smoothen the time series using a moving average / lowpass filter. In Matlab this can be done by using the function 'smooth' (Curve Fitting Toolbox).

3. Detect peaks of the absolute value of the smoothened signal to get both positive and negative peaks. It can be helpful to use a peak detection algorithm that can discard values smaller than a certain tolerance and require the peaks to be separated by a certain time span. In Matlab this can be done using the function 'findpeaks' (Signal Processing Toolbox).

4. Divide the data set into separate segments of free flight. This can be done by

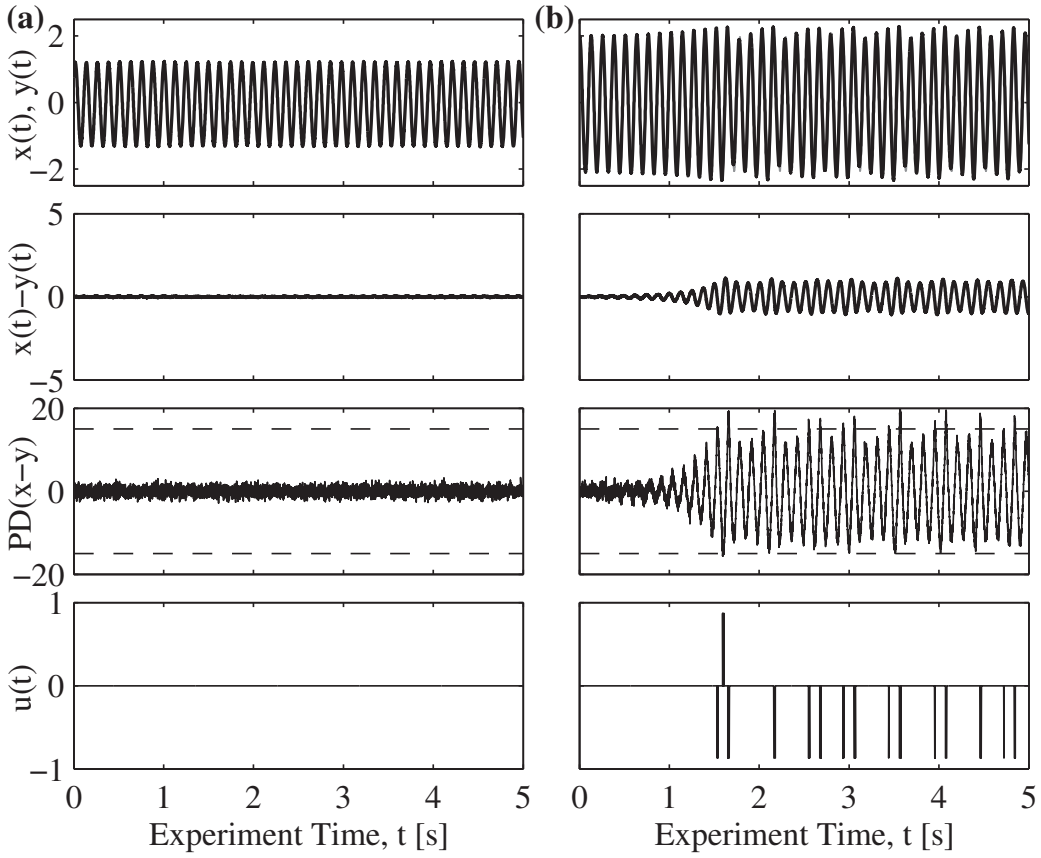

Figure 5.6: Time series for deadband control stability tests at (a) a stable state (#5) and (b) an unstable state (#10). Deadband limits (- - -) are shown together with controller output in the third panel and the deadbanded control signal which is sent to the actuators is shown in the fourth panel. Note that the control is only active for the unstable state (b) and that it only allows a limited divergence. Taken from [P4].

checking the control signal, as this is zero when the system is in free flight, cf. Figure 5.7.

5. Evaluate the Cooks' distance [27] for each segment and use this information to remove statistical outliers from the data sets.

6. Perform linear interpolation on each set of peak data and average the slopes to get the finite-time Lyapunov exponent λ.

Figure 5.7 shows an example of the method successfully applied at an unstable equilibrium state. The postprocessing is automated and implemented in the stability test functions, which are a part of the Continex-toolbox.

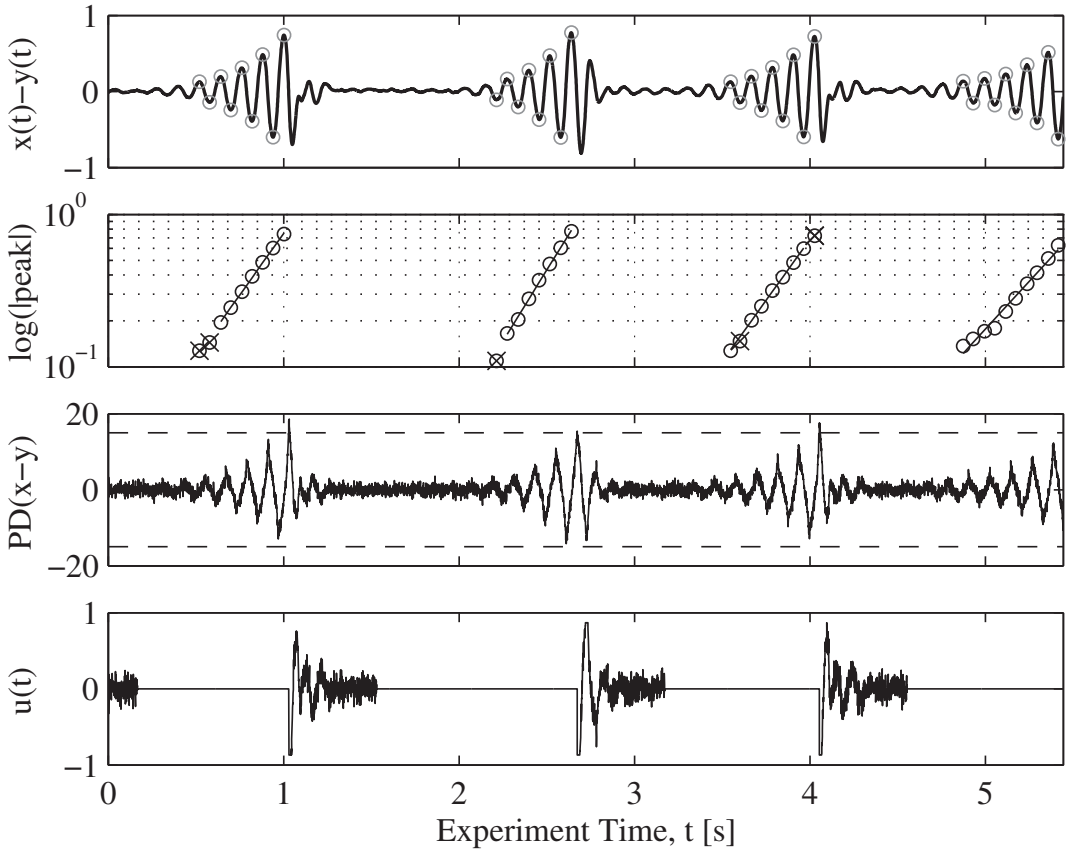

Figure 5.7: Deadband-limited free flight stability check at an unstable state (#16). Removed outliers are marked by (×) in fit. Average Lyapunov exponent: $\lambda = 3.65 \pm 0.58$. Taken from [P4].

5.3 Results

In the following we present results of applying the stability tests during continuation. The complete set of results can be found in [P4].

5.3.1 Continuation with stability information

A continuation run with a continuous measure of instability, estimated using the free-flight method, is shown in Figure 5.3. In contrast Figure 1.1c shows a frequency response with a distilled binary measure of stability. Both results are noted to be in good agreement with theory and parameter sweeps. Figure 5.8 shows the stability estimators for five consecutive continuation runs using the free-flight and the deadband limited free-flight method. Since the continuation uses an adaptive step-length, the number of points used in each continuation run varies. To allow for comparison, the curves are normalized with respect to the total arclength of the corresponding branch. The two methods estimate the onset of instability at the same place, but only the deadband limited free-flight gives quantitative information about the stability. The stability is noted to change smoothly when continuing across a fold point, which can also be seen in Figure 5.9. This agrees with the observation that divergence is slow near the fold points.

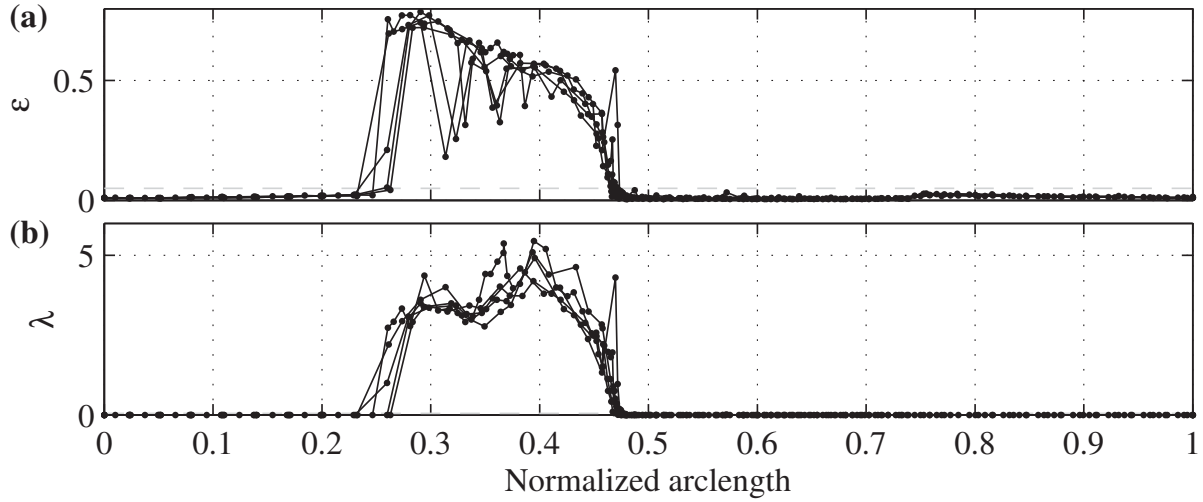

Figure 5.8: Stability estimator (normalized with respect to arclength of the branch in the bifurcation diagram) of multiple continuation runs. Chosen stability threshold $\varepsilon_t = 0.05$ is marked by (- - -). Top panel shows the normalized root mean square error ε for a free-flight test. Bottom panel shows the averaged Lyapunov exponent estimated by the deadband-limited free flight method. [P4].

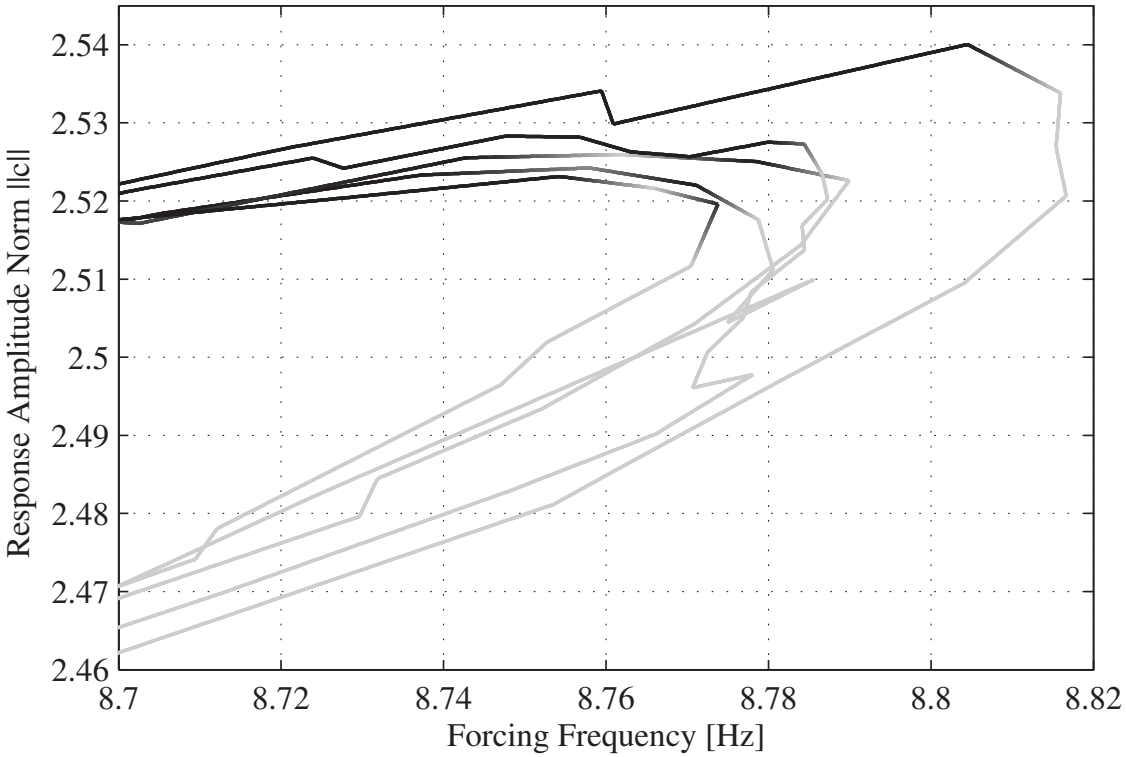

Figure 5.9: Continuation around a fold point. Five overlaid bifurcation diagrams for forcing strength $A = 0.5$ with stability estimator plotted in grayscale (dark for small values, light for larger values). Taken from [P4].

5.3.2 Special case: Stability at an isola

Figure 5.10 presents an experimentally found isola, by which we mean a family of stable and unstable equilibrium branches that are detached from the primary resonance peak. This isola is created by a 1:3 subharmonic resonance, at which the impactor is forced at approximately three times its fundamental resonance frequency, but the response is approximately at its fundamental resonance frequency. The isola serves as a good test case for both the continuation and stability check: It is difficult to initialize and perform parameter sweeps in this region since several branches of stable as well as unstable equilibria coexist and are connected through the unstable equilibrium branches. Using the control-based continuation method it is possible to follow the unstable equilibrium states and obtain a more complete bifurcation diagram. Performing stability checks during continuation is in this case only possible using the deadband control method. If the system is allowed to diverge, the control is not able to restore the equilibrium state and continuation cannot be resumed. The deadband had to be adjusted to only allow divergence just above the noise level. Hence, a few control bursts were allowed at stable equilibrium states due to noise. Unstable equilibrium states were characterized by a factor of 100 or more control bursts than at the stable states.

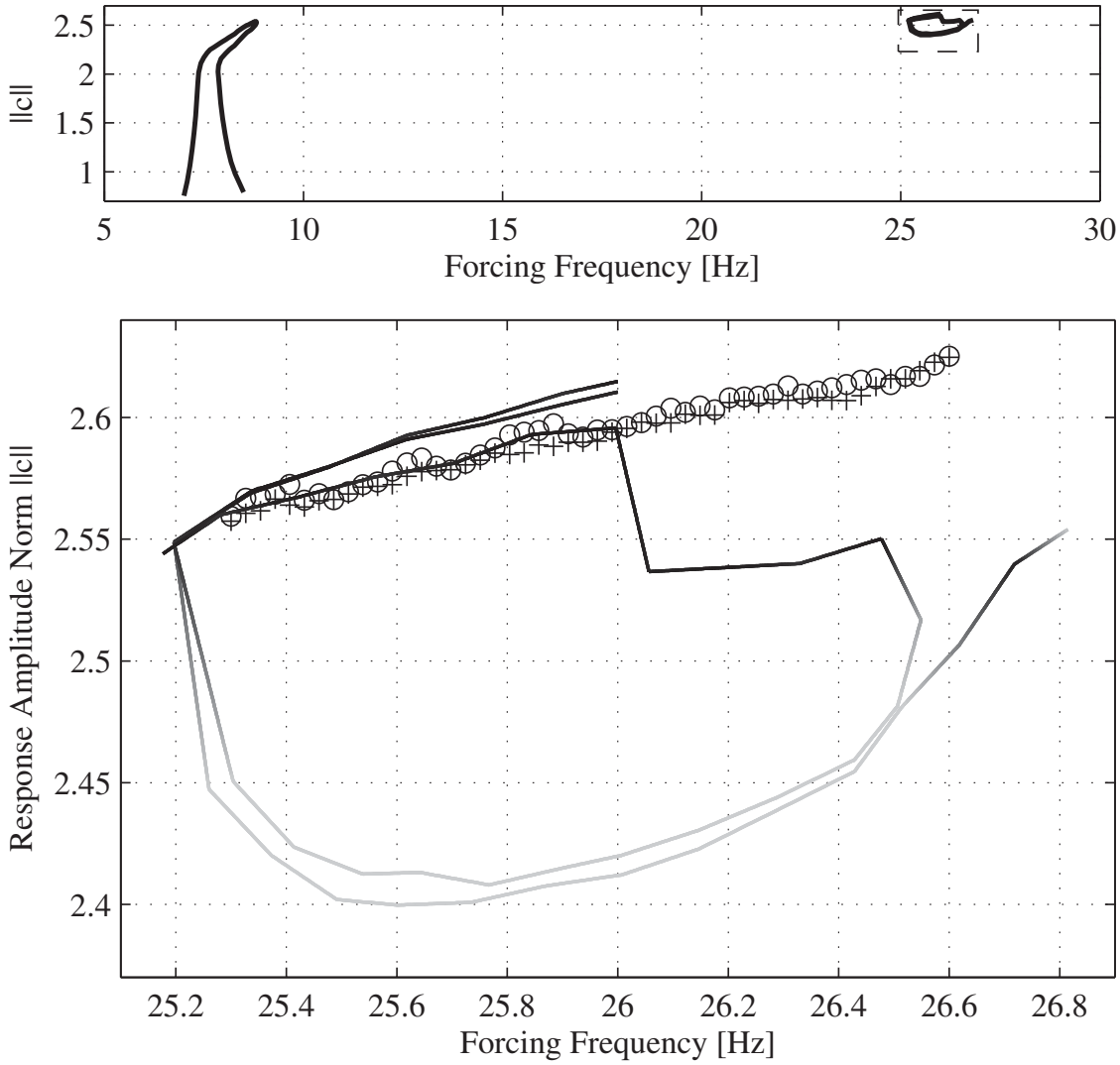

Figure 5.10: Family of isolated equilibrium branches (isola). Top panel shows the primary resonance (Fig. 5.1) at 7-10 Hz and the isola around 25-26 Hz. The bottom panel shows the isola composed of the stable and unstable equilibrium branches of a 1:3 subharmonic resonance found by a parameter sweep and two consecutive continuation-runs, using different settings for tolerances and step size. The sweep is denoted by (+) for increasing and (∘) for decreasing frequency. Stability information is assessed using deadband control and the number of control bursts are used as a continuos measure of stability. Taken from [P4].

5.4 Further remarks

All three suggested methods have been successfully applied to determine stability during experimental continuation, and each of the methods is shown to be suitable in different situations. The free-flight method and deadband control are robust and easy to implement. In contrast the deadband limited free-flight method is more advanced and puts more requirements on the experiment, but in turn provides statistically weighted Lyapunov-exponents for the unstable equilibria. All three methods requires the tolerance with which the corrector accepts a state x as an equilibrium state to be sufficiently strict, while otherwise the residual drift upon disabling control will be mistaken for instability. Quantifying the instability in terms of its finite-time Lyapunov exponent, requires the divergence to be well behaved: Divergence has to occur over several periods, and the coexisting equilibria cannot lie too close in phase space. Note that it is at this point only possible to quantify instability. Quantifying stability using a method similar to the free-flight stability test would require the equilibrium to be perturbed. In our test rig, however, the damping is high, such that for stable equilibria states, the transients are damped out within few oscillations. Increasing the magnitude of the perturbation effectively changes the response due to the nonlinear nature of the impact oscillator. This problem might be addressed by using a fitting method that makes use of the full set of acquired data as opposed to only fitting the peaks.

6 Simulating control-based continuation experiments

Simulating control-based continuation experiments has two purposes. Firstly, it is a quick, cheap and safe way to test experiment designs, actuators and tune the control prior to entering the laboratory. Secondly, the provided framework for simulating experiments mirrors the set of functions for performing control-based continuation in experiments. This means that with the Continex-toolbox and COCO continuation core [21] at hand, it will be possible to run simulated experiments out of the box. This is helpful for gaining insight in how the code works and how to connect it to an experiment with sensors and actuators. Our hope is that downloading a code that runs out of the box encourages people to setup a control-based continuation experiment, and in that way helps to spread and develop the method. For testing the implementation, we simulate an externally forced Duffing oscillator. Finally a control-based continuation experiment of a controlled nonlinear Jeffcott rotor is simulated to investigate and discuss the feasibility of applying the control-based continuation method to rotating machinery.

6.1 Simulation strategies

Figure 6.1 presents different strategies for exchanging the experiment with a simulation. The experiment and continuation runs asynchronously with control and forcing being generated by the Continex real-time model, cf. Figure 3.8. The continuation algorithm (COCO) interacts with the experiment through Continex, by changing parameters, the reference trajectory and reading out the Fourier-modes of the response. Figure 6.1 indicates three different ways to substitute the experiment by a simulation. The first and simplest option is to use Matlab's ODE solver to integrate a set of differential equations describing the dynamics of a system and appending

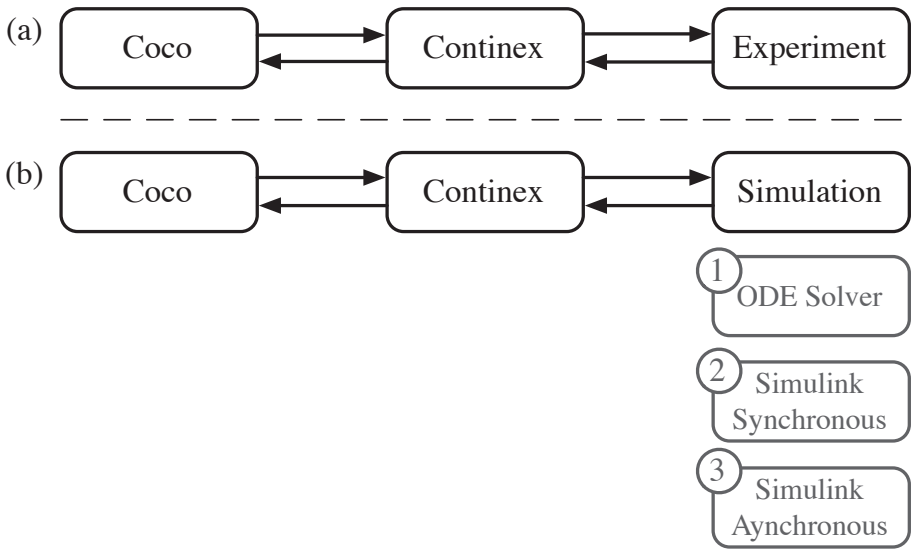

Figure 6.1: Different ways of simulating control-based continuation experiments. (a) Interaction of a control-based continuation experiment. (b) Different way of substituting the experiment with a simulation: 1) Using a Matlab ODE solver. 2) Interacting synchronously with a Simulink model. 3) Interacting Asynchronously with a Simulink model.

them with a non-invasive control signal. This option makes it possible to set up simulated control-based continuation experiments without using Simulink, but is also the option that has the least similarity with a real experiment. The second option is to run the Continex Simulink model (sketched in Figure 6.2) synchronously with the continuation-code. The Continex Simulink model is similar to the real-time model (cf. Figure 3.8), but it runs entirely in Simulink and hence does not require a real-time control board. It uses a discrete solver with a fixed step-size, which gives signals similar to what a sampled experiment produces. In addition, it includes a model of the experiment and actuators. The last option is running the Continex Simulink model and continuation code asynchronously. This is similar to running a control-based continuation experiment, but requires the Simulink model to be continuously running and hence requires more computational power. An advantage of using the Continex Simulink model is that it is easy to log and view all internal signals in the model, which is helpful when choosing suitable parameters for the continuation or tuning the control.

6.1.1 Matlab ODE-solver

Denoting the output state of a simulated experiment r and a reference trajectory set by the continuation algorithm s, a non-invasive PD-control can be constituted

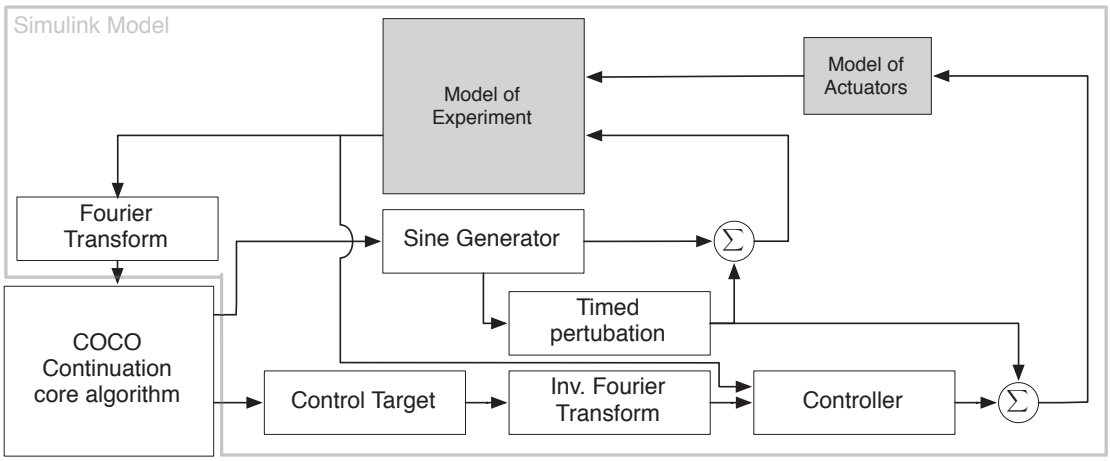

Figure 6.2: Sketch of the Continex Simulink model for simulating control-based continuation experiments.

as

$$u = K_p P + K_d D, \tag{6.1}$$

where the proportional and derivative term can be estimated as

$$P = r - s \tag{6.2}$$

$$D = \frac{1}{w}[P - \delta], \tag{6.3}$$

with

$$\dot{\delta} = \frac{1}{w}[P - \delta] \quad (\Delta t < w \ll 1). \tag{6.4}$$

Here Δt is the integration step size (which may vary) and w is a real constant. The derivative is approximated using equation (6.3) and (6.4). The control-signal (6.1) is calculated for each integration step and added to the equations of motion. Equation (6.4) is added to the system of equations and integrated along with the rest of the equations. This trick was provided in a set of unpublished notes by Jan Sieber.

For each iteration step, the continuation algorithm sets parameters μ and a control target c, which is inverse Fourier transformed to obtain the reference trajectory $s(t)$. The equations of motion with added control are simulated until transients have settled. Then exactly one forcing period of steady state behavior is simulated and Fourier-transformed after which the residuum $\mathcal{F}(r) - c$ is returned.

6.1.2 Simulink synchronous

The code listing 6.1 shows how to synchronously evaluate the Simulink model (cf. Figure 6.2). The function sets the control-target and parameter and then calls a function `run_sim`, which runs the simulation and handles saving/resuming of the simulation state, such that each new simulation continues from the last state of the previous simulation. At this point the function waits for the Simulink model to simulate for the specified time `wait_tm` and then returns the logged signals, which are written when the Simulink model terminates. Finally `get_res` calculates and returns the residuum as the difference between the final value of the Fourier-modes and the control target c.

```
function [data, y] = evaluate_sim_sync(data,c,p)
set_ctrltarget(c);
set_pars(p);
[data] = run_sim(data,data.wait_tm());
y = data.get_res();
end
```

Code 6.1: Synchronous evaluation of the Continex Simulink model.

6.1.3 Simulink asynchronous

The Continex Simulink model (Figure 6.2) is started and is running continuously and asynchronous to the continuation code, similar to what would be the case for an experiment. The code listing 6.2 shows how to evaluate the simulated experiment. In comparison to the synchronous evaluation an explicit pause command is used for allowing transients to settle after the parameters p and control target c has been set. Since the Simulink model does not run in real time, the wait time parameter `wait_tm` depends on the transient time, integration step-size and processor speed, and must be estimated. The function `get_data` forces Simulink to write the logged signals to the disk, after which the residuum can be calculated and returned.

```
function [data, y] = evaluate_sim_async(data,c,p)
set_ctrltarget(c);
set_pars(p);
pause(data.wait_tm());
data.get_data;
y = data.get_res();
end
```

Code 6.2: Asynchronous evaluation of the Continex Simulink model.

6.2 Simulation results for a Duffing oscillator

In the following we test the implementation of the methods by simulating an externally excited Duffing oscillator

$$\ddot{r} + 2\beta\omega_0\dot{r} + \omega_0^2 r + \gamma r^3 = q \sin 2\pi f t, \tag{6.5}$$

where β is the damping ratio, ω_0 is the undamped linear natural frequency of the system, γ is the coefficient of a cubic nonlinearity, and q and f the amplitude and frequency (in Hz) of an external harmonic excitation. This is a generic case treated extensively in literature, see for example [28, 29]. Figure 6.3 presents simulation results using Continex with both the ODE-solver and the Simulink model. The results are for both cases compared with results from parameter sweeps, and are noted to be in perfect agreement.

6.3 Applying control-based continuation in rotating machinery

In the following we discuss the feasibility of applying the control-based continuation method to rotating machinery. The method would allow to perform experimental bifurcation analysis: Investigate how the response depends (nonlinearly) on variable bearing parameters, obtain frequency responses for nonlinear rotor systems, trace out stability boundaries, study the onset of instability and much more. Nonlinearities may be introduced into rotating machinery in many ways, e.g. through foil bearings, oil-film bearings, clearances in roller bearings, impacts and rubbing. Nonlinear phenomena such as sub/super harmonic resonances, hysteresis, impacts and chaotic behaviour are encountered in real machinery. A review of practical observations of nonlinear phenomena in rotor dynamics can be found in [30].

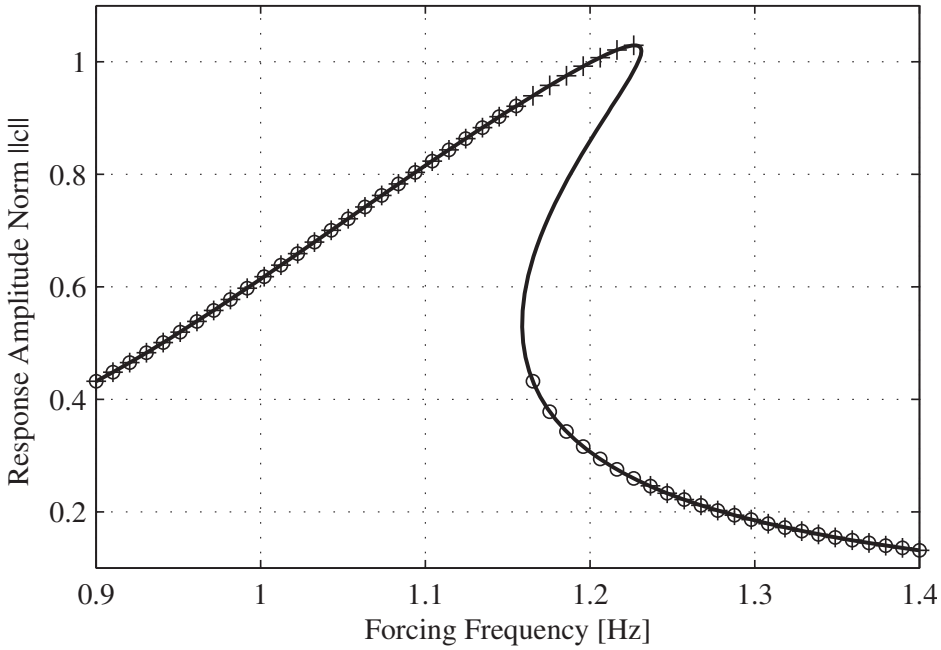

(a) Simulation using Continex and Matlab ODE45.

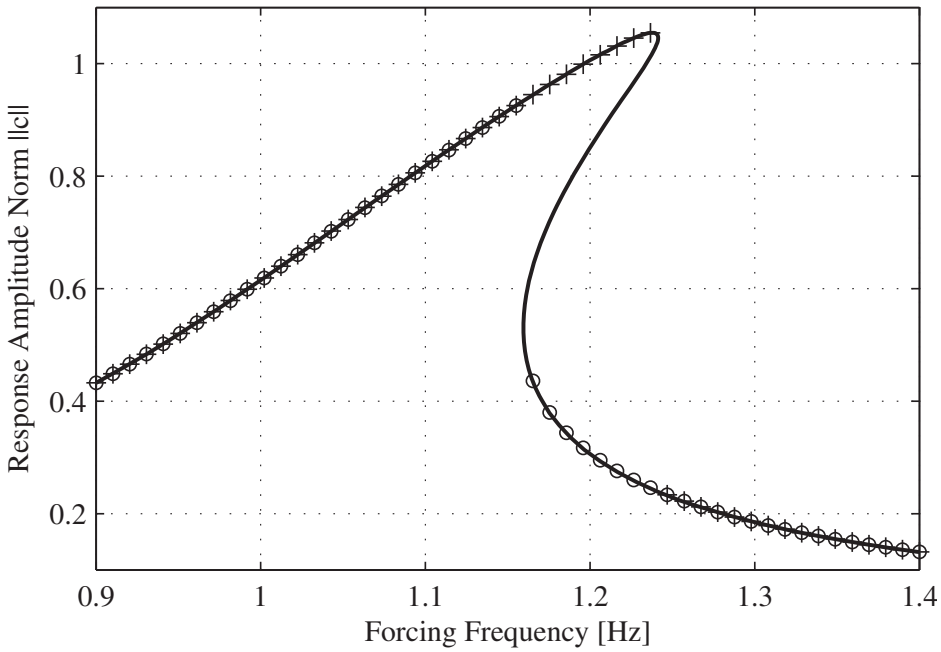

(b) Simulation using Continex and Simulink synchronously.

Figure 6.3: Simulated results for the duffing oscillator with parameters: $q = 5, \beta = 0.05, \omega_0 = 2\pi, \gamma = 25$. Parameter sweep is denoted by (+) for increasing frequency and (o) for decreasing and control-based continuation result is denoted by (—). Control gains was for both cases chosen to $K_p = K_d = -1$. Stability check is omitted.

The electromagnetic actuators used in our test rig (cf. Figure 3.1) serves as a prototype for electromagnet bearings and other nonlinear actuators with no direct contact. This type of actuators are important for rotating machinery, as they can exert a force directly on the rotor while it is operating. Note that control-based continuation does not require large amounts of control energy and that it is not necessary to know the dynamics of the actuator. The use of smart machine elements such as electromagnetic bearings is becoming more common in applications, making the control-based continuation method readily available as a software extension. This will allow in-situ bifurcation analysis and dynamical tests, and since the method uses a stabilizing control it might be possible to overcome instabilities as well as operate in regions where multiple stable and unstable states exist. Additionally, the methods for determining stability makes it possible to safely map out stability boundaries of the uncontrolled system. Finally, the method makes it possible to perform hybrid-tests to investigate how a rotor-system will behave as a part of a simulated structure or during faults, e.g. with an unbalanced impeller.

6.3.1 Simulations for a nonlinear Jeffcott rotor

To investigate the feasibility of applying control-based continuation we construct a simulated experiment. We simulate a simple model of a two degree of freedom Jeffcott rotor with a symmetric cubic nonlinear restoring force presented in [31]. The equations of motion for this model are

$$\begin{aligned} m\ddot{x} + d\dot{x} + kx + \beta(x^2 + y^2)x &= me_d\omega^2 cos\omega t \\ m\ddot{y} + d\dot{y} + ky + \beta(x^2 + y^2)y &= me_d\omega^2 sin\omega t - mg, \end{aligned} \tag{6.6}$$

where m denotes the mass of the rotor disc which is displaced from the geometric center by the eccentricity e_d, d is the damping coefficient, k is the linear stiffness, β is a coefficient of the nonlinearity which for example can account for an aerodynamic coupling, ω is the rotational speed and g is the gravitational acceleration. For simplifying the simulations, we set the gravity to zero $g = 0$, making the model symmetric corresponding to a vertical rotor. The gravitational acceleration g can later be varied to investigate how the asymmetry affects the continuation and the bifurcation diagram. Since the x and y-directions are coupled, it might be possible to affect both directions applying control in only one of the directions. This allows to perform bifurcation analysis in each direction independently. It is possible to constitute a control in both directions and perform continuation in multiple parameters, but for simplicity we restrict ourself to the simple single-input-single-output (SISO) case. We add the non-invasive PD-control signal to the x-direction direction and perform a simulated control-based continuation experiment in that

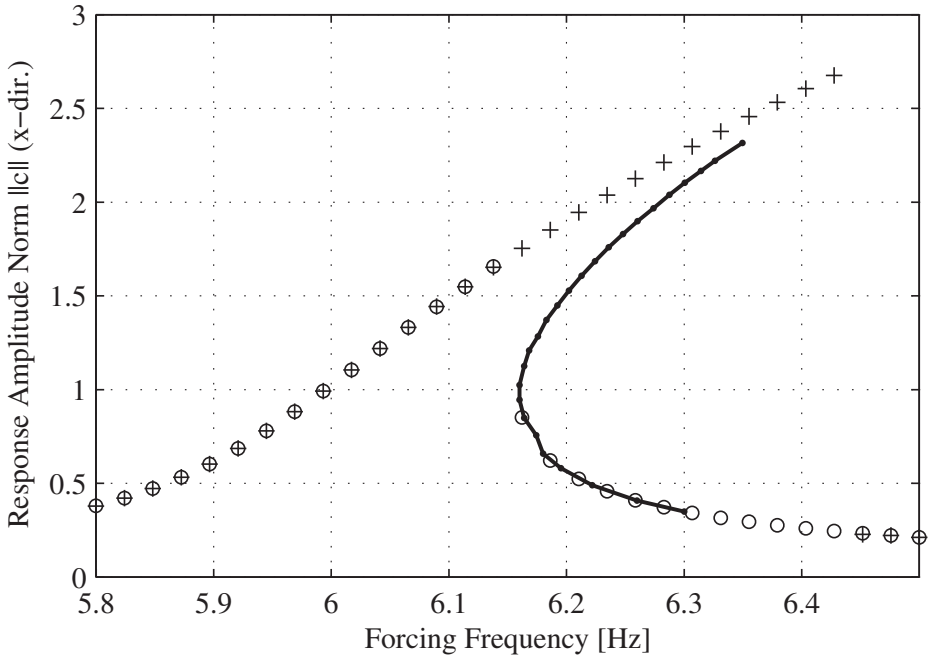

Figure 6.4: Continex Simulation of the nonlinear Jeffcott rotor. Model parameters: $m = 0.7, k = 1000, d = 0.7, \beta = 20, e_d = 1.2, g = 0$. Control-gains: $K_p = -12.5, K_d = 125$.

direction using the synchronous Continex model. Adding the control signal directly to the equations of motion simplifies the problem by assuming an ideal control actuator, but this is sufficient for proof of concept.

The result of a parameter-sweep and a continuation in the x-direction (starting at 6.3 Hz) are shown in Figure 6.4. The results of parameter sweep and continuation are in good agreement and the control is able to non-invasively stabilize most of the unstable equilibria along the response curve, making it possible for the continuation to track it. The continuation is observed to fail along the unstable equilibrium branch, because the controller at this point fails to stabilize the equilibrium states. In order to overcome this limitation, and compute the full frequency-response, one must perform a tuning of the control and continuation parameters as explained in Chapter 4. Nevertheless, the results are sufficient to indicate both the feasibility and usefulness of applying control-based continuation to a rotor dynamic experiment.

7 Conclusion

7.1 Summary and discussion

The work comprising this thesis is focused on implementing and developing techniques for performing experimental bifurcation analysis of nonlinear dynamical systems. The work has been centered around the newly developed control-based continuation method, and we show how to apply this method to track stable and unstable frequency response curves for a harmonically forced impact oscillator. An effort has been made to make the method available to the mechanical engineering community. Publication [P2] provides a thorough description of the method along with details on how to implement it. Moreover, a software toolbox, by the name Continex, which implements control-based continuation for experiments has been developed. This will be made freely available together with the Matlab continuation-platform COCO from [21]. It will also include examples of simulated control-based continuation experiments that only requires Matlab/Simulink to run.

A prerequisite for applying control-based continuation in an experiment is the constitution of a non-invasive and locally stabilizing control. Since the purpose of control-based continuation is to investigate nonlinear systems for which no good model exist, a method for tuning the control must be purely experimental. We propose a series of experiments that allow to tune a non-invasive control without a-priori study of a model. These experiments are carried out for the impact oscillator with electromagnetic actuators, resulting in a set of optimal control gains and parameters for the continuation method. Using these, we show that it is possible to reliably retrieve complete frequency responses including the unstable part. Some important conclusions are: It is necessary to investigate how well the control performs at an unstable equilibrium state. Secondly, the filtering of high-frequency

noise in the differential term of a PD-controller has a large influence on the control. Furthermore, the choice of parameters in combination with the use of Broyden updates or finite differences, for calculating the Jacobian, has an impact on how well the correction step of the continuation performs.

It is possible to assess stability of equilibrium states during control-based continuation by modifying or momentarily turning off the control. Three different methods for determining the stability have been proposed and successfully applied to determine stability during experimental continuation. Each method has advantages and drawbacks and they are suitable in different situations. The free flight stability check is robust and easy to implement, but requires the divergence to be completely reversible by the control. The deadband control method allows to check stability while only allowing minimal divergence, but it does not provide information about the rate of divergence. Finally the deadband-limited free flight method can provide an estimate of the finite-time Lyapunov exponent, while only allowing a limited divergence. In turn the method puts more requirements on the experiment, is more difficult to implement and has more parameters that needs to be tuned.

In conclusion we have shown how it is possible to reliably produce (and reproduce) complete frequency response diagrams with indication of stability. Frequency responses for both the primary resonance and a 1:3 subharmonic resonance have been tracked for the impact oscillator. The time necessary for tracking a frequency response for our test rig is approximately one hour and of the same order as a parameter sweep with fine resolution. One reason for this is that the addition of control causes a shorter transient period. Furthermore, the results from experimental continuation are statistically weighted and ensured to be correct to the order of the convergence criteria of the corrector algorithm.

The framework for performing simulated control-based continuation experiments has been developed and will be included with Continex. The simulations use either Matlab's ODE-solver or a Simulink model similar to the one used when applying the method to experiments. This allows to test experiment designs, actuators and tune the control before going to the laboratory. Most importantly running a simulated experiment gives valuable insight in how the method and Continex works, which will hopefully help to make the method more widely used in the field of experimental mechanics.

7.2 Future work

The control-based continuation method is in its infancy, but with that being said, the method has shown to work well and reliable for suitable experiments. There is still much work in making the method reliable for a broader range of experiments as well as making it more robust and user-friendly.

Two concepts from numerical continuation, namely bifurcation detection and branch switching, still needs to be implemented. By applying so-called test-functions, it is possible to detect bifurcation points and determine the type of bifurcation. Knowing the type of bifurcation, it is possible to automatically continue the equilibrium paths branching out from the bifurcation point. Constructing such test functions relies on the ability to determine stability during continuation.

The proposed method for experimentally tuning the control may be further developed to construct an auto-tuning control. For simpler types of actuators it might also be possible to apply an adaptive control. For experiments that cannot be allowed to be run close to their stability boundary, it might be possible to modify the tuning method to accomodate it. One simple idea could be to monitor the divergence while testing sets of control-gains and parameters, and as soon as the divergence exceeds a certain level the control parameters are substituted with ones that are guaranteed to stabilize the equilibrium state.

Another point of improvement could be to extend the quantification of stability in terms of finite-time Lyapunov exponents to stable equilibrium states. This could be done by applying a perturbation and measuring how fast transients settle. Unfortunately, for most stable equilibrium states in our test rig, the transients settle within few oscillations, not giving enough data for our estimation method. This problem might be overcome by implementing a fitting method that makes better use of the recorded data.

There are many application for the control-based method, but one particularly interesting is in rotating machinery. In this area nonlinear phenomena are frequently encountered and for rotors with smart machine elements, such as electromagnetic bearings, the necessary hardware for sensing and actuation is already present. Section 6.3 discuss and investigate the feasibility of applying the method to rotor dynamic experiments, but the task of testing this in a real experiment remains.

Finally, an interesting perspective of the method is that it might help overcome delay induced instability when performing hybrid testing, as reported in [14]. Hybrid testing is an interesting technique which combines real time experiments with computer simulations. The method has big potential and many applications, so a

natural next step in the research would be to put the method proposed in [14] to test in a real experiment.

Bibliography

[P1] E. Bureau, F. Schilder, I. F. Santos, J. J. Thomsen, and J. Starke. Experimental bifurcation analysis for a driven nonlinear flexible pendulum using control-based continuation. In *7th European Nonlinear Dynamics Conference*, 2011.

[P2] E. Bureau, I. F. Santos, J. J. Thomsen, F. Schilder, and J. Starke. Experimental bifurcation analysis of an impact oscillator - tuning a non-invasive control scheme. *Journal of Sound and Vibration*, 332(22):5883–5897, 2013.

[P3] E. Bureau, I. F. Santos, J. J. Thomsen, F. Schilder, and J. Starke. Experimental Bifurcation Analysis By Control-based Continuation - Determining Stability. In *Proceedings of the ASME 2012 International Design Engineering Technical Conferences & Computers and Information in Engineering Conference*, 2012.

[P4] E. Bureau, F. Schilder, M. Elmegård, I. F. Santos, J. J. Thomsen, and J. Starke. Experimental bifurcation analysis of an impact oscillator - determining stability. *Accepted for publication in: Journal of Sound and Vibration*, January 2014.

[P5] E. Bureau, F. Schilder, I. F. Santos, J. J. Thomsen, and J. Starke. Experiments in nonlinear dynamics using control-based continuation: Tracking stable and unstable response curves. In *8th European Nonlinear Dynamics Conference*, 2014.

[P6] F. Schilder, E. Bureau, J. Starke, H. Dankowicz, and J. Sieber. A Matlab Continuation Toolbox for Response Tracking in Experiments. In *7th European Nonlinear Dynamics Conference*, 2011.

[P7] F. Schilder, E. Bureau, I. F. Santos, J. J. Thomsen, and J. Starke. Continex: A toolbox for continuation in experiments. In *8th European Nonlinear Dynamics Conference*, 2014.

[8] K. Pyragas. Continuous control of chaos by self-controlling feedback. *Physics Letters A*, 170(6):421 – 428, 1992.

[9] E. Ott, C. Grebogi, and J. A. Yorke. Controlling chaos. *Phys. Rev. Lett.*, 64: 1196–1199, Mar 1990.

[10] M. A. Savi, F. H. I. Pereira-Pinto, and A. M. Ferreira. Chaos control in mechanical systems. *Shock and Vibration*, 13(4):301–314, 2006.

[11] J. Sieber and B. Krauskopf. Control based bifurcation analysis for experiments. *Nonlinear Dynamics*, 51(3):365–377, 2008.

[12] R. Seydel. *Practical bifurcation and stability analysis*. Springer, 2010.

[13] E. J. Doedel. Lecture Notes on Numerical Analysis of Nonlinear Equations. In B. Krauskopf, H. M. Osinga, and J. Galán-Vioque, editors, *Numerical continuation methods for dynamical systems*, pages 1–49. Springer Netherlands, 2007.

[14] J. Sieber and B. Krauskopf. Tracking oscillations in the presence of delay-induced essential instability. *journal of sound and vibration*, pages 781–795, 2007.

[15] J. Sieber, A. Gonzalez-Buelga, S. Neild, D. Wagg, and B. Krauskopf. Experimental Continuation of Periodic Orbits through a Fold. *Physical Review Letters*, 100:244101, 2008.

[16] B. Krauskopf, D. Wagg, J. Sieber, A. Gonzalez-Buelga, and S. Neild. Control-based continuation of unstable periodic orbits. *Journal of Computational and Nonlinear Dynamics*, 6(1), 2011.

[17] D. Barton and S. Burrow. Numerical continuation in a physical experiment: investigation of a nonlinear energy harvester. *ASME Journal of Computational and Nonlinear Dynamics*, 6(1):011010, 2011.

[18] D. Barton, B. Mann, and S. Burrow. Control-based continuation for investigating nonlinear experiments. *Journal of Vibration and Control*, 18(4):509–520, 2012.

[19] D. A. W. Barton and J. Sieber. Systematic experimental exploration of bifurcations with noninvasive control. *Physical Review E*, 87(5):052916, May 2013.

[20] C. G. Broyden. A class of methods for solving nonlinear simultaneous equations. *Mathematics Of Computation*, 19(92):577–593, 1965.

[21] H. Dankowicz and F. Schilder. Coco - continuation core and toolboxes. http://sourceforge.net/projects/cocotools/, January 2014.

[22] H. Dankowicz and F. Schilder. An extended continuation problem for bifurcation analysis in the presence of constraints. *Journal of Computational and Nonlinear Dynamics*, 6(3):031003, 2011.

[23] H. Dankowicz and F. Schilder. *Recipes for continuation*, volume 11 of *Computational Science & Engineering*. Society for Industrial and Applied Mathematics (SIAM), 2013.

[24] Y. Uchiyama, M. Mukai, and M. Fujita. Robust control of electrodynamic shaker with 2dof control using formula not shown filter. *journal of sound and vibration*, 326(1-2):75–87, 2009.

[25] J. Ziegler and N. Nichols. optimum settings for automatic controllers. *journal of dynamic systems measurement and control-transactions of the asme*, 115 (2B):220–222, 1993.

[26] F. Haugen. Basic dynamics and control. *TechTeach (http://techteach.no)*, 2010.

[27] R. D. Cook. Detection of influential observation in linear regression. *Technometrics*, 42(1):65–68, 2000.

[28] J. J. Thomsen. *Vibrations and stability: advanced theory, analysis, and tools*. Springer, 2003.

[29] B. Balachandran and T. Kalmár-Nagy. Forced harmonic vibration of a duffing oscillator with linear viscous damping. *Duffing Equation: Nonlinear Oscillators and Their Behaviour*, pages 139–174, 2011.

[30] F. F. Ehrich. Observations of Nonlinear Phenomena in Rotordynamics. *Journal of System Design and Dynamics*, 2:641–651, 2008.

[31] H. Yabuno, T. Kashimura, T. Inoue, and Y. Ishida. Nonlinear normal modes and primary resonance of horizontally supported jeffcott rotor. *Nonlinear Dynamics*, 66(3):377–387, 2011.

P1 Publication 1

The following paper [P1] was submitted to and presented on the 7th European Nonlinear Oscillations Conferences (ENOC) in Rome, Italy 2011. It presents the framework for making continuation possible in our experiment, and reports on the early stages of the work in developing a systematic and purely experimental method for tuning a non-invasive locally stabilizing control scheme, necessary for control-based continuation.

Experimental bifurcation analysis for a driven nonlinear flexible pendulum using control-based continuation

Emil Bureau*, Frank Schilder **, Ilmar F. Santos*, Jon Juel Thomsen* and Jens Starke **
*Department of Mechanical Engineering, Technical University of Denmark (embu@mek.dtu.dk)
**Department of Mathematics, Technical University of Denmark

Summary. We present a software toolbox that allows to apply continuation methods directly to a controlled lab experiment. This toolbox enables us to systematically explore how stable and unstable steady state periodic vibrations depend on parameters. The toolbox is implemented partly in MATLAB and partly on a dSPACE realtime controller board. Its functionality is tested on a driven mechanical oscillator with a strong impact nonlinearity, controlled with electromagnetic actuators. We show how to tune a controller so that the steady state dynamics of the controlled experiment matches that of the corresponding *un*-controlled experiment.

Introduction

Being able to observe stable as well as unstable steady state responses directly in experiments has many interesting perspectives. It allows to perform bifurcation analysis in experiments for which no good model exist - or helps to validate and improve existing models by comparing them with experimental data for both stable and unstable dynamics. Furthermore, stable branches in bifurcation diagrams might be connected via unstable branches, thus following an unstable branches might reveal otherwise overlooked dynamics, and in the case of multi-stability, conventional parameter sweeps might not detect all stable states.

The recently developed method of *control-based continuation* makes such investigations of both unstable and stable states possible. The method was first introduced in [1] and its application was further developed in [2, 3, 4]. It allows for a direct systematic exploration of the dependency of a physical system on parameters, including tracking unstable vibrations not otherwise observable in the lab. The prerequisites for this method are measurement of the modes of interest (observability) and the possibility to control the system via actuators (controllability). This makes the method immediately applicable to actively controlled machinery, such as rotors supported in active lubricated bearings [5], since all the necessary hardware for sensing, actuation and control is already present.

The focus of our work is the development of a software toolbox that implements experimental bifurcation analysis using an already existing continuation package COCO [6]. The mechanical system that is used for testing the implementation is a driven nonlinear flexible pendulum with hardening spring-stiffness and impact. The test rig design was chosen to be simple but still have sufficiently rich nonlinear dynamic behavior. Since the system shows multi-stability and has a hard impact it is a good example for the usefulness of the method, as these effects are hard to deal with, both for theoretical and experimental approaches. The type of actuators and sensors were chosen because they can be used with rotating machinery, which facilitates the intended transition into more advanced test rigs in the field of rotor dynamics, investigating bearing properties for advanced hybrid bearings.

Methods

Theoretical Background

Continuation packages employ a path-following algorithm to systematically trace curves of steady state dynamic responses under variation of parameters. These curves can then be collected to produce a bifurcation diagram. Typically, path-following methods implement a predictor-corrector scheme. Starting from an initially known dynamical state, the predictor makes a small step in the tangent direction of the response curve. In the correction step the predicted point is used as an initial guess for a nonlinear solver, which is applied perpendicular to the tangent direction and corrects the state back to the curve. In order to apply a continuation package a user must provide some function that implicitly defines the dynamical response of interest, which is straightforward if a model is known.

The method of control-based continuation seeks to apply the continuation technique to a suitably controlled real experiment, making it possible to directly trace out bifurcation diagrams for physical systems. The key idea is to locally stabilize the dynamical equilibrium states of the system without perturbing them. This makes it possible to trace unstable response curves, as well as preventing the system from jumping between stable states in case of multi-stability. In order to use already existing continuation packages, it is necessary to formulate a function, a so called *zero problem*, that enables the continuation algorithm to evaluate and change the controlled experiment. This function must take a control target defining the control force exerted to the experiment as an input argument. Applying the nonlinear solver to the zero problem, convergence must imply that the system is at a *un*-controlled dynamical equilibrium. This requires the control to be *non-invasive*, which means that a control force will only be exerted when the system is *not* at a dynamical equilibrium. This implies that the steady state dynamics of the controlled experiment is identical to the steady state dynamics of the uncontrolled experiment. This idea was first introduced in [7] and later applied to continuation in [1, 2]. This paper will describe how to formulate a zero problem, enabling COCO [6] to perform control-based continuation in experiments.

Particular focus will be on the implementation and tuning of the locally stabilizing non-invasive control scheme.

To make the above conditions more precise, we consider an experiment as a process that runs over time t and depends on a number of parameters μ, and taking a single measurement can be thought of as a function evaluation $y(\mu, t)$. Since we are interested in periodic states we need to sample the experiment over an interval of time covering at least one period. We represent one such sample as a finite sequence of the form

$$Y(\mu, N) = \{y_0, \ldots, y_{N-1}\}, \tag{1}$$

where N denotes the number of sampled points. The measurements are taken with a constant sampling interval h, that is, that the k-th measurement is $y_k = y(t_0 + kh)$, where t_0 denotes the starting time of the measurement. Similarly, we denote a sample of a controlled experiment as

$$Z(\mu, N, u) = \{z_0, \ldots, z_{N-1}\}, \tag{2}$$

where u is a control force applied to the experiment. The control scheme must be chosen to satisfies the following conditions:

1. For zero control the controlled experiment must be identical to the original experiment: $Z(\mu, N, 0) \equiv Y(\mu, N)$.
2. The control scheme must be *locally stabilizing*, that is, any equilibrium state y of Y must become an asymptotically stable equilibrium state of Z. In other words, if a controlled experiment Z is initialized close to a equilibrium state of Y, then the state z must converge to the state y over time.
3. The control must be *non-invasive*, that is, the control force must satisfy the inequality $||u|| \leq \delta||y - z||$.

All these conditions can be satisfied using a PD-Controller G with appropriately chosen gains. Let us express the control signal as

$$u(t) = G(x(t)) := PD(x(t) - z(t)) \tag{3}$$

where $x(t)$ is a predefined control target set by the continuation algorithm, and $z(t)$ is the measurement of the controlled experiment Z taken at time t. Furthermore, we denote a discrete Fourier transform of a sample by

$$c = \mathcal{F}(Y(\mu, N)). \tag{4}$$

Note that the Fourier transform $\mathcal{F}$ and the number of samples N must be chosen such that (4) is independent of the starting time of the measurement frame t_0. Using the above definitions we can now construct a function

$$F(c, \mu; N) := \mathcal{F}\{Z[\mu, N, G(\mathcal{F}^{-1}(c))]\} - c, \tag{5}$$

which can be passed as a zero problem to a standard continuation package. Our control scheme is non-invasive, because (under simplifying assumptions on smoothness and noise)

$$||u|| = ||PD(x - z)|| \leq \delta||x - z|| \leq \delta\kappa||\mathcal{F}(x) - \mathcal{F}(z)|| = \delta\kappa||F(c, \mu; N)|| \tag{6}$$

holds, which implies that the control force vanishes whenever the difference between control target x and measurement z is zero. In the implementation we use $||F(c, \mu; N)|| <$ TOL as a criteria for convergence, and typically TOL can be chosen at the order of the measurement error.

Experimental Setup and Implementation

Figures 1a and 1b show the experimental test rig, which consists of a mechanical system, sensors, actuators and a data acquisition- and control system. The mechanical system comprises a clamped flexible pendulum (1) which, when vibrating with large enough amplitudes, impacts a mechanical stop (2) causing an increase of stiffness. This nonlinearity causes a change of natural frequency with oscillation amplitude, and the appearance of a hysteresis loop when varying the frequency of the external excitation (figure 1c). The pendulum is mounted on a platform (3), which can be moved in the horizontal plane by means of an electromagnetic shaker (4). The displacement of the platform and the displacement of the pendulum is measured using two laser displacement sensors (5). An electromagnetic actuator (6) is mounted on each side of the pendulum mass. Using an amplifier and a power supply, the strength and direction of the magnetic field can be varied using a control signal. Data acquisition and control is realized using a computer equipped with a dSPACE DS1104 board and MATLAB/Simulink.

Figure 2 shows how the communication between different parts of the software is implemented. The tasks that have to be executed in real time run on the dSPACE board, while the continuation core algorithm runs asynchronously on the computer. The real time application generates the excitation signal that is sent to the shaker and constructs the control signal based on the difference between the control target and the measured relative displacement. The control is implemented using a standard MATLAB/Simulink PD-controller block. Communication between the computer and the board

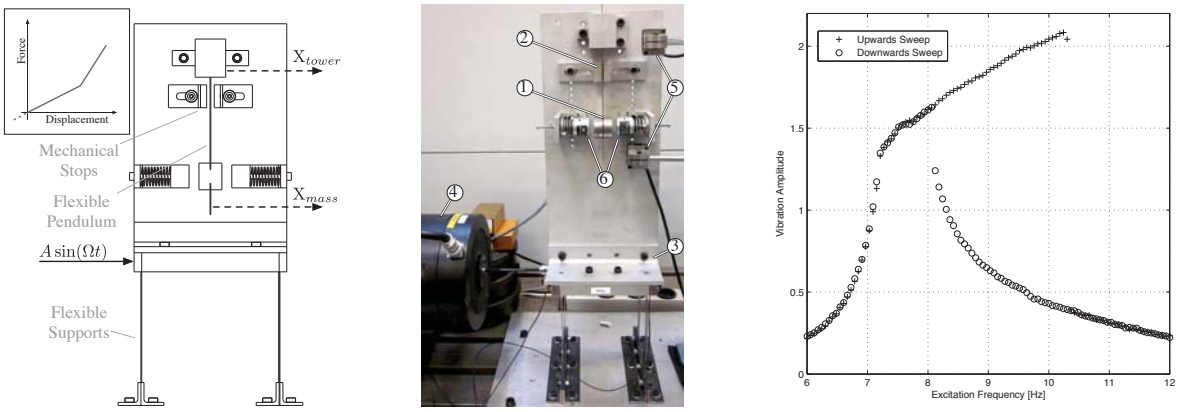

(a) (b) (c)

Figure 1: a) Main elements and input/output of the mechanical system. b) Experimental test rig. c) Frequency response found by frequency-sweep, keeping constant amplitude of the shaker voltage signal.

is achieved by reading and writing coefficients of Fourier modes using the MLIB/MTRACE MATLAB interface libraries provided by dSPACE. On the dSPACE card Simulink blocks are implemented in order to both compose and decompose periodic signals from and to their approximated Fourier coefficients in real time. The computer also runs dSPACE ControlDesk, which is used to monitor different parameters during the experiments.

An important task is the tuning of the gains for the PD-controller. Conventionally the tuning process is performed using a model of the physical system to be controlled. However, since the method presented intends to investigate properties of dynamical systems without models, inherently this approach cannot be used in our experiment. The gains are experimentally adjusted to constitute a control that meets a number of criteria: Firstly the control should never destabilize or disturb the equilibrium states. Secondly the control should be aggressive, meaning that it should have short reaction time and exerting large forces when the state deviates from the control target. This constitutes two competing targets and therefore the goal of the tuning process is to find a suitable compromise between control aggressiveness and non-invasiveness.

Figure 3 shows a number of parameter sweeps made on the control gains. The top row illustrates the level of invasiveness of the control. The results were obtained by measuring a stable steady state response to a certain excitation frequency and then setting this response as control target, while keeping the external excitation and varying the control gains. The plots show the resulting control signal, which for complete non-invasiveness should be zero (as is the case for zero control gains). The bottom row presents a measure for the aggressiveness of the control. A zero control target was chosen in order to keep the pendulum at the down-hanging static equilibrium while disturbing it with a harmonic excitation from the shaker and varying the control gains. The plots show the resulting control error simply being the amplitude of vibration for the pendulum. This can be thought of as the inverse of the aggressiveness. For both cases hysteresis was observed depending on the sweep direction and so, in order to have a conservative estimate, the maximum value is plotted. For both the invasiveness and aggressiveness, high and low plateaus are observed depending on the overall gain G. When choosing an appropriate set of gains one should aim at a low plateau for both conditions.

It is important that the continuation core algorithm can change the frequency of external excitation without causing the

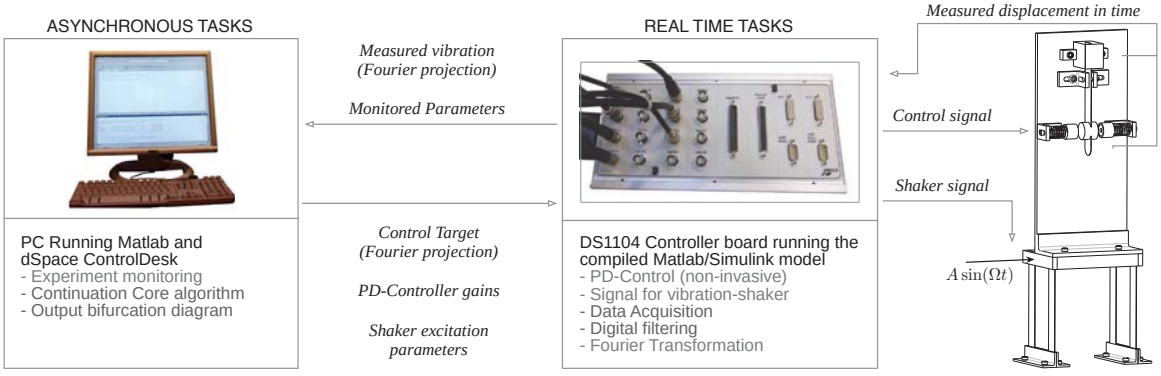

Figure 2: Overview of the communication between different parts of the hardware and software.

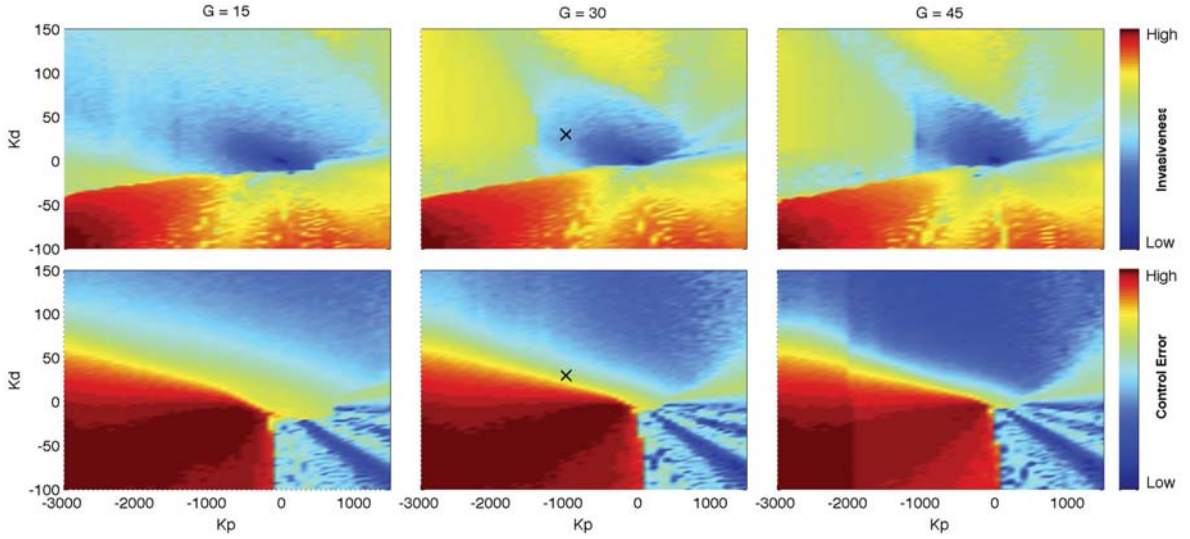

Figure 3: Experimentally obtained parameter sweeps of gains for the PD-Controller for different overall gains G applied to the controller output. K_p denotes proportional gain and K_d denotes differential gain. The top row illustrates the level of invasiveness of the control while the bottom row illustrates the aggressiveness. $\times$ denotes the chosen gain combination for the continuation.

phase of the excitation signal to shift abruptly. Such a jump in the phase might cause unwanted perturbations of the mechanical system. Let us illustrate this: Figure 4a (top) shows an abrupt jump in phase due to two signals with very close frequencies slowly drifting in and out of phase as the experiment time elapses. The phase jump is avoided using a scaled time defined by the differential equation $\dot{\tau} = \omega(t) \Rightarrow \tau = \int_0^t \omega(s)ds$, which is in general not equal to ωt. Even when the frequency is changed discontinuously, the resulting excitation will change continuously, which implies that a phase jump is avoided. The result of implementing the scaled time is shown in Figure 4a (bottom) and the implementation in Simulink is illustrated in Figure 4b.

We use a Fourier transformation applied with a shifted and averaged window function to decompose the buffered measured response into n Fourier modes. Starting from the k^{th} sample, the window $\xi(t_k, w, t)$ of the width w holds one forcing period, that is,. $\xi(t_k, w, t) = 1$ inside and zero elsewhere. A full sampling interval $[0, N]$ of N points can hold $M = N - floor(1/\omega)$ such windows. The number of points in the buffer and the sampling frequency are limited by the available processing power of the dSPACE card, and thus the frequency range that is possible to measure has an upper and a lower bound. These bounds are determined by the number of points stored in the buffer and the sampling rate, because at least one whole period must fit in the buffer $(w \leq N)$ and high frequency oscillations must be sampled with a sufficient number of measurements in order to avoid aliasing. The Fourier coefficients are computed as

$$c_n = \int_{t_0}^{t_0+hN} \psi(t)y(t)\varphi_n(t)dt, \quad \text{where} \quad \psi(t) = \frac{1}{M}\sum_{k=0}^{M-1} \xi(t_k, k, t) \tag{7}$$

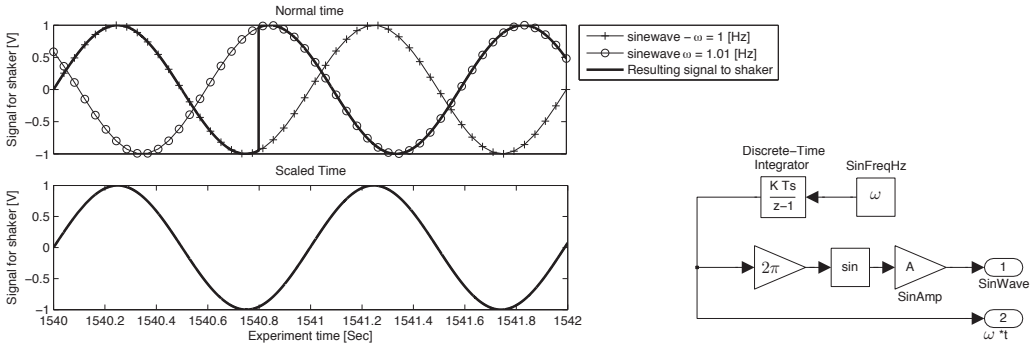

(a) (b)

Figure 4: Example of the phase jump problem and the implemented solution. (a) Shows the effect of incrementing the frequency of excitation by 1% for the system without scaled time (top) and with scaled time (bottom). (b) Shows the Simulink block used for implementing the scaled time.

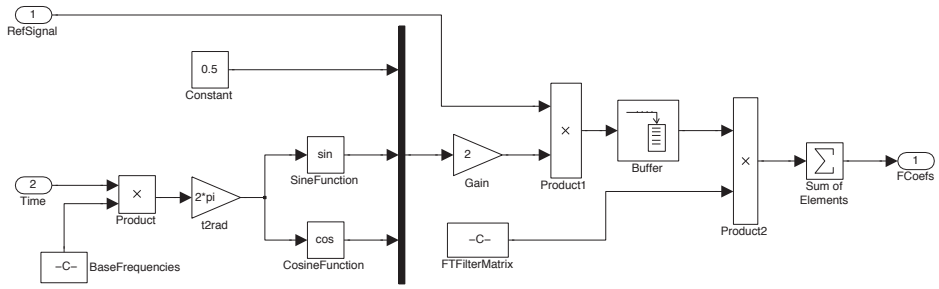

Figure 5: Simulink implementation of Fourier transform with a shifted averaged window.

where $\varphi_n(t)$ denotes the n^{th} Fourier base functions that is projected onto and h is the sampling interval. The Fourier transform is implemented using the block shown in figure 5. Note that the averaged window can be calculated *a priory* and loaded as a matrix into the model.

Results

Figures 6 illustrates the frequency and amplitude responses of the testrig. Figure 6a shows the result of a series of parameter sweeps for the amplitude of the signal sent to the shaker. As expected the response amplitude (calculated as the euclidian norm of the Fourier coefficients) is seen to jump abruptly at the point where the pendulum starts impacting the stops. The amplitude at which the jump occurs is seen to change with the excitation frequency. Finally, for increasing excitation frequencies, hysteresis is seen depending on the sweep direction. Figure 6 shows the result of corresponding series of frequency sweeps. A similar hysteresis behavior is observed for increasing amplitudes, the lowest amplitude essentially represents a linear system, since the amplitude of the pendulum is never sufficient to hit the stops. Note that the sweeps only find stable responses and will not necessarily find all stable responses in case of multiple stability.

Figure 7 shows the frequency response found by a continuation run plotted on top of the corresponding frequency sweep. It should be noted that there is very good agreement between the results obtained by the two methods and that the continuation is able to track the unstable part of the response curve connecting the two stable parts. At high amplitudes (> 1.8) the influence of higher order bending modes seems to become important and quasi periodic dynamics is observed, giving rise to a number of smaller hysteresis loops along the curve. This serves as a good example for the usefulness of the method, as these phenomena would probably not have been captured studying a simple two degree of freedom piecewise linear model of the system. When the system is on a equilibrium state only small amounts of control force are exerted and we also observe that the control is normally seen not to have any low frequency content. Since the method stabilizes unstable states we have no other ways to determine the stability of a current state, than turning off the control and observe if the system diverges from the dynamical state. However, this might both cause damage to the experimental testrig and the available control energy might not be sufficient to return to the branch and resume the continuation run. This presents a problem to be tackled in our future work.

Discussion

A suitably simple controlled experiment with sufficiently rich nonlinear dynamics was set up. A toolbox for using an existing continuation software to track stable and unstable branches of bifurcation diagrams directly in an experiment was

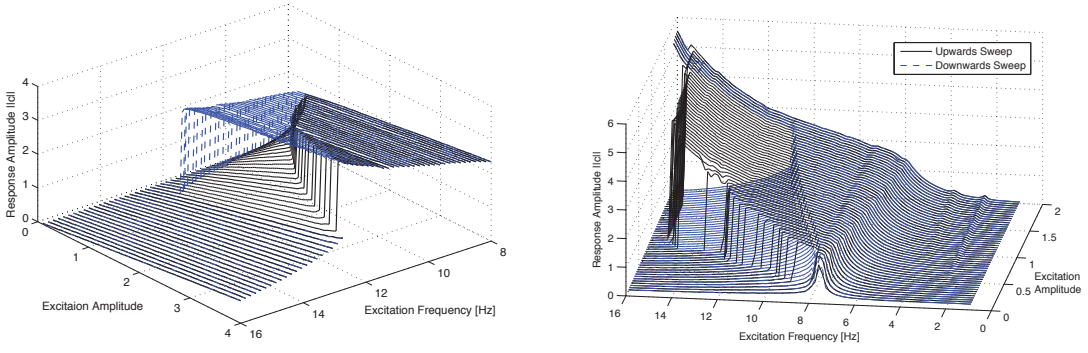

(a) (b)

Figure 6: Experimental steady state response amplitudes recorded by parameter sweeps made by keeping one parameter fixed in steps. a) Amplitude sweep for fixed steps in frequency. b) Frequency sweep for fixed steps in amplitude.

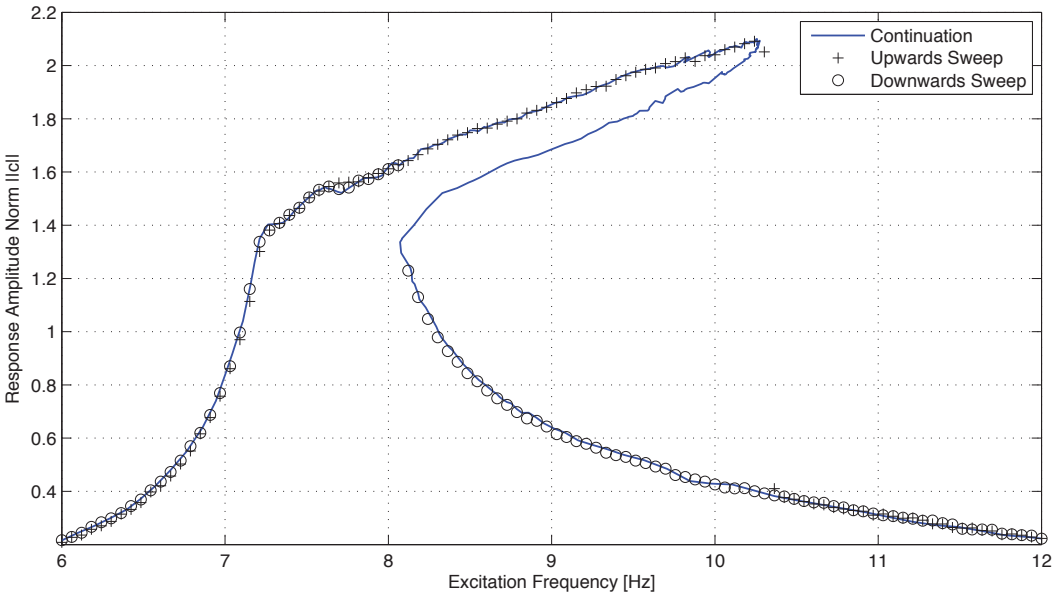

Figure 7: Bifurcation diagram (frequency response) for the driven pendulum observed experimentally by control-based continuation. The whole diagram was traced in one continuous run. The sweep was made for a excitation signal with amplitude, $A = 0.4$.

successfully developed and tested. In order to make the controlled experiment match the steady state dynamics of the corresponding *un*-controlled experiment, a method for tuning locally stabilizing non-invasive control was presented.

Perspectives to be tackled in future work includes; determination of stability, development of auto- or systematic tuning of control-parameters while avoiding unstable control, adaptive control during continuation runs, determination of bifurcation-points and branch switching at such point. Finally we aim at applying the method in the field of rotor dynamics, in order to explore vibrations dependency on properties of active and hybrid bearings, such as active and passive magnetic bearings, actively lubricated bearings and gas foil bearings.

Acknowledgments

This work was funded by the Danish Research Council FTP. The authors wish to thank Jan Sieber, David Barton and Bernd Krauskopf for helpful comments when setting up the experiments.

References

[1] Sieber J. and Krauskopf B. (2008). Control based bifurcation analysis for experiments. *Nonlinear Dynamics*, **51(3)**:365–377.

[2] Barton D.A., Mann B.P. and Burrow S.G. (2010). Control-based continuation for investigating nonlinear experiments. *Journal of Vibration and Control* (Accepted).

[3] Dankowicz, H., Schilder, F. (2011) An Extended Continuation Problem for Bifurcation Analysis in the Presence of Constraints. *Journal of Computational and Nonlinear Dynamics*, **6(2)** (Accepted).

[4] Sieber J., Krauskopf B., Wagg D., Neild S. and Gonzalez-Buelga A. (2011) Control-based continuation of unstable periodic orbits. *Journal of Computational and Nonlinear Dynamics*, **6(1)**:011005–1–9

[5] Santos. I.F. (2009) Trends in controllable oil film bearings. In *IUTAM Symposium on Emerging Trends in Rotor Dynamics* (in print). Springer Verlag.

[6] http://sourceforge.net/projects/cocotools/

[7] Pyragas, K. (1992) Continuous control of chaos by self-controlling feedback. *Physics Letters A*, **170(6)**:421-428.

[8] Sieber J., Gonzalez-Buelga A., Neild S., Wagg D. and Krauskopf B. (2008) Experimental continuation of periodic orbits through a fold. *Physical Review Letters*, **100(24)**:244101–1–4.

P2 Publication 2

The following paper [P2] was published in Journal of Sound and Vibration, Volume 332, Issue 22 on October 28, 2013. It extends the work started in the previous paper by proposing and testing a sequence of experiments for tuning a non-invasive control-scheme that does not require a-prior study of a model. It also contains a detailed description of the control-based continuation method and its implementation, specifically minded for the mechanical engineering community.

Journal of Sound and Vibration 332 (2013) 5883–5897

Contents lists available at SciVerse ScienceDirect

Journal of Sound and Vibration

journal homepage: www.elsevier.com/locate/jsvi

Experimental bifurcation analysis of an impact oscillator—Tuning a non-invasive control scheme

Emil Bureau [a,*], Frank Schilder [b], Ilmar Ferreira Santos [a], Jon Juel Thomsen [a], Jens Starke [b]

[a] Department of Mechanical Engineering, Technical University of Denmark, Denmark
[b] Department of Applied Mathematics and Computer Science, Technical University of Denmark, Denmark

ARTICLE INFO

Article history:
Received 27 November 2012
Received in revised form
8 May 2013
Accepted 20 May 2013
Handling Editor: D.J. Wagg
Available online 10 July 2013

ABSTRACT

We investigate a non-invasive, locally stabilizing control scheme necessary for an experimental bifurcation analysis. Our test-rig comprises a harmonically forced impact oscillator with hardening spring nonlinearity controlled by electromagnetic actuators, and serves as a prototype for electromagnetic bearings and other machinery with build-in actuators. We propose a sequence of experiments that allows one to choose optimal control-gains, filter parameters and settings for a continuation method without a priori study of a model. Depending on the algorithm for estimating the Jacobian required by Newton's method we find two almost disjoint sets of suitable control parameters. Control-based continuation succeeds reliably in producing the full bifurcation diagram including both stable and unstable equilibrium states for an appropriately tuned controller.

1. Introduction

Experimental bifurcation analysis is possible directly in experiments using the control-based continuation method, but it requires an appropriate feedback control. We study a *non-invasive*, *locally stabilizing* proportional-derivative (PD) control scheme, where the control force is generated through nonlinear electromagnetic actuators. Our test-rig comprises an actively controlled impact oscillator, which serves as a prototype for smart machinery with build in sensor and actuation systems. We propose a sequence of experiments that allows one to choose optimal control-gains, filter parameters and settings for a continuation method used for experimental bifurcation analysis of the impact oscillator. A particular requirement of this tuning process is that it does not rely on the availability of a model for the actuators and test-specimen under investigation. Depending on settings for the continuation method, we find two sets of optimal control parameters for which bifurcation analysis employing control-based continuation reliably succeeds in producing the full bifurcation diagram including both stable and unstable equilibrium states.

The method of control-based continuation provides means to explore nonlinear features in experiments, which are not observable with traditional methods like sweeps. An example is coexisting stable and unstable steady-state periodic vibration of a nonlinear oscillator. Comparing the theoretical frequency response of a linear system with an example nonlinear counterpart (Fig. 1a), the response-curve of the nonlinear system bends over to one side, creating a range of frequencies in which two stable and one unstable steady state coexist. Depending on the separation of the response-curves,

* Corresponding author. Tel.: +45 2843 5906.
E-mail address: embu@mek.dtu.dk (E. Bureau).

0022-460X/$ - see front matter © 2013 Elsevier Ltd. All rights reserved.
http://dx.doi.org/10.1016/j.jsv.2013.05.033

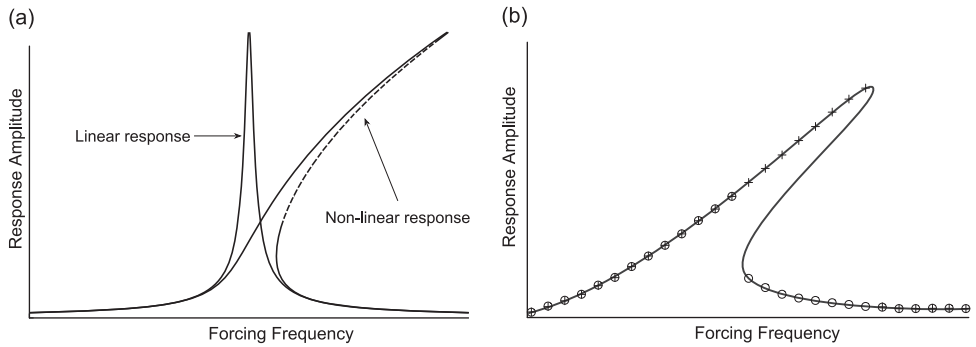

Fig. 1. Panel (a) compares a theoretical linear and nonlinear frequency–response curves with stable (—) and unstable (- - -) steady states. (b) shows how a frequency response can be obtained experimentally by upwards (+) and downwards (○) frequency sweep or by control-based continuation (—).

it might not be possible to initialize the system at a certain desired steady state, nor ensure that the system stays on a certain state. Control-based continuation overcomes these problems by applying a stabilizing feedback-control.

Parameter sweeping is the conventional method for experimental investigation of nonlinear mechanical systems. In a parameter sweep, the system is initialized on a desired steady state and a parameter (e.g. the frequency or amplitude of external excitation) is swept up and down while recording the response. The curve marked by + and ○ in Fig. 1b is the result of such a sweep. If the steps in the sweep parameter are sufficiently small compared with the phase-space separation of the response curves, the system stays on the response curve on which it is initialized as long as there are no bifurcations. Sweeping the parameter both up and down can reveal hysteresis, as is shown in Fig. 1b. However, the method does not allow one to follow unstable periodic motion, which could provide valuable information about the size of the basin of attraction of the stable equilibrium states.

Control-based continuation was developed in [1] and has been successfully applied to experiments in [2–5]. The method consists of applying to the experiment a *non-invasive* and *locally stabilizing* control together with a path-following algorithm. By this we mean a control that modifies the stability of the system without altering the steady states. The contribution of this paper is an experimental and systematic method to tune such a control for a test-rig with unknown dynamics. Fig. 1b compares the parameter-sweep method and control-based continuation. The two methods give similar results for the stable branches, but the continuation method is able to track around the two fold-points and trace out the branch of unstable periodic motion, as it is stabilized by the control.

2. Methods

Experimental bifurcation analysis using control-based continuation can be thought of as a guided experiment. Starting with an equilibrium state of an uncontrolled experiment, a path-following algorithm produces a prediction of a new equilibrium state for a new set of system parameters. A correction algorithm then seeks to modify this prediction such that it again matches with an actual equilibrium state of the uncontrolled experiment. Iterating a series of such prediction and correction steps while constantly applying a stabilizing control allows one to trace a so-called *path* of states irrespective of their stability.

Let us illustrate the basic principle with a simple example: Fig. 2 shows a ball in a landscape with peaks and valleys, representing respectively unstable and stable equilibria for the ball. The task is to roll the ball along the center ridge using a simple algorithm: roll the ball a small distance in the direction tangential to the center ridge (prediction) followed by rolling to the nearest equilibrium position (correction). Since several stable and unstable steady states coexist, the prediction step-length must be small enough not to move the ball onto one of the other equilibria. In case if this happens, the continuation algorithm might follow the equilibrium branch on which the new equilibrium resides. The control is necessary for realizing the state requested by the prediction. The stable state created by the control might be thought of as artificial as the system would never settle there in the absence of control. Furthermore, a non-invasive control-scheme will make the control effort vanish once the ball is exactly on an equilibrium-state for the uncontrolled system. This means that the control is only enabled when the ball starts to roll off the ridge. This keeps the ball on the ridge without altering the steady-state dynamics of the system.

To apply control-based continuation to a test-specimen the experiment must be set up such that a pseudo arc-length continuation algorithm implemented e.g. in COCO [6] or AUTO [7] can be applied to it. This requires the formulation and experimental evaluation of a so-called *zero-problem* and its Jacobian. Furthermore, applying pseudo arc-length continuation to an experiment requires the use of statistical methods since experimentally obtained data are subject to noise and measurement uncertainties. Finally, a non-invasive and locally stabilizing control must be realized. Sections 4.1–4.3 review the fundamentals of pseudo arc-length continuation and how to apply it to experiments.

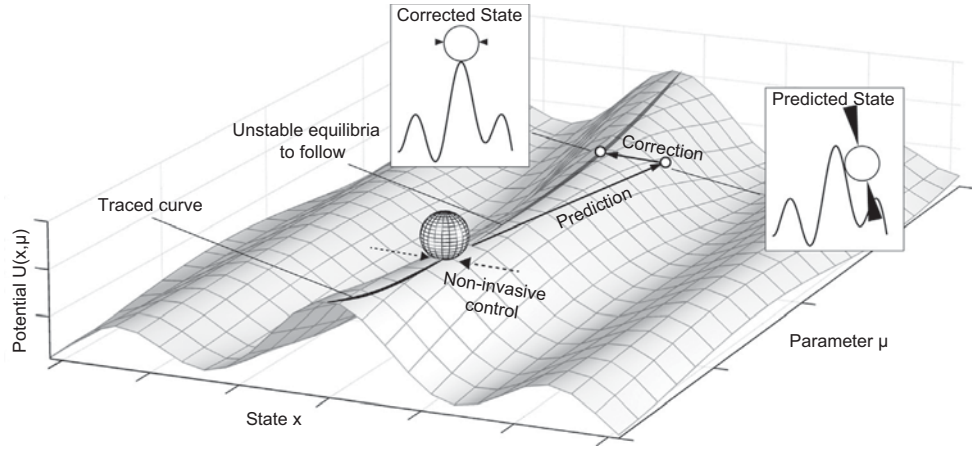

Fig. 2. General illustrative example: non-invasive control and control-based continuation for a ball in a landscape of peaks and valleys. The branch of unstable equilibria created by the center ridge is followed as μ is varied. When the correction step converges to an equilibrium state for the un-controlled system, the control force vanishes.

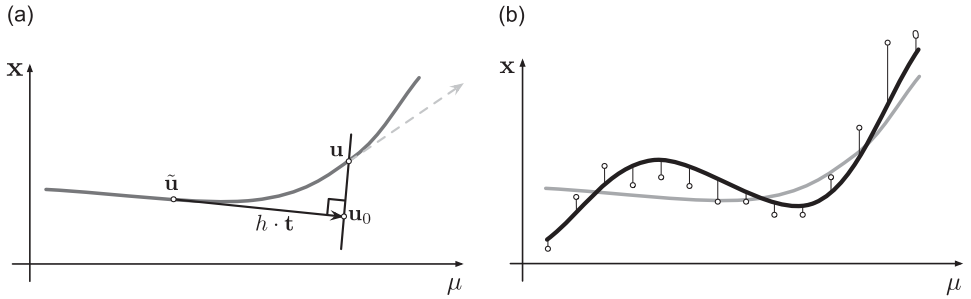

Fig. 3. Basic components of experimental continuation. (a) Pseudo arc-length continuation: from an initial point $\tilde{\mathbf{u}}$ a prediction step of length h is done in a tangent direction $\mathbf{t}$. The predicted point $\mathbf{u}_0$ is then corrected to the point $\mathbf{u}$, using Newton's method in a direction perpendicular to the tangent, after which the whole procedure is repeated. (b) Approximation of noise contaminated measurements. The actual path is shown as (——), but due to noise contamination of the measurements (○) a third-order polynomial fit (——) is used.

2.1. Path following and pseudo arc-length continuation

Consider the system of nonlinear equations, which we will refer to as a *zero problem*

$$\mathbf{F}(\mathbf{x},\mu)=\mathbf{0}, \quad \mathbf{F}:\mathbb{R}^n\times\mathbb{R}\to\mathbb{R}^n, \tag{1}$$

where $\mathbf{x}$ represents an equilibrium state to be determined and μ is a design parameter. If the function $\mathbf{F}$ satisfies the conditions of the implicit function theorem, there exists a function $\mathbf{x}(\mu)$ of solutions in some neighborhood of a known initial solution of (1). In other words, for a given design parameter μ it is possible to compute the corresponding state $\mathbf{x}$.

The idea of pseudo arc-length continuation [8,9] is to consider the equivalent geometrical problem of computing a curve or path $\mathbf{u}(s):=(\mathbf{x}(s),\mu(s))$, with $\mathbf{u}(s)\in\mathbb{R}^n\times\mathbb{R}$, where s refers to a parametrization of this curve, such that

$$\mathbf{F}(\mathbf{u}(s))=\mathbf{F}(\mathbf{x}(s),\mu(s))=\mathbf{0} \tag{2}$$

holds for all s. The algorithm is initialized with some known state $\mathbf{u}(0)=\tilde{\mathbf{u}}=(\tilde{\mathbf{x}},\tilde{\mu})$ and proceeds by predicting a new point $\mathbf{u}_0=\tilde{\mathbf{u}}+h\mathbf{t}$ along the tangent vector $\mathbf{t}$, which will be close to this curve for small enough step sizes h; see Fig. 3a. In the subsequent correction step a root finding algorithm solves for the point $\mathbf{u}$ at the intersection of the solution path and the plane through $\mathbf{u}_0$ and normal to $\mathbf{t}$, which amounts to supplementing (2) with the so-called pseudo arc-length constraint

$$(\tilde{\mathbf{x}}')^{\mathrm{T}}(\mathbf{x}-\tilde{\mathbf{x}})+\tilde{\mu}'(\mu-\tilde{\mu})=h \tag{3}$$

where a prime denotes differentiation with respect to s. This is equivalent to solving Eqs. (2) and (3) simultaneously as

$$\mathbf{H}(\mathbf{u})=\begin{bmatrix}\mathbf{F}(\mathbf{u})\\ (\tilde{\mathbf{u}}')^{\mathrm{T}}(\mathbf{u}-\tilde{\mathbf{u}})-h\end{bmatrix}=\mathbf{0}, \tag{4}$$

where h denotes the (adaptive) step length in s used by a continuation algorithm.

A typical implementation uses Newton's method for correcting the predicted solution $\mathbf{u}_0$ to the corrected solution $\mathbf{u}$. The sequence of Newton steps is given by

$$\mathbf{u}_{i+1} = \mathbf{u}_i - \mathbf{J}(\mathbf{u}_i)^{-1}\mathbf{H}(\mathbf{u}_i), \quad i = 1, 2, \ldots, \tag{5}$$

where $\mathbf{J}$ is the Jacobian

$$\mathbf{J} = \mathbf{H}_{\mathbf{u}} = \begin{bmatrix} \mathbf{F}_{\mathbf{u}} \\ \tilde{\mathbf{u}}' \end{bmatrix} = \begin{bmatrix} \mathbf{F}_{\mathbf{x}} & \mathbf{F}_{\mu} \\ (\tilde{\mathbf{x}}')^{\mathrm{T}} & \tilde{\mu}' \end{bmatrix} \tag{6}$$

and $\mathbf{F}_{\mathbf{u}}$, $\mathbf{F}_{\mathbf{x}}$ and $\mathbf{F}_{\mu}$ denote the partial derivatives with respect to $\mathbf{u}$, $\mathbf{x}$ and μ, respectively. After successful correction this process repeats with a new prediction step along the new tangent direction $\mathbf{t}$. For the k-th iteration we have the update formula

$$\mathbf{J}(\mathbf{u}_k) \cdot \mathbf{t} = \begin{bmatrix} \mathbf{0} \\ 1 \end{bmatrix} \tag{7}$$

for the new tangent vector.

As this brief review illustrates, for applying a path-following algorithm we at least need to construct a system of nonlinear equations $\mathbf{F}$, the solutions of which represent the state of an experiment, and possibly their derivatives with respect to the state vector and the design parameters. The derivatives with respect to arc-length can be computed from this data using (7). A more detailed explanation of the pseudo arc-length continuation can be found for example in [10].

2.2. Approximation of noisy paths

While it is possible to apply pseudo arc-length continuation to a set of equations defining a smooth path, dealing with experimentally obtained data presents difficulties, as the data will be subject to noise and measurement uncertainties. Therefore, it is necessary to use statistical methods to ensure that the correct path is followed. Here, we sample several points and use least-squares approximation as illustrated in Fig. 3b, where pseudo arc-length continuation of a smooth path is compared with a least-squares approximation of a path defined by noise contaminated sampled points. In the present implementation we fit a user-defined number of sample points to a third-order polynomial, in our experiment observations suggest that 15–20 points are sufficient. Another difference to standard pseudo arc-length continuation as described in the previous section is that instead of solving Eq. (7) to obtain an updated tangent, we use the tangent of the approximation polynomial at the end point of the path. A trade-off of this modification is that measuring a larger number of points per continuation step will give (statistically) more accurate results, while the time for obtaining a bifurcation diagram increases. It is important to highlight that the time for data acquisition is the dominant contribution to the overall run time.

2.3. Control based continuation

Consider an experiment Y running over time t and depending on a parameter μ. Making a single measurement can be thought of as evaluating a function $y(\mu, t)$. Since we are interested in time periodic equilibrium states,[1] several periods of experimental data need to be sampled. We represent one such measurement as a finite sequence of the form

$$Y(\mu, N) = \{y_0, \ldots, y_{N-1}\}, \tag{8}$$

where N denotes the number of sampled points taken with a constant sampling increment. For experimental continuation, we construct a suitably controlled experiment

$$Z_{u_c}(\mu, N, x) = \{z_0, \ldots, z_{N-1}\}, \tag{9}$$

where $u_c = u_c(t)$ denotes a control signal, and $x = x(t)$ is a reference trajectory provided by the continuation algorithm; see Fig. 5. The controller and the controlled experiment must satisfy a number of conditions:

1. The controlled experiment must be *consistent*, that is, for zero control $Z_0 \equiv Y$ holds and the controlled experiment Z_{u_c} converges uniformly to the *un*-controlled experiment as $u_c \to 0$.
2. The control must be *locally stabilizing*, meaning that any equilibrium state of Y (stable or unstable) must become an asymptotically stable equilibrium state of Z_{u_c}.
3. The control must be *non-invasive*, that is, the control-signal u_c must vanish whenever the requested state x is a equilibrium state of the *un*-controlled experiment.

The first condition requires the control actuator not to alter the dynamics of the system when the control signal is zero. Many actuators, e.g. servo-motors and hydraulic actuators, add inertia, stiffness and damping to the system and, hence, are

[1] By this we mean the so-called ω−limit set, i.e. the state approached when transients due to initial conditions has decayed (in mathematical models corresponding to particular solution of the differential equation of motion). For periodic/quasi-periodic motions in particular, the stationary state can be characterized simply by the stationary value of amplitude(s) and phase(s).

likely to violate this requirement. Another workaround is to add the control force to the external excitation force as in [2]. The second requirement makes it possible to observe unstable equilibrium states and distinguish coexisting steady states as long as they are sufficiently separated in phase-space compared to the accuracy of measurements and control. The third condition is satisfied by controllers that generate a control signal that is bounded by the difference between the reference trajectory and the measurement of the controlled experiment

$$\|u_c\| \leq \delta \|x - z\|, \tag{10}$$

which corresponds to Lipschitz continuity with appropriately chosen norms. Linear control, for example, PD control, will satisfy this requirement.

A control-scheme for experimental continuation should satisfy all the above conditions and seek to minimize the difference between the requested reference trajectory and the current state of the system. We accomplish this by using a PD control, G, with appropriately chosen gains K_p and K_d. The control signal $u_c(t)$ is thus expressed as

$$u_c(t) = G(x(t), z(t)) := K_p(x(t) - z(t)) + K_d(\dot{x}(t) - \dot{z}(t)), \tag{11}$$

where $z(t)$ is the measurement of the controlled experiment taken at time t. For the control signal (11) to satisfy (10) a low-pass filter must be applied in order to ensure that the time-derivative $\dot{z}(t)$ of the measurements is well-behaved. This filter must balance the two competing targets of removing high-frequency noise while not making the control too slow.

Denoting the discrete Fourier transform of a sequence by $\mathcal{F}_Q$, where Q is the number of Fourier-modes that is projected onto, the Fourier-projection of the reference trajectory is given by

$$c = \mathcal{F}_Q(x). \tag{12}$$

Using this, it is possible to formulate a zero-problem

$$F(c, \mu; N) := \mathcal{F}_Q(Z_{u_c}(\mu, N, \mathcal{F}_\infty^{-1}(c))) - c = 0, \tag{13}$$

which compares the Fourier coefficients of a settled response Z_{u_c} (discarding transients) with those of the reference trajectory c. The correction-step of the continuation algorithm seeks to minimize the difference between reference trajectory and current response by changing the reference-trajectory and parameters μ. When the difference between the Fourier coefficients of the reference trajectory and those of the measured response, and the change in parameters $\mu - \mu_0$ between two iterations are below a certain tolerance, we assume that the correction has converged and that the reference trajectory is an approximation of a periodic equilibrium state of the *un*-controlled system. Typically the tolerance for this convergence criterion can be chosen to be of the same order as the noise-level. Appendix A presents a sketch of a proof that these convergence criteria implies vanishing control as long as a sufficient number of modes Q are used in the Fourier transform.

2.4. Experimental evaluation of the Jacobian

The correction step relies on the (experimental) evaluation of the Jacobian defined in (6). One can approximate the upper part using either Broyden's method [11] or a finite difference formula, while the lower part is explicitly available in the continuation code. Broyden's update for the Jacobian[2] of the i-th (correction) iteration is

$$\mathbf{J}_i = \mathbf{J}_{i-1} + \frac{\Delta \mathbf{F}_i - \mathbf{J}_{i-1} \Delta \mathbf{u}_i}{\|\Delta \mathbf{u}_i\|^2} \Delta \mathbf{u}_n^T. \tag{14}$$

Broyden's update requires only one measurement and is therefore very efficient. Due to noise in the measurements, Broyden's updates are sometimes not accurate enough to ensure convergence. Therefore, we recompute a finite difference approximation of the Jacobian from time to time, which requires at least $2Q+2$ measurements. In the experiment this is implemented by perturbing the different input parameters and variables one by one and recording the response, where the size of the perturbation is chosen to be greater than 10 times the noise level.

3. Experimental setup

3.1. Hardware

The experimental test-rig is depicted in Fig. 4; it comprises a flexible beam with a concentrated tip mass, which can be harmonically forced transversally by means of an electromagnetic shaker (B&K type 4809). When the vibration-amplitude of the beam exceeds a certain value, it starts to impact the mechanical stops, which causes a sudden increase in stiffness, effectively creating a hardening nonlinearity. The shaker is not feedback controlled, which means that the amplitude of the exerted displacement varies nonlinearly with the forcing frequency due to back-coupling of vibrations from the impactor to

[2] Even though the Jacobian $\mathbf{J}$ is not a square matrix ($\mathbf{u}$ has more elements than $\mathbf{F}$), Broyden's update can still be computed since the dimensions of the last term in (14) are $(([m \times 1] - [m \times n][n \times 1])/[1 \times 1])[1 \times n] = [m \times 1][1 \times n] = [m \times n]$.

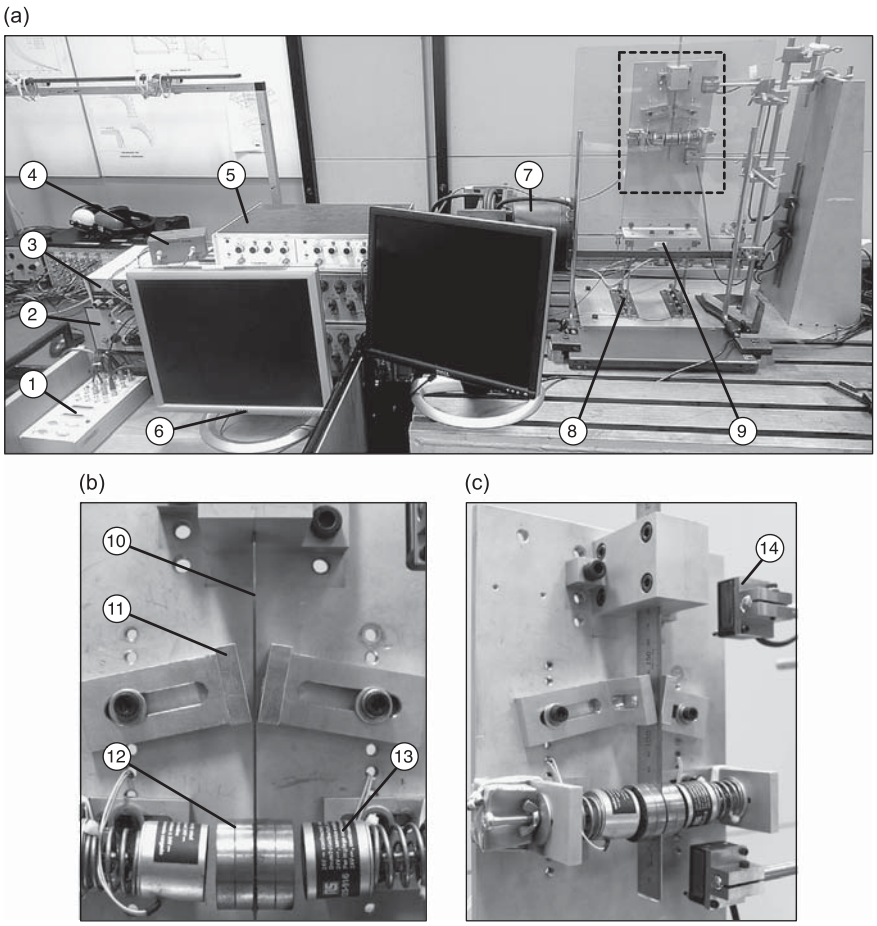

Fig. 4. Experimental test rig: (1) DSpace DS1104 board for data-acquisition and real-time control, (2) amplifier and power-supply for shaker, (3) power supply for electromagnets, (4) amplifier for electromagnets, (5) analog signal-filters and conditioners, (6) computer running DSpace control-desk, Matlab and Matlab/Simulink, (7) electromagnetic shaker, (8) flexible supporting legs, allowing movement only in one horizontal direction, (9) platform, (10) flexible beam, (11) adjustable mechanical stops, (12) beam tip mass, (13) electromagnetic actuators, (14) laser displacement sensors. (a) Overview of the experimental test rig. (b) Impactor front view. (c) Impactor side view.

the shaker. In consequence, we measure the coupled response of the shaker, platform and impactor as a function of the signal being sent to the shaker. Similar mechanical systems have been studied in [12–14].

A control-force can be exerted directly on the tip mass by means of two electromagnetic actuators. The displacements of the platform and the tip mass of the impactor are measured by two OmronZX-LD40 laser displacement sensors. Data acquisition and the generation of the shaker- and control-signal are performed by a computer running Matlab, Simulink and DSpace Control Desk. The electromagnetic actuators are suitable for realizing non-invasive control since they do not add damping or inertia to the impactor itself as they have no direct mechanical contact with the tip mass. Due to the use of a steel tip mass it is only possible to exert pulling forces with our electromagnetic actuators. Therefore, the direction of the control force is varied by sending the signal through an amplifier to either one of the two electromagnets, depending on the polarity of the control-signal. It is important to note that the control-force depends nonlinearly on both the control-signal and the distance to the mass. As a consequence, the control might exhibit hysteresis and multi-stability for certain control-parameter.

3.2. Simulink implementation

Fig. 5 shows a simplified sketch of the experimental setup and the real-time application, which is programmed in Simulink and then compiled and uploaded to run on the DSpace board. The computer which is executing the continuation algorithm runs asynchronously to the experiment, and communication occurs only to change forcing parameters (amplitude and frequency), set a new reference trajectory and read Fourier coefficients of the current state. Since several parameters in the real-time application and continuation code can be modified at run time, it is possible to sweep control and filter parameters, as well as adjust parameters in the continuation code, such as continuation step-size and settings for the correction.

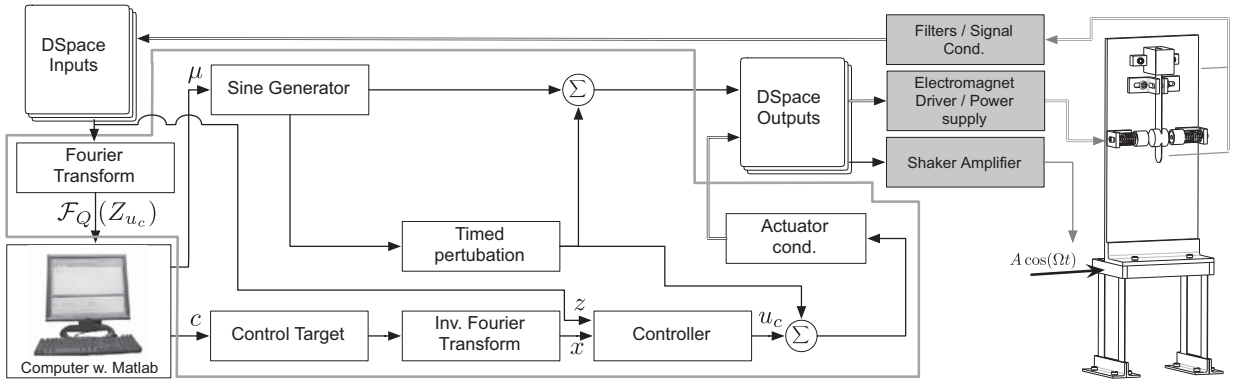

Fig. 5. Simplified Simulink model and its interaction with the continuation code and experiment.

Several re-scalings of signals are applied inside the real-time application (Fig. 5) to make the measured signals be of the same order as the parameters. This is necessary in order to make their relative errors comparable when checking for convergence of the correction-algorithm as described in Section 2.3. The applied rescaling in turn makes the control-gains and filter-coefficients dimensionless.

3.2.1. PD controller

The control strategy described by (11) is implemented in the model using the standard Simulink PD-block. As shown in Fig. 5 the controller is designed to eliminate the difference between reference trajectory $x(t)$, set in the code as the inverse Fourier transform of the control target c, and the current measured trajectory $z(t)$. In addition to the proportional and derivative gains (K_p,K_d), a low-pass filter is used in the differential term of the controller to avoid amplification of high-frequency noise. The pole location and, hence, the cut-off frequency of the filter is controlled by the parameter PDFC.[3] The output of the PD-block is scaled by an overall gain, CFGain, which can also be varied.

3.2.2. Smooth parameter ramping

It is important that the forcing signal sent to the shaker changes smoothly in time when the forcing parameters are updated, so that unwanted perturbations are avoided. When using the standard sine-block in Simulink to create the shaker signal, a change in the excitation frequency can cause a phase jump, as illustrated in Fig. 6. This is because two sine-waves with very close frequencies will slowly drift in and out of phase as experiment time elapses. Sending the signal depicted in Fig. 6 to the shaker would cause a perturbation that could result in the system settling onto a different steady state. The phase-jump can be avoided by using a scaled time defined by $\dot{\tau} = \omega(t) \Rightarrow \tau = \int_0^t \omega(s)\, ds$, since the integration will smoothen out any discontinuous changes to the frequency ω.

3.2.3. Timed perturbation

The real-time application (Fig. 5) also includes a 'Timed Perturbation' block, which is used to create a perturbation with the shaker and magnets. Fig. 7 shows the perturbation signal, which is constructed from a sine-wave at the resonant-frequency of 7.5 Hz multiplied with an envelope function. The multiplicative envelope ensures that the signal sent to the shaker is continuous. The timed perturbation is used during control-gain sweeps as the control (due to the nonlinear actuators) is observed to be multi-stable for certain choices of control-parameters. After changing control-parameters, the perturbation-signal is applied to the control and forcing signal in order to verify that the control is in fact stabilizing, even under large perturbations.

3.2.4. Fourier transformation

We communicate dynamical states between the continuation code and the real-time application by passing Fourier coefficients. The transform c of a signal $y(t)$ consisting of N sampled points recorded with the interval h computed as

$$c_n = \int_{\tau_0}^{\tau_0+hN} y(\tau)\varphi_n(\tau)\psi(\tau)\, d\tau, \quad n = 0, \ldots, 2Q. \tag{15}$$

Here

$$\varphi_n(\tau) = \begin{cases} 1, & n = 0, \\ 2\sin(n\tau), & 1 \le n \le Q, \\ 2\cos((n-Q)\tau), & Q+1 \le n \le 2Q, \end{cases} \tag{16}$$

[3] PDFC corresponds to the parameter N in the standard Matlab/Simulink PD-control block (w. forward Euler and discrete time integration).

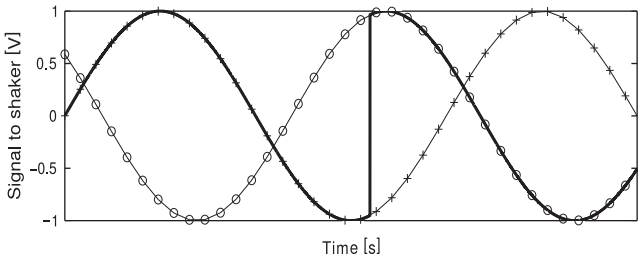

Fig. 6. Illustration of phase jumps when changing excitation frequency. Time-series of a 1 Hz (+) and 1.01 Hz sine-wave (○) slowly drifting in and out of phase: a small change in frequency can result in the non-smooth signal (−) being sent to the shaker.

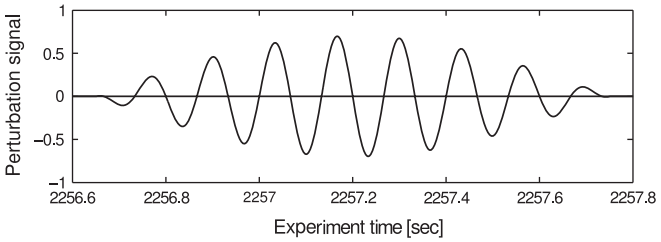

Fig. 7. Perturbation signal, which can be added to shaker and control signal. The perturbation is constructed of a sine-wave of 7.5 Hz multiplied by an (half-sine) envelope function.

is the n-th Fourier base-function that is projected onto, Q is the number of Fourier-modes used in the projection and $\psi(t)$ is a weight function, which is calculated as the shifted average

$$\psi(t) = \frac{1}{M}\sum_{k=0}^{M-1} \xi(t_k, k, t), \tag{17}$$

where

$$\xi(t_k, w, t) := \begin{cases} 1 & \text{for} \quad t_k \le t \le t_{k+w}, \\ 0 & \text{else}, \end{cases} \tag{18}$$

is a window function of width w. The window $[t_k, t_{k+w}]$ holds one forcing period and is necessary since the transform (15) assumes $y(t)$ to be periodic. The full sample interval $[0,N]$ holds $M = N - \text{round}(\omega_s/\omega)$ windows, where ω_s denotes the sampling frequency. The frequency range that can be represented by the Fourier-transform is limited by upper and lower bounds. The lower limit is determined by the width of the window function, since at least one whole period must fit in the buffer ($w \le N$). The upper bound is determined by Q and the sampling-frequency of the real-time application, as high frequency oscillations must be sampled with at least two points per period to avoid aliasing (the Nyquist–Shannon sampling theorem). In our experiments we used $Q = 5$ modes.

3.3. Continex toolbox

Continuation is applied to the controlled experiment using the Matlab continuation-platform COCO [6]. A toolbox named *Continex* (Continuation in experiments) has been specifically developed to handle the communication between COCO and the real-time application running on the DSpace board. It also implements the experimental evaluation of the Jacobian using either finite differences or Broyden's updates (cf. Section 2.4) as well as the polynomial approximation of noise contaminated measured data (cf. Section 2.2). The continuation code uses Broyden's updates by default, but it is possible to force a full recomputation of the Jacobian using finite differences every N_{Jac} step through the N_{Jac}-parameter. The toolbox utilizes Matlab/MLib functions included in the software for the DSpace board, and implements features for automating experiments, managing and plotting recorded data, resuming previous continuation-runs, etc. Continex is publicly available via Sourceforge [15].

3.4. Experimental modal analysis of the impact oscillator

An overview of the dynamical response of the mechanical system to different types of harmonic excitation is given in Fig. 8 in the form of waterfall diagrams. Panels (a) and (c) show a set of frequency–response curves obtained by sweeping the frequency of the shaker signal up and down. In (a) we observe larger hysteresis loops for increasing amplitude of the shaker signal. We also observe smaller hysteresis loops for driving frequencies of $\omega \approx 7.5$ Hz and $\omega \approx 11$ Hz indicated by the small steps on the upper branches of the response curves, which are due to subharmonic resonances and the nonlinear

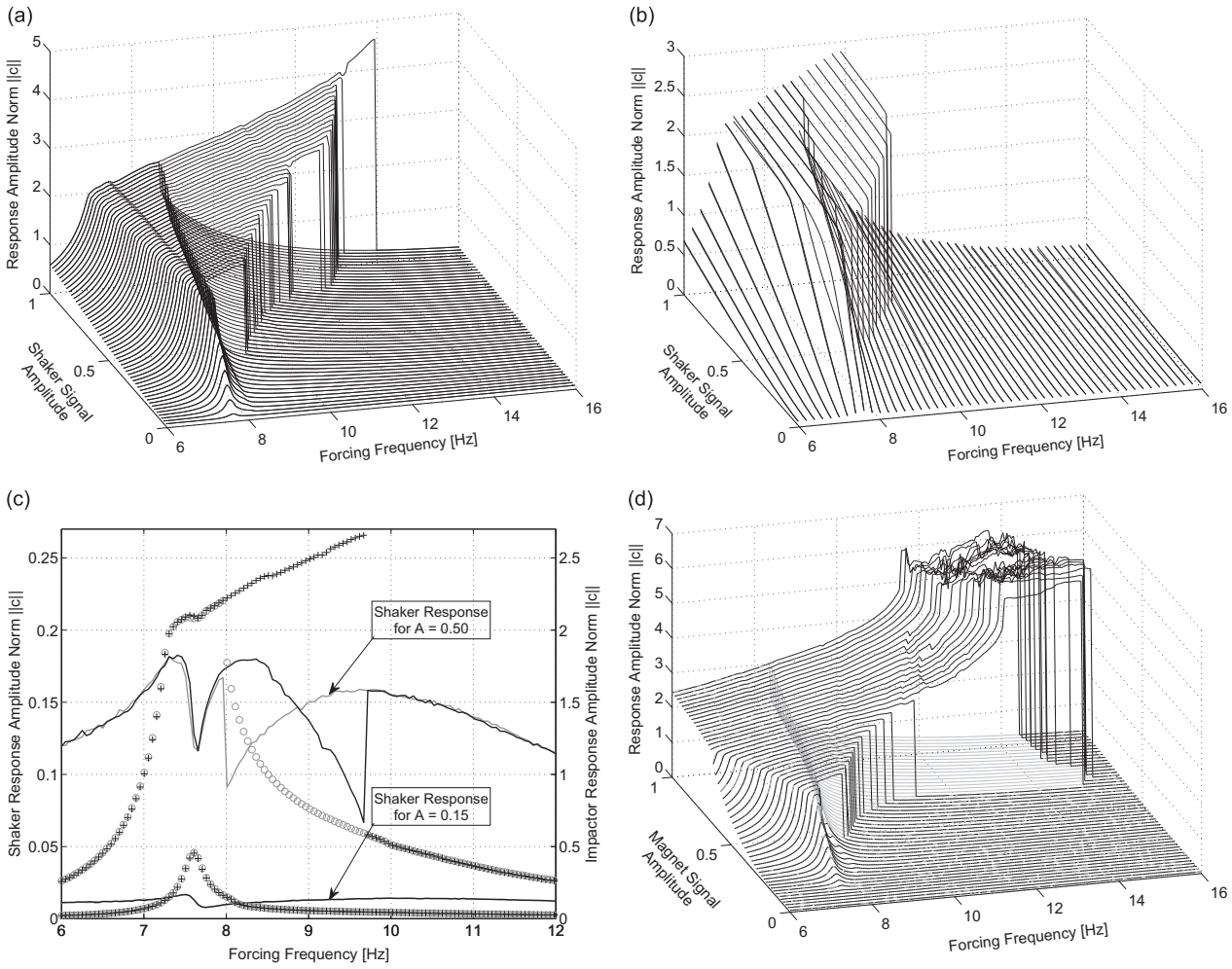

Fig. 8. Results of different parameter sweeps performed on the experimental test rig (Fig. 4). Panels (a) and (b) show series of frequency and amplitude responses for the coupled system consisting of impactor, base-structure and shaker. The response amplitude is given as the Euclidean norm of the Fourier-coefficients $\|c\|$. Panel (c) presents the displacement of the base produced by the shaker for two different fixed amplitudes of the shaker signal. The lower set of curves ($A=0.15$) has been scaled down by a factor of 75 percent to make the figure less cluttered. The upwards sweep is denoted by the black curves (——) and the downwards by gray (——). For the overlaid frequency response curves + marks the upwards while ○ marks the downwards sweep. Panel (d) presents series of frequency sweeps obtained by using the electromagnetic actuators as source of excitation. Each of the sweeps took 30 h to complete and has a resolution of 200×50 measurement points, with the highest resolution being in the swept parameter.

coupling between shaker and impactor. For our subsequent tests we chose to use the forcing frequency as the bifurcation parameter for a fixed forcing amplitude $A_{\text{shaker}} = 0.5$, since for this amplitude our oscillator shows a large hysteresis loop with moderate response amplitudes well within the measurement range of the laser sensors. We also observe evidence for detached responses similar to observations made in [16,17].

Fig. 8c compares the displacement of the base-structure (for different amplitudes of the shaker signal) with the corresponding response curve for the impactor. Note that a different scale is used for the left and right y-axis and that the lower set of curves ($A_{\text{shaker}} = 0.15$) has been reduced by 75 percent in order not to clutter the plot. Comparison of the two curves gives an indication of the coupling between shaker, base structure and impactor. For larger amplitudes of the shaker signal ($A_{\text{shaker}} = 0.5$) the base-structure displays a hysteresis behavior in the range $\omega \approx [8, 10]$ Hz reflecting the behavior of the impactor. Around the impactors primary linear resonance frequency $\omega \approx 7.5$ Hz, a considerable attenuation of the amplitude of the base-structure is seen. At this frequency, the impactor is seen to act almost as a tuned mass damper. For our studies this is not a problem as the mechanical system serves well as a test case for control-based continuation as well as a prototype of systems with build in actuators. In fact it creates a favorable amplitude-attenuation around resonance, making it possible to make better use of the measurement-range of the displacement-sensors.

For comparison, in a second sweep we also produced the set of amplitude response curves shown in Fig. 8b, where we sweep the amplitude of the shaker signal up and down. Although the hysteresis loops are significantly larger when sweeping the amplitude instead of the frequency, the amplitude is less suitable as a bifurcation parameter, because we find that some response amplitudes exceed the measurement range of our sensors (not shown in the figure). As a third sweep

we produced a set of frequency response curves using the electromagnetic actuators as the source of excitation (d). There are three important differences to the previous tests. Firstly, since the input/output relation is different, we do not expect the exact same response as in panel (8a). The second important observation is that although the signal sent to the magnet driver is sinusoidal, the actual forcing is not due to cut-off of the voltage at 26 V. Therefore, for increasing driving amplitudes the signal starts containing higher harmonics and will eventually turn into a rectangular wave resulting in bang-bang drive. Finally, for driving amplitudes $A_{\text{magnets}} > 0.7$ and larger driving frequencies we observe the effect of the nonlinearity of the actuation system. There is a sharp increase in amplitude and the mass starts impacting the magnets. As a result we restrict the amplitude of the driving signal to the range of safe (impact free with respect to the magnets) operation.

4. Control tuning

We propose and test a method for tuning the control parameters, which consists of a systematic sequence of experiments that neither requires a model nor any other prior knowledge about the object under test. We arrived at the proposed tuning procedure in a trial-and-error process that included many failing continuation runs with a subsequent investigation of the reason of failure and a revision of the tuning process that we will outline below along with the experiments.

4.1. Stabilizing the static equilibrium state

The most simple experiment to gain insight into the performance of our control system is to stabilize the static equilibrium position under the influence of a harmonic excitation exerted by the shaker under variation of the control gains. To this end, we set the reference trajectory to $x(t)=0$ and apply a harmonic forcing with amplitude $A_{\text{shaker}} = 0.5$ and frequency $\omega = 7.75$ Hz. One can then vary the various control parameters and use the resulting amplitude of the impactor as a measure of the control power.

Since we intend to use the control scheme for control based continuation, this basic set-up is not sufficient. During the prediction–correction cycle a path following method will frequently change the system's parameters and the reference trajectory. This amounts to applying perturbations to the system and an obvious requirement for a non-invasive, locally stabilizing control scheme is robustness with respect to such perturbations that may not be small. Therefore, we augment this experiment with the application of a large perturbation (created by the timed perturbation block) during a test of a set of control gains. For each pair (K_p, K_d) we applied a perturbation with a duration of 0.5 s, let the system settle and extract the amplitude of the response from a 5 s measurement frame. Fig. 9 shows the displacement of the impactor mass for one such measurement cycle with stabilizing control. For sets of gains resulting in unstable control, the response often leads to the impactor mass hitting and sticking to the electromagnets, resulting in a square-wave-like response with a large amplitude.

Fig. 10 shows the result of three such investigations for different values of the overall scaling gain CFGain. As expected, the control becomes more effective for larger control gains. Less expected, but resulting from the nonlinearity of the actuation system is the region of inefficient control appearing in the top-right corner of the graphics. Also somewhat counter-intuitive is the observation that negative proportional gain seems to improve the control. In conclusion, these results suggest to use a pair of gains that is close to the boundary of effective control as the control strength increases with increasing gains.

4.2. Stabilizing a stable impacting equilibrium state

The previous experiment provides quantitative information about the ability of our control system to stabilize a target state. Different from the situation in continuation, the target state was not close to any equilibrium position, hence, the results do not provide information about whether the control scheme is invasive or not. In order to obtain information about the latter requirement, we perform a modified experiment where we set the target state to an actual equilibrium response of the impactor and repeat the previous experiment with this target reference trajectory.

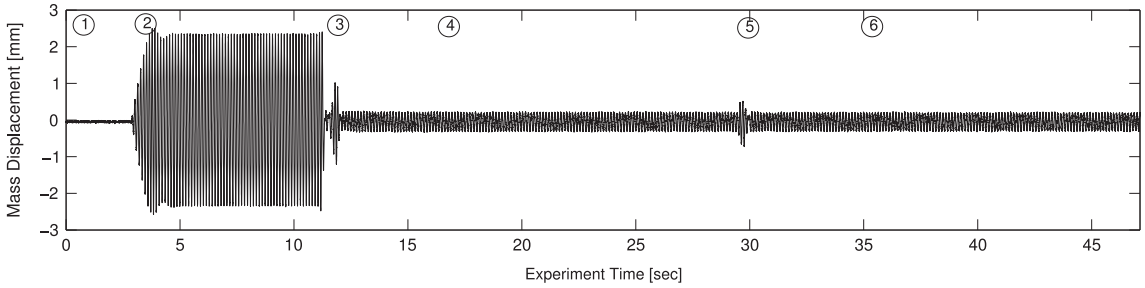

Fig. 9. Time series for the impactor mass during one measurement cycle for the experiment of stabilizing the static equilibrium. (1) No harmonic forcing is applied, (2) harmonic forcing ($A_{\text{shaker}}=0.5$ and $\omega = 7.75$ Hz) is applied and transients are allowed to die out, (3) control is enabled with parameters $K_d=0.5$, $K_p=5$, CFGain=0.750 (stabilizing control) and the system is allowed to settle, (4) extra wait-time to allow for a possible instability of the control to grow, (5) an in-phase perturbation is added to shaker and control-signal to test the controls' robustness against large perturbations, and transients are allowed to die out, and (6) the response is measured and Fourier-transformed.

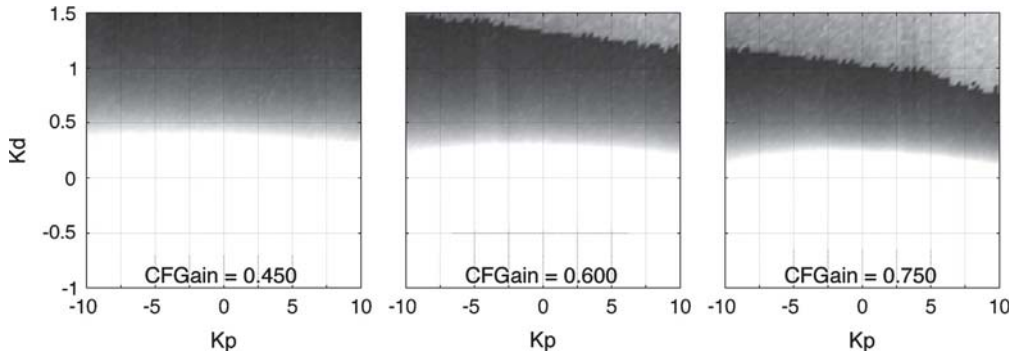

Fig. 10. Stabilization of the static equilibrium state of the impactor as the control-gains K_p and K_d are varied for different but fixed values of the scaling gain CFGain and a fixed filter coefficient PDFC = 180. The gray scale indicates the amplitude of the response, where a darker shade corresponds to smaller amplitude and, hence, to more effective control. We observe an improvement of the control for increasing K_d, but also an onset of inefficient control indicated by the light-gray area appearing at the top-right corner of the diagram for increasing overall gain. Each set of sweeps has a resolution of $[75 \times 75]$ measurement-points with each point measured twice (the worst case value is used) and took around 50 h to complete.

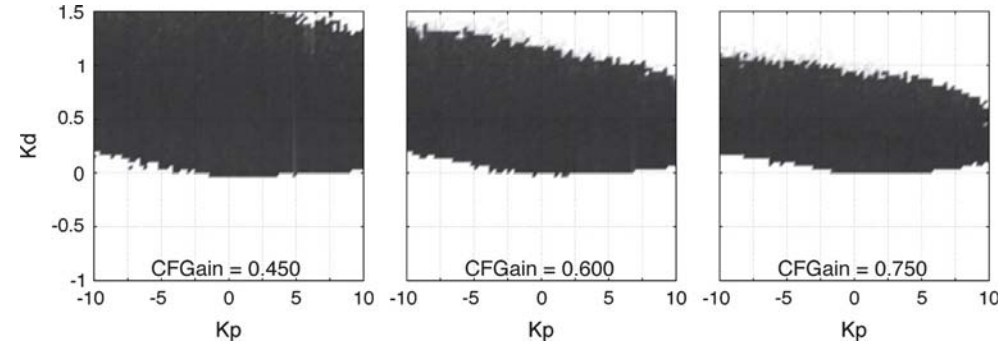

Fig. 11. Stabilization of an impacting stable equilibrium state as the control gains K_p and K_d are varied for different but fixed values of the scaling-gain CFGain and a fixed filter coefficient PDFC = 180. The gray scale indicates the deviation of the measured response from the reference trajectory, which is generated from the Fourier-coefficients of the stable equilibrium state. Darker shade corresponds to smaller deviation and, hence, to less invasive control. We observe that proportional control increases invasiveness as the region of low invasiveness is further away from the line $K_d = 0$ as stronger proportional control is applied. A good choice is $K_p \approx 2$. We also observe high invasiveness for control gains that led to inefficient control in the previous experiment; cf. Fig. 10. The set of sweeps is recorded with the same resolution as the previous experiment and took roughly the same time to run.

To this end, we again excite the impactor with a harmonic forcing with amplitude $A_{\text{shaker}} = 0.5$ and frequency $\omega = 7.75$ Hz. These parameters are chosen such that the impactor has a unique impacting equilibrium state; see Fig. 8. We chose to perform this test with an impacting state, because we are interested in the behavior of the control system applied to a nonlinear response. To initialize the reference trajectory we record the equilibrium state and compute its Fourier transform. As before, for each pair of control gains we apply a perturbation and extract the amplitude of the difference between the reference trajectory and the observed response. If this difference is large, we have to assume that the control scheme perturbs the experiment as the control is not even able to leave a known equilibrium state unchanged. Ideally, we are able to identify control gains for which we have effective control as indicated in the previous experiment as well as vanishing perturbation of an equilibrium state.

Fig. 11 shows the result for the same values of the overall scaling gain CFGain as in the previous experiment. We observe a strip of control gains that result in non-invasive control, which is bounded from below and above. The results indicate that, for CFGain = 0.6, a good choice of gains is $K_p \approx 2$ and $K_d \in [0.5, 0.75]$, resulting in stabilizing and non-invasive control. Indeed, using these settings it is possible to apply control based continuation to our test rig with some success: In a sequence of continuation runs we were able to obtain a bifurcation diagram including unstable equilibrium states. However, the continuation using these gains turned out to be quite unreliable, repeating the same experiment several times would often result in unsuccessful runs. As a first conclusion, we obtained useful gains, but further refinement was necessary.

4.3. Stabilizing an unstable impacting equilibrium state

The previous tuning experiments resulted in a choice of control gains that enabled control based continuation for our test rig, although with varying success. To improve the performance further, we investigate the dependence of the properties of the control system on the filtering implemented in Matlab's PD block. The pole location and, hence, the cut-off frequency of the filter is controlled by the parameter PDFC. For this investigation we fix CFGain = 0.65 and restrict the control gains to the

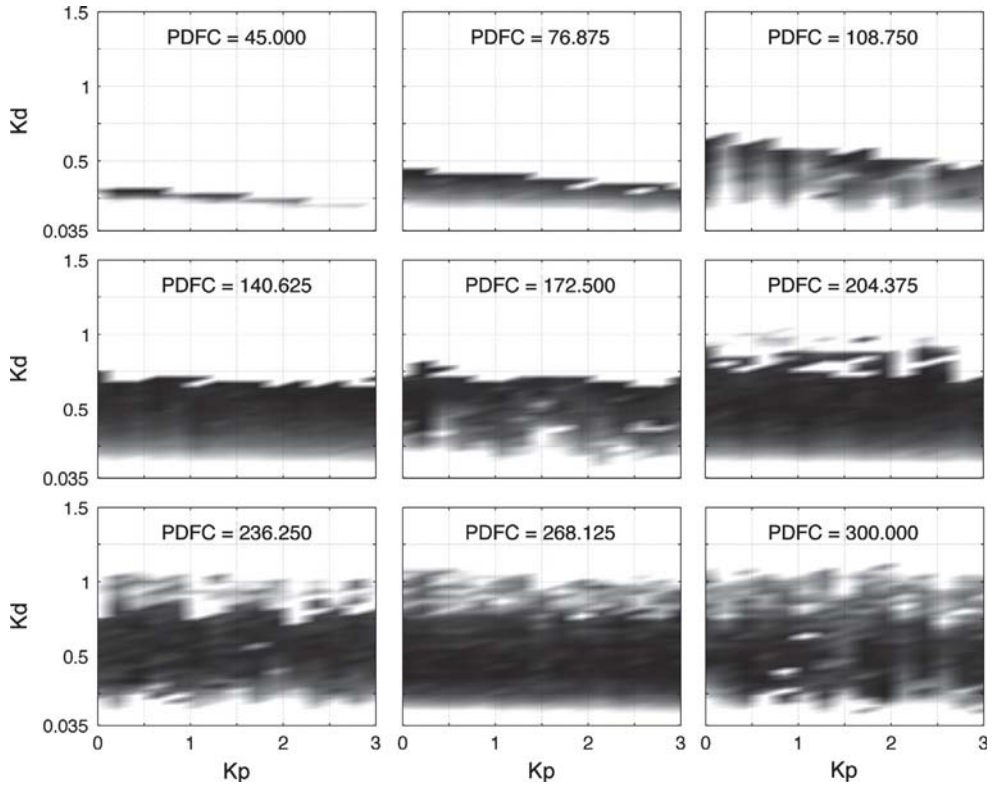

Fig. 12. Stabilization of an impacting unstable equilibrium state as the control-gains K_p and K_d are varied for different but fixed values of the filter coefficient PDFC and a fixed scaling-gain CFGain=0.65. The gray scale indicates the deviation of the measured response from the reference trajectory, which is set to the Fourier-coefficients of an unstable equilibrium state. Darker shade corresponds to smaller deviation and, hence, to both more effective and less invasive control. We observe the emergence of a strip of effective control parameters around K_d=0.5. Each panel has a resolution of $[K_p : 15 \times K_d : 45]$ with each point measured twice (worst case value used) and took around 15 h to complete.

strip $(K_p, K_d) \in [1, 3] \times [0, 1.5]$. To initialize the reference trajectory we use the Fourier-coefficients of an unstable equilibrium state obtained in a successful continuation run. Since ambient conditions, like temperature, change over the course of these experiments, such previously obtained solutions are only approximations and not precise enough to guarantee consistent results. To ensure that the tests for all control gains are executed under the same conditions, we run Newton's method in regular intervals to adapt the reference trajectory to changes in the environment. Otherwise, the experiment is identical to the previous one, in particular, the criterion for the quality of the control.

Fig. 12 presents sweeps of control gains conducted for different values of the filter-coefficient PDFC, while stabilizing a resumed unstable (stabilized) naturally occurring equilibrium state. We observe the emergence of a strip of efficient and non-invasive control around K_d=0.5 as well as a dramatic improvement for PDFC up to 150, with seemingly little improvement for larger values. The proportional gain K_p is seen to have very little influence for PDFC > 140. This test did not lead to much improvement for the continuation, because our previous value of PDFC=180 was already good.

During the tests with the filter-coefficient, we observed that with higher values of PDFC the time for the transient behavior of the impactor becomes shorter, meaning that the time Newton's method would have to wait for transients to settle might be shorter for higher PDFC gains. Putting this hypothesis to test, it turned out that the choice of parameters for the control had a significant impact on how fast and consistent Newton's method would converge.

4.4. Optimizing performance of Newton's method

In the previous experiments we investigated how the control-parameters influence the controls' ability to locally stabilize the system in a non-invasive way. Using these results it was possible to obtain effective control, but it turned out to be important also to investigate how the control parameters influenced the convergence of Newton's method used in the correction-step. For some sets of parameters that gave very stable and efficient control, Newton's method would converge very slowly or even fail to converge. Recomputing the Jacobian every N_{Jac} iteration steps, rather than relying completely on Broyden's updates would improve the convergence, at the cost of increased experiment time. A reason for this might be the noise contamination of the measurements resulting in Broyden's updates that are sometimes not accurate enough to ensure convergence.

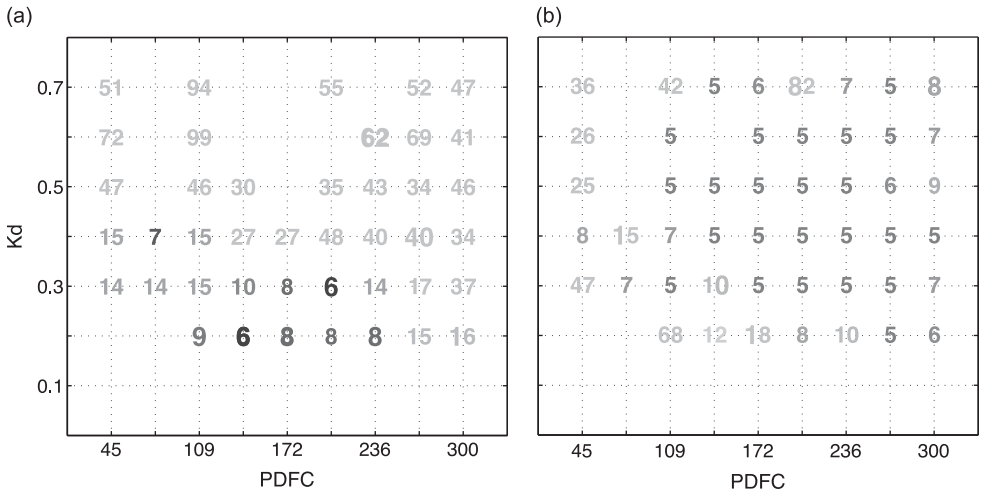

Fig. 13. The number of corrector-iterations required for one correction-step to converge depending on control parameters K_d and PDFC. In panel (a) only Broyden's updates are used to calculate the Jacobian whereas in panel (b) the Jacobian is re-computed initially and every $N_{\text{Jac}}=45$ steps using finite difference approximations. The integers indicate the number of iterations necessary for convergence, and are shaded according to computation time with black corresponding to low computation time and gray high. Note that computation time and number of iterations do not correlate, as re-computing the Jacobian using finite differences is expensive. Also a minimum of five steps are used in order to provide statistical evidence that the correction did not satisfy the convergence criteria by chance. Non-converging parameter sets are removed leaving empty spaces. The sweeps were made using a fixed proportional gain of $K_p=2$ and CFGain$=0.650$. Each sweep is done twice and the worst case value is used for both calculation time and number of iterations. Each panel took approximately 20 h to obtain.

Failure of Newton's method to converge usually happens while tracking a branch of unstable equilibria or while tracking around a fold point. In contrast, when correcting to a properly separated stable equilibrium-state, its attracting nature helps to stabilize the convergence of Newton steps. Thus, an experiment to investigate Newton's method dependence on control-parameters and recomputation of the Jacobian must seek to stabilize an otherwise unstable equilibrium state. Similar to the previous experiment, we find the convergence of Newton's method not to be sensitive to changes in proportional gain K_p, but very sensitive to the derivative gain K_d and the filter coefficient PDFC.

Fig. 13 presents the result of a series of convergence tests depending on the control-parameters and the number (N_{Jac}) of steps between each full finite difference re-computation of the Jacobian. Similar to the experiment in Fig. 12 we resume an unstable equilibrium-state obtained from a previous continuation run, and then test how well Newton's method converges depending on control-parameters. Fig. 13a shows the results of this test with Broyden's updates only. There is a triangular island of low iteration numbers and short convergence time for PDCF$=$[109;236] and $K_d=$[0.2;0.3]), where the correc tion succeeds reliably. Furthermore, as shown in Fig. 13b, more frequent re-computation of the Jacobian stabilizes the convergence for a larger range of the control-parameters at the expense of longer experiment times, as Broyden's update is much faster than a full Jacobian re-computation. The set of gains for which Broyden only is very effective is observed to be almost disjoint from the set of gains for which finite difference approximations are effective. In conclusion, this explains our previous observation of unreliability in Newton's method when using only Broyden's updates, a small K_d is optimal here, while a larger K_d is optimal when using both finite difference approximation and Broyden's updates. For our subsequent continuation runs we used $K_p=2$, $K_d=0.35$, PDFC$=180$ and CFGain$=0.65$.

5. Continuation results

Fig. 14a presents a comparison of experimental frequency–response curves found by a conventional parameter-sweep and by control-based continuation using the control-parameters obtained in the previous section. The results of the two methods are seen to be in good agreement, while in addition to finding the stable branches the continuation method is able to track around the two fold-points and trace out also the unstable part of the response-curve. Fig. 14b presents a number of consecutive continuation-runs, which verifies that the continuation does in fact run very consistently when using the control-parameters obtained by the presented tuning method. Fig. 14c and d shows zooms of Fig. 14b. Panel (c) shows a small bubble of hysteresis around $\omega=7.7$ Hz. This is not an artifact of the continuation-algorithm, but actual measurable dynamical behavior. Currently all continuation-runs terminate at this point. The method terminates because the stable states coexisting at this point lie closer together in phase-space than is possible to distinguish by both measurement and the control. Panel (d) shows the continuation tracing the upper fold point. At this point it is harder for the continuation algorithm to approximate the data, as the curvature is increasing drastically. Furthermore, during experiments, we observe that quasi-periodic vibrations seem to exist in the high-amplitude range. To properly distinguish these from normal periodic

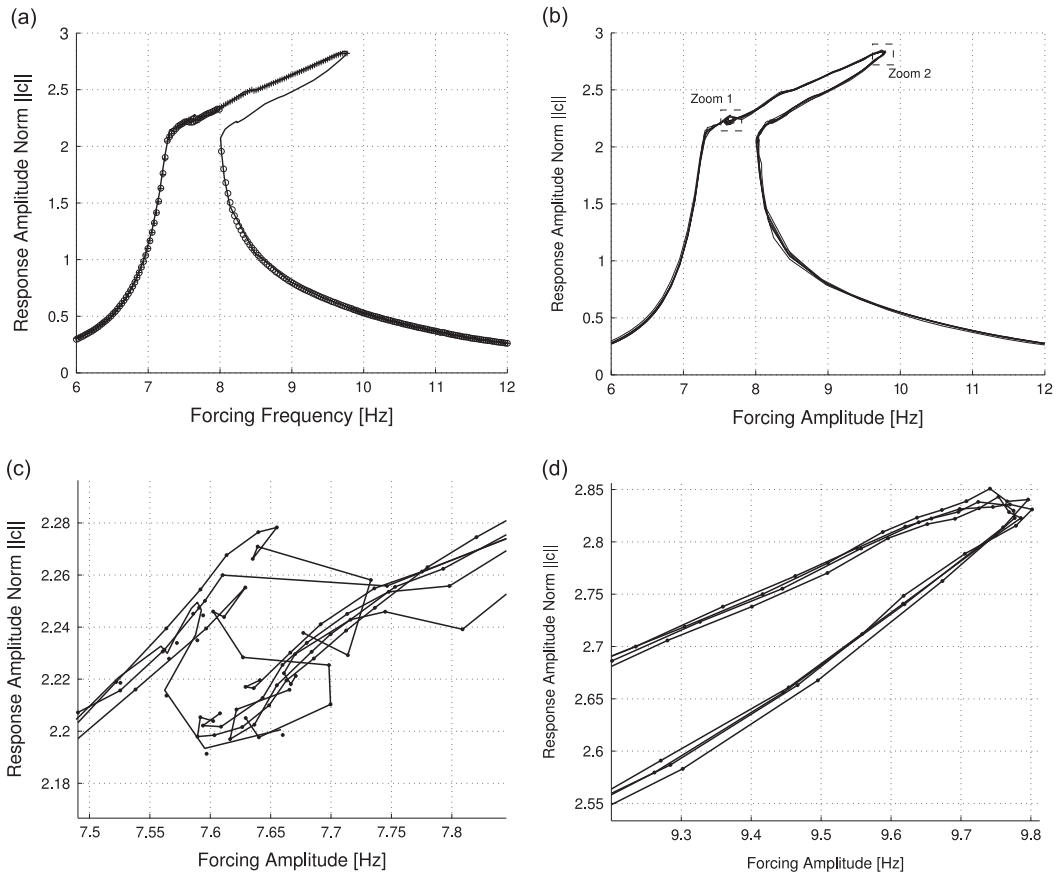

Fig. 14. Frequency responses for the impact oscillator obtained by control-based continuation. Panel (a) compares the result of the continuation method with those of a parameter-sweep (explained in Section 3.4), showing (for the stable branches) good agreement between the two methods. Panel (b) shows several consecutive continuation-runs overlaid, and confirms that the method provides consistent results. Panel (c) shows the occurrence of a small hysteresis bubble. Currently all continuation runs terminate at this point, since the accuracy of measurements and actuation is not sufficient to distinguish the coexisting states at this point. Panel (d) shows a zoom of the upper part of the frequency–response, and confirms that the continuation method is able to track around the upper (as well as the lower) fold point. A full frequency response, as the one shown in panel (a), is a combination of two separate runs started on each side of the point where the method terminates and takes a total of approximately 8 h to complete.

steady states require longer measurements to be used in the Fourier-transform. Nevertheless, the continuation algorithm seems to be quite robust and perform very consistently.

6. Conclusions

Our experiments show that it is possible to construct a non-invasive and locally stabilizing control using electromagnetic actuators despite the resulting nonlinearity of the actuation force. As a consequence, it becomes feasible to conduct experimental bifurcation analysis for certain types of smart machinery using control-based continuation. The sequence of experiments proposed here shows how to tune a controller without a model for control or actuators, which is important if one wishes to apply the method to test-subjects for which no sufficiently good models are available. An interesting observation is that more frequent recomputation of the Jacobian using finite difference approximations seems to improve convergence of the Newton corrector for a large range of control parameters.

The experimental tuning process as presented here required about one month of consecutive experiments. However, since we used a high resolution over the full range of gains for producing the graphics, there are opportunities to shorten the required time dramatically. For example, in our study we observe the control to be most sensitive to changes in the derivative gain K_d and the filter coefficient PDFC. A significant speed up will, therefore, already result from restricting a detailed study to the most influential parameters, which may be identified rather quickly in simple experiments. Furthermore, using coarser grained parameter sweeps seems to be sufficient in many cases and allows one to reduce the required time even further. Another idea to improve the performance of the tuning process is to locate only the boundary of stability in Figs. 9 and 11. This would either speed up the tests, or allow the inclusion of an additional parameter in the tuning process without loss of performance.

Further problems we plan to address are monitoring of stability of steady-state responses, studies of a test rig with three degrees of freedom, and applications to rotating machinery with foil-bearings, mounted on rotors with actively controllable bearings. First experiments testing the feasibility of monitoring stability of steady-state responses by disabling the controller in different ways for short periods of time have been presented in [18]. We aim at refining these ideas such that robust and reliable stability tests become available in the near future.

The Continex toolbox we developed to interface experiments with the existing Matlab continuation-platform COCO [6] is publicly available via Sourceforge [15].

Acknowledgments

This work was supported by the Danish Research Council FTP under the project number 09-065890/FTP. The authors wish to thank Jan Sieber, David Barton, Harry Dankowicz and Bernd Krauskopf for helpful comments when setting up the experiments.

Appendix A. Non-invasiveness of the control-scheme

That the convergence criterion for the correction-step indeed implies a vanishing control signal follows from *non-invasiveness*, which holds for the linear PD scheme, since

$$\begin{aligned} \|u_c\|_\infty = \|G(x-z)\|_\infty &= \|K_p(x-z) + K_d(\dot{x}-\dot{z})\|_\infty, \\ &\le K_p\|x-z\|_\infty + K_d\|\dot{x}-\dot{z}\|_\infty, \\ &\le \max\{K_p, K_d\}(\|x-z\|_\infty + \|(\dot{x}-\dot{z})\|_\infty), \\ &\le \delta\|x-z\|_1, \end{aligned} \tag{A.1}$$

which in turn implies that the control signal is bounded by the residual

$$\begin{aligned} \|u_c\| = \|G(x-z)\| &\le \delta\|x-z\|, \\ &\le \delta\kappa\|\mathcal{F}_\infty(x)-\mathcal{F}_\infty(z)\|, \\ &\le \delta\kappa(\|F(c,\mu;N)\| + R_{Q+1}), \end{aligned} \tag{A.2}$$

where R_{Q+1} is the residual term that arises because the Fourier-transform uses a finite number of modes for the projection. This underlines the necessity for using a sufficient number of modes in order for the Fourier-transform to represent the dynamics of the system within measurement accuracy. In our experiments we found that $Q=5$ is more than sufficient.

References

[1] J. Sieber, B. Krauskopf, Control based bifurcation analysis for experiments, *Nonlinear Dynamics* 51 (3) (2008) 365–377, http://dx.doi.org/10.1007/s11071-007-9217-2.
[2] J. Sieber, A. Gonzalez-Buelga, S. Neild, D. Wagg, B. Krauskopf, Experimental continuation of periodic orbits through a fold, *Physical Review Letters* ; 100 (2008) http://dx.doi.org/10.1103/PhysRevLett.100.244101.
[3] J. Sieber, B. Krauskopf, D. Wagg, S. Neild, A. Gonzalez-Buelga, Control-based continuation of unstable periodic orbits, *Journal of Computational and Nonlinear Dynamics* 6 (1) (2011). 011005–011005-9.
[4] D.A.W. Barton, S.G. Burrow, Numerical continuation in a physical experiment: *investigation of a nonlinear energy harvester*, *Journal of Computational and Nonlinear Dynamics* 6 (1) (2011). 011010–011010-6.
[5] D.A. Barton, B.P. Mann, S.G. Burrow, Control-based continuation for investigating nonlinear experiments, *Journal of Vibration and Control* 18 (4) (2012) 509–520, http://dx.doi.org/10.1177/1077546310384004.
[6] H. Dankowicz, F. Schilder, An extended continuation problem for bifurcation analysis in the presence of constraints, *Journal of Computational and Nonlinear Dynamics* 6 (3) (2011) 031003.
[7] E.J. Doedel, A.R. Champneys, T.F. Fairgrieve, Y.A. Kuznetsov, B. Sandstede, X. Wang, Auto 97: Continuation and Bifurcation Software for Ordinary Differential Equations (with homcont), ⟨http://cmvl.cs.concordia.ca/auto/⟩, 1997.
[8] H.B. Keller, Numerical solution of bifurcation and nonlinear eigenvalue problems, *Applications of Bifurcation Theory (Proc. Advanced Sem., Univ. Wisconsin, Madison, Wis. 1976)*, Academic Press, New York, 1977, pp. 359–384. Publ. Math. Res. Center, No. 38.
[9] H. Schwetlick, Ein neues Prinzip zur Konstruktion implementierbarer, global konvergenter Einbettungsalgorithmen, *Beiträge zur Numerischen Mathematik* 4 (1975) 215–228.
[10] E.J. Doedel, Lecture notes on numerical analysis of nonlinear equations, in: B. Krauskopf, H.M. Osinga, J. Galán-Vioque (Eds.), *Numerical Continuation Methods for Dynamical Systems*, Springer, Netherlands2007, pp. 1–49, http://dx.doi.org/10.1007/978-1-4020-6356-5.
[11] C.G. Broyden, A class of methods for solving nonlinear simultaneous equations, *Mathematics of Computation* 19 (92) (1965) 577–593.
[12] E. Bureau, F. Schilder, I. Santos, J.J. Thomsen, J. Starke, Experimental bifurcation analysis for a driven nonlinear flexible pendulum using control-based continuation, *Proceedings of the Seventh European Nonlinear Dynamics Conference*, Rome, Italy, 2011.
[13] S. Shaw, Forced vibrations of a beam with one-sided amplitude constraint: *theory and experiment*, *Journal of Sound and Vibration* 99 (2) (1985) 199–212.
[14] J. Ing, E. Pavlovskaia, M. Wiercigroch, S. Banerjee, Bifurcation analysis of an impact oscillator with a one-sided elastic constraint near grazing, *Physica D*: *Nonlinear Phenomena* 239 (6) (2010) 312–321, http://dx.doi.org/10.1016/j.physd.2009.11.009.
[15] Continex on Sourceforge, ⟨http://www.sourceforge.net⟩; project cocotools, toolbox continex, April 2013.
[16] N.A. Alexander, F. Schilder, Exploring the performance of a nonlinear tuned mass damper, *Journal of Sound and Vibration* 319 (1–2) (2009) 445–462, http://dx.doi.org/10.1016/j.jsv.2008.05.018.
[17] Y. Starosvetsky, O. Gendelman, Dynamics of a strongly nonlinear vibration absorber coupled to a harmonically excited two-degree-of-freedom system, *Journal of Sound and Vibration* 312 (1–2) (2008) 234–256, http://dx.doi.org/10.1016/j.jsv.2007.10.035.
[18] E. Bureau, I. Santos, J.J. Thomsen, F. Schilder, J. Starke, Experimental bifurcation analysis by control-based continuation—determining stability, *Proceedings of the ASME 2012 International Design Engineering Technical Conferences & Computers and Information in Engineering Conference*, Chicago, USA, 2012.

P3 Publication 3

The following paper [P3] was submitted to and presented on the ASME 24th Conference on Mechanical Vibration and Noise (part of the ASME IDETC/CIE conference) in Chicago, USA 2012. It propose methods for determining stability during control-based continuation by momentarily turning off or modifying the control. Furthermore, it presents a study of the behaviour of our test rig upon disabling the control at different stabilized equilibrium states.

Proceedings of the ASME 2012 International Design Engineering Technical Conferences & Computers and Information in Engineering Conference
IDETC/CIE 2012
August 12-15, 2012, Chicago, IL, USA

DETC2012-70616

EXPERIMENTAL BIFURCATION ANALYSIS BY CONTROL-BASED CONTINUATION - DETERMINING STABILITY

Emil Bureau *
Department of Mechanical Engineering
Technical University of Denmark
Kongens Lyngby, 2800, Denmark
Email: embu@mek.dtu.dk
WWW: http://www.continex.mek.dtu.dk

Ilmar Ferreira Santos &
Jon Juel Thomsen
Department of Mechanical Engineering
Technical University of Denmark
Kongens Lyngby, 2800, Denmark

Frank Schilder &
Jens Starke
Department of Mathematics
Technical University of Denmark
Kongens Lyngby, 2800, Denmark

ABSTRACT

The newly developed control-based continuation technique has made it possible to perform experimental bifurcation analysis, e.g. to track stable as well as unstable branches of frequency responses directly in experiments. The method bypasses mathematical models, and systematically explores how vibration characteristics of dynamical systems change under variation of parameters. The method employs a control scheme to modify the response stability. While this facilitates exploration of the unstable branches of a bifurcation diagram, it unfortunately makes it impossible to distinguish previously stable and unstable equilibrium states. We present the ongoing work of developing and applying the control-based continuation method to an experimental mechanical test-rig, consisting of a harmonically forced nonlinear impact oscillator controlled by electromagnetic actuators. Furthermore we propose and test ideas on how to determine the stability of equilibria states during continuation.

INTRODUCTION

Experimental investigations of nonlinear mechanical systems present many difficulties. While it is straightforward to extract frequency and amplitude responses of linear systems in an experiment, this is no longer true for nonlinear systems. The co-existence of multiple dynamically stable equilibria separated by unstable ones cause problems since the experiment can jump between equilibrium states. To illustrate this, we consider the classical example of a frequency response for a system with a softening or hardening nonlinearity (cf. Fig. 1). Comparing with its linear equivalent, the nonlinear system will have its resonance peak bent over to one side, creating a frequency region in which two stable and one unstable dynamic equilibrium co-exist.

The conventional way of investigating such nonlinear systems experimentally is by parameter sweeps, where a parameter (in this case the frequency of external excitation) is swept up and down, and the stationary response is recorded. Figure 2 shows an example of an experimental parameter sweep for the mechanical system investigated in this paper. Since the equilibria associated with the stable branches of the bifurcation diagram are (locally) asymptotically stable, the system will continue along the branch on which it is initiated as the sweep parameter is varied. In Fig. 2 this property is exploited in order to reveal both stable branches, as the upwards sweep is initiated on the upper branch, and the downwards sweep on the lower.

It is evident that this method only works under certain conditions, which cannot always be expected to hold. First of all, it must be possible to initialize the system on the desired equilibrium state, which might not be possible in regions with multiple co-existing stable equilibrium states. Secondly the system must not accidentally jump between different stable equilibrium states, which puts requirements on both the external excitation and the dynamics of the system. The perturbations introduced by the external excitation and noise should be small enough not

*Address all correspondence to this author.

to cause an accidental jump between equilibrium states, which again requires the equilibrium states to be sufficiently separated in phase-space. Comparing Figs. 1 and 2 illustrates another important point; the parameter-sweep only detects stable equilibrium states. This is because the unstable equilibria act as separators between the stable ones, and the system will always diverge from unstable equilibria. Nevertheless, the unstable equilibrium states influence the transient behavior of the system and, therefore, hold important information for fitting a correct model. Furthermore, seemingly unconnected branches of stable steady state dynamics in the bifurcation diagram might be connected through branches of unstable equilibrium states. Thus following these unstable equilibrium states can be a key for obtaining a more complete picture of the dynamics. Finally, because unstable equilibrium states cannot be observed in experiments, they are sometimes considered as hypothetical artifacts, while our results support the point of view that they are not.

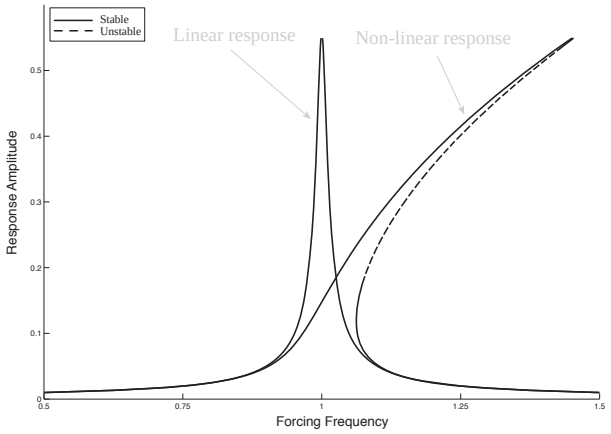

FIGURE 1. COMPARISON OF A LINEAR AND NONLINEAR (THEORETICAL) FREQUENCY RESPONSE.

Control-based continuation provides a more systematic approach to investigate the nonlinear dependency of vibration characteristics on system parameters directly in an experiment. Most importantly, it provides a mean to follow and measure branches of unstable dynamics. The method was first introduced in [1] and developed further in [2–7]. The fundamental idea is to apply a control force to the system under investigation and then use a predictor-corrector path-following algorithm to systematically trace out branches of a bifurcation diagram. The controller locally stabilizes the state requested by the prediction-step and will in turn stabilize otherwise unstable steady states. It is essential that the control scheme is *non-invasive*, meaning that the steady state dynamics of the controlled and the *un*-controlled system

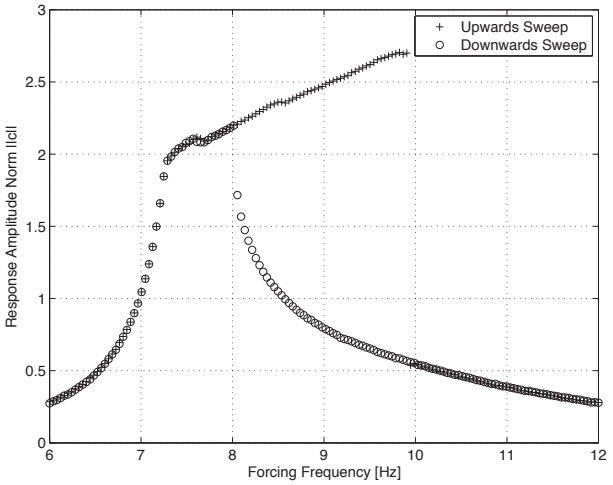

FIGURE 2. EXPERIMENTAL FREQUENCY RESPONSE BY PARAMETER SWEEP.

are identical. While the modification of the systems' stability facilitates exploration of the unstable branches of the bifurcation diagram, it makes it impossible to differentiate easily between previously (*un*-controlled) stable and unstable equilibria.

We present the ongoing work of improving the method of control-based continuation and apply it to an experimental mechanical test-rig, consisting of a harmonically forced nonlinear impact oscillator controlled by electromagnetic actuators. Results from the experimental bifurcation analysis are presented and discussed in the light of evaluating the method. Furthermore we propose new ideas on how to determine the stability of bifurcation branches during continuation. These are based on momentarily switching off or scaling the control, while monitoring the resulting behavior of the uncontrolled system. The implementation and experimental tests of these ideas have not been carried out at the time of writing. More resent results will be presented at the conference.

METHOD

Control Based Continuation

The fundamental idea of the method of control-based continuation is to construct a suitably controlled experiment and apply a continuation algorithm to it. By suitably controlled experiment we mean that the controller should only facilitate the measurement of steady state dynamics, not alter the equilibrium states from those of the corresponding *un*-controlled experiment.

Continuation algorithms employ a predictor-corrector path-following algorithm to systematically trace curves of steady state dynamic responses under variation of parameters. In an experiment, a prediction step in a tangent direction of the parametrized

curve can be understood as requesting the experiment to go to a specific equilibrium state. This state might not be a *natural* state, by which we mean an equilibrium state that exists for both the controlled and *un*-controlled experiment, but rather an artificial state, that can be stabilized by the control. The correction step then applies an iterative nonlinear (Newton-like) solver in order to correct the predicted state, until the system reaches a natural state that we are interested in measuring. As will be explained in the following, the method implies constraints on the control and requires the formulation of a zero-problem, which can be used with continuation algoritms such as COCO [8,9] or AUTO [10].

We consider an experiment to be a process that runs over time t and depends on parameters μ. Making a single measurement can be thought of as a function evaluation $y(\mu,t)$. If we are interested in measuring periodic states we need to sample the experiment over a time interval covering several periods. We represent one such measurement as a finite sequence of the form

$$Y(\mu,N) = \{y_0,\ldots,y_{N-1}\}, \tag{1}$$

where N denotes the number of sampled points. The measurements are taken with a constant sampling interval h, meaning that the k-th measurement is $y_k = y(t_0+kh)$, where t_0 denotes the starting time of the measurement. Similarly, we denote a measurement of a corresponding controlled experiment as

$$Z_u(\mu,N,x) = \{z_0,\ldots,z_{N-1}\}, \tag{2}$$

where $u = u(t)$ denotes the control signal and $x = x(t)$ is the reference trajectory requested by the continuation algorithm. The controller and the controlled experiment must satisfy a number of conditions:

1. The controlled experiment must be *consistent*. That is, for zero control the controlled experiment must be identical to the original experiment: $Z_0 \equiv Y$, and the controlled experiment Z_u must converge smoothly and continuously to the *un*-controlled experiment Y when the control $u \to 0$.
2. The control scheme must be *locally stabilizing*, i.e. any equilibrium state of Y (stable or unstable) must become an asymptotically stable equilibrium state of Z_u.
3. The control must be *non-invasive*, meaning that the control signal should be bounded by the difference between the requested reference trajectory and the measurement of the controlled experiment: $||u|| \leq \delta||x-z||$ (Lipschitz continuity with appropriately chosen norms). This implies that the control-signal u will vanish whenever the requested state x is a natural state for the system.

The first point implies some intuitive but quite important restrictions on the control actuator. When the control signal is zero, the controller should not alter the dynamics of the system. Many actuators, e.g. servo-motors and hydraulic actuators, add additional inertia, stiffness and damping to the system, effectively changing the *un*-controlled experiment. This is the motivation for choosing electromagnetic actuators for the setup investigated in this paper. There is no direct contact between the actuator and the mechanical system and residual magnetization is found to be small. Another workaround is simply adding the control force to the external excitation force as in previous studies [3].

The second point makes it possible to follow unstable equilibrium states as well as dealing with multiple co-existing steady states, as long as these are sufficiently separated in phase-space compared to the quality of measurements and control.

The control-scheme should satisfy all the conditions above, and seek to minimize the difference $x(t)-z(t)$. This can be obtained by using a PD-Controller, G, with appropriately chosen gains G_P and G_D. The control signal can be expressed as

$$u(t) = G(x(t)) := PD(x(t),z(t)), \tag{3}$$
$$= G_P(x(t)-z(t)) + G_D(\dot{x}(t)-\dot{z}(t)) \tag{4}$$

where $x(t)$ is a reference trajectory set by the continuation algorithm, and $z(t)$ is the measurement of the controlled experiment taken at time t. This control scheme satisfies the inequality $||u||_0 \leq \delta||x-z||_1$, where $||u||_0 := \sup|u(t)|$, $t \in \mathrm{D} \subseteq \mathbb{R}$, denotes the supremum norm and $||u||_1 := ||u||_0 + ||u'||_0$ denotes the C^1 norm. The utilization of the C^1 norm on the right-hand side implies a need for smoothing noise contaminated measurements using signal filtering, which must balance the two competing targets of not amplifying high frequency noise while not making the control too slow.

We denote a discrete Fourier transform of a sequence by $\mathscr{F}_Q$, where Q is the number of Fourier-modes that is projected onto. With this notation, the Fourier-projection of the reference trajectory is given by

$$c = \mathscr{F}_Q(x). \tag{5}$$

Now a zero-problem can be formulated as

$$F(c,\mu;N) := \mathscr{F}_Q\{Z_u(\mu,N,\mathscr{F}_Q^{-1}(c))\} - c, \tag{6}$$

which will set a reference trajectory and parameters, wait for transients to die out and compute Fourier transform of the response. Then the Fourier coefficients of the obtained response are compared with those of the target trajectory. We assume that the reference trajectory is an approximation of a natural response when its Fourier coefficients are identical to those of the measured response. Our control is *non-invasive* since the PD control

scheme is linear and

$$||u|| = ||PD(x-z)|| \leq \delta||x-z|| \quad (7)$$
$$\leq \delta\kappa||\mathscr{F}_\infty(x) - \mathscr{F}_\infty(z)|| \quad (8)$$
$$\leq \delta\kappa(||F(c,\mu;N)|| + R_{Q+1}), \quad (9)$$

where R_{Q+1} denotes residual terms that arises because a finite number of Fourier-modes is used in the projection. This means that it is important to include sufficiently many terms in the Fourier-projection to correctly represent the dynamics of the system. In our experiments we have used $Q = 5$.

As a criteria for convergence, we use $||F(c,\mu;N)|| < \text{TOL}$, where TOL is typically of the order of the measurement error. In other words; if the control signal is sufficiently small, the measurement is accepted as a natural state. This indirect measure for convergence is necessary, since it is not possible to measure the *un*-controlled experiment for comparison.

Note that the zero-problem F can be evaluated asynchronously to the experiment, meaning that the experiment and control can run in real-time, while the continuation algorithm can run separately on a computer.

Determining Stability

Since control-based continuation locally turns both stable and unstable equilibrium states into asymptotically stable ones, it is no longer possible to determine stability using traditional methods of dynamical systems theory. The key idea for enabling measurements of stability is to modify the control signal for a certain amount of time and study the resulting behavior of the system. Three approaches that seem feasible are:

1. Turning off the control and monitor if the system diverges. If we sample a Poincaré-map it should become possible to quantify the stability using classic Lyapunov stability criteria, for example, the rate of divergence (Lyapunov-exponent). Sampling multiple Poincaré-sections should allow for obtaining statistically reliable estimates.
2. Turning off the control inside a *trust region* in phase-space and monitor if the system diverges. The control should be turned back on as soon as the system exits the trust-region. This region could, for example, be defined by comparing the current state with the reference trajectory. We assume unstable behavior if the system leaves the trust region.
3. Applying a nonlinear scaling function, u_{sc} to the control-signal; cf. Fig 3. Stability might be determined applying statistical analysis on a sampled orbit, assuming that the nonlinear scaling results in different distributions of points for stable and unstable equilibrium states.

Which strategy can be used during continuation depends on two properties: how quickly the system diverges from an unstable state, and if the state can be restored by the control-system. The latter might not be possible if divergence causes damage to the system, or if the control-energy is insufficient to restore the state of the system once diverged. Strategy 1 requires the system to either diverge slowly over several periods and any natural state to be restorable by the control system. Strategies 2 and 3 implement precautions to prevent catastrophic divergence, which means that the controller does not have to be able to restore the system after divergence. On the other hand, strategy 1 provides a quantitative characterization of stability, while the other two only indicate if an equilibrium state is stable or not. Note also, that due to the fact that we can observe divergence only over a finite amount of time, equilibrium states with strong transient growth of perturbations will be classified as unstable.

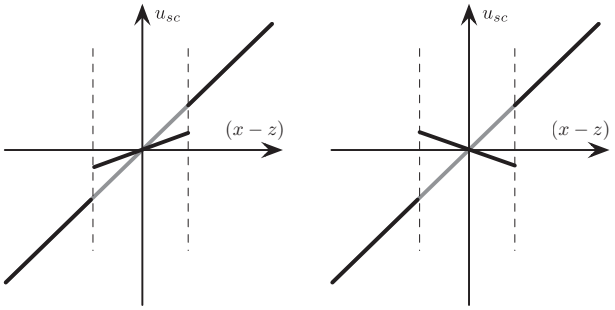

FIGURE 3. STRATEGIES FOR SCALING OF THE CONTROL.

EXPERIMENTAL SETUP AND IMPLEMENTATION

The experimental test rig is shown in Fig. 4. It comprises an impact-oscillator with a hardening nonlinearity, controlled by electromagnetic actuators. The impactor is a flexible pendulum (1) which, when vibrating with large enough amplitudes, impacts a mechanical stop (2) causing a steep increase in stiffness. The pendulum is mounted on a base (3), that can be moved in the horizontal plane by means of an electromagnetic shaker (4). The horizontal displacement of the platform and the pendulum is measured using two laser displacement sensors (5). An electromagnetic actuator (6) is mounted on both sides of the pendulum mass. The resulting magnetic field in the gap can be varied using an amplified control signal. Data acquisition and real-time control is realized using a computer equipped with a dSPACE DS1104 board and MATLAB/Simulink.

Figure 2 presents a frequency response obtained by a frequency-sweep. It is seen that the backbone of the frequency response is bent, creating a region, where multiple steady states co-exist. This is recognized as a typical feature of systems with a hardening nonlinearity. Note that the shaker does not have a feedback control, meaning that the dynamics of the base-structure affects the displacement produced by the shaker.

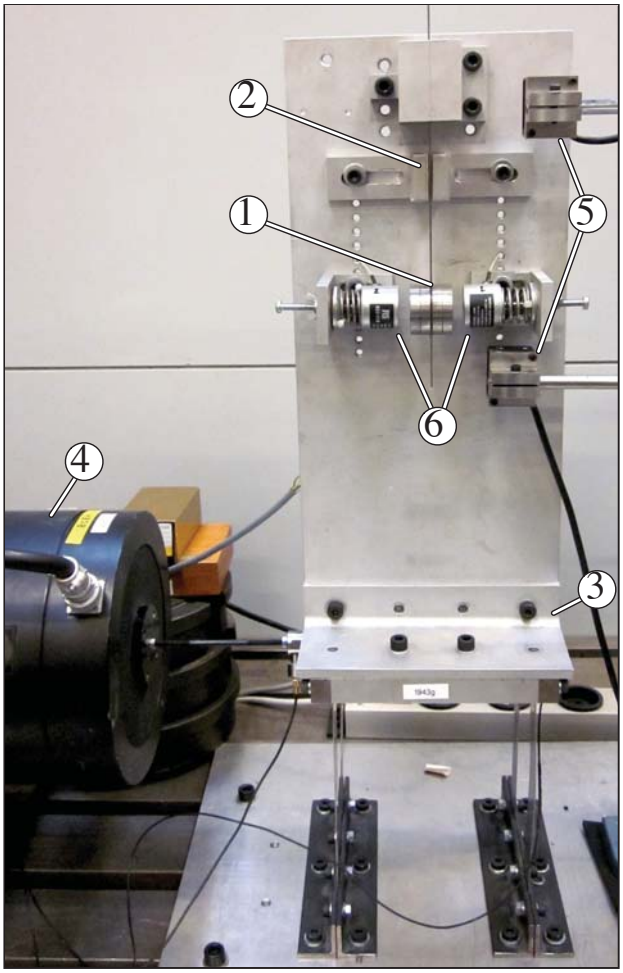

FIGURE 4. THE EXPERIMENTAL TEST RIG. (1) FLEXIBLE PENDULUM, (2) MECHANICAL STOPS, (3) BASE STRUCTURE, (4) ELECTROMAGNETIC SHAKER, (5) LASER DISPLACEMENT SENSORS, (6) ELECTROMAGNETIC ACTUATORS.

For our experiments, this is not a problem; the test-rig can still be used for proof of concept, and it introduces a scaling, which lowers the forcing amplitude around the resonance. This means that we can use more force overall, making better use of the resolution of the sensors. A similar experimental test rig was investigated in [11, 12] showing many of the same dynamical features.

Figure 5 illustrates the communication between software and hardware. Tasks that have to be executed in real time run on the dSPACE board, while the continuation core algorithm and plot routines run asynchronously on the computer. The real time application generates the excitation signal that is sent to the electromagnetic shaker and constructs the control signal based on the difference between the reference trajectory and the measured relative displacement. The control-scheme is implemented using a standard MATLAB/Simulink PD-controller block. Communication between the computer and the board is performed by using the MLIB/MTRACE MATLAB interface libraries provided by dSPACE. Simulink-blocks for composing and decomposing periodic signals from and to their approximated Fourier coefficients in real time are implemented on the dSPACE board. The computer also runs dSPACE ControlDesk, which is used to monitor various parameters during the experiments.

The PD-controller was tuned using a brute-force sweep method. Different sets of gains was tested in terms of stability and non-invasiveness of the control, in order to find an optimal combination af gains. Details can be found in [7].

RESULTS

Continuation

Figure 6 shows frequency responses for the experimental test-rig obtained by both control-based continuation and frequency-sweep. Note that the curve obtained by continuation matches the result found by the frequency sweep, but also captures a branch of unstable steady states. The traced curve is seen to be irregular for high amplitudes. To some extend, this is an artifact of the interpolation algorithm used by the continuation

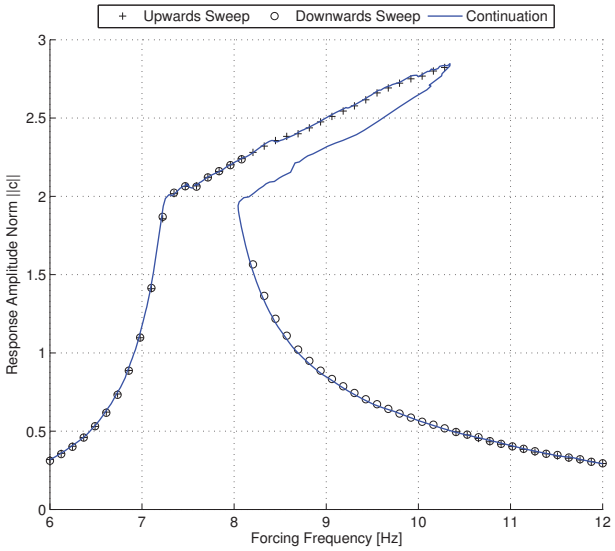

FIGURE 6. FREQUENCY RESPONSE OBTAINED BY CONTROL-BASED CONTINUATION AND PARAMETER SWEEP

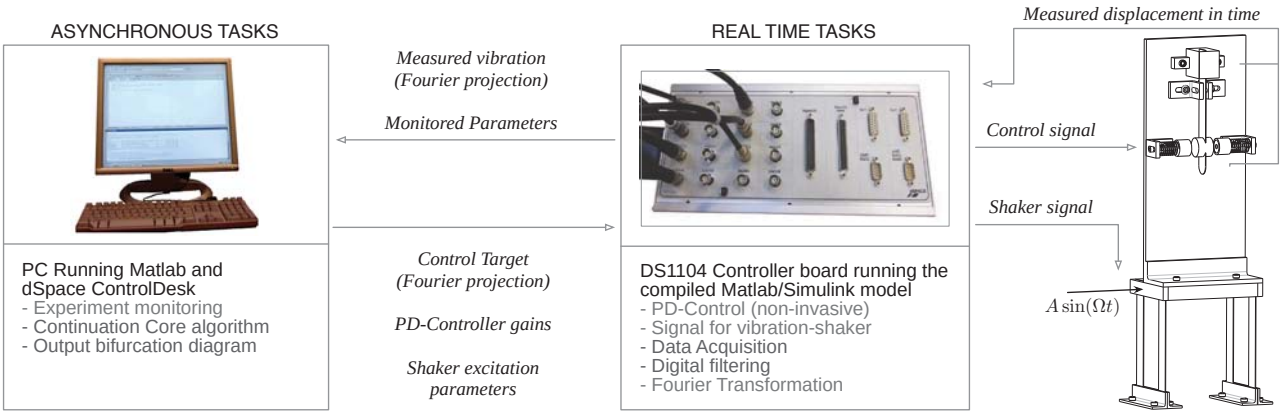

FIGURE 5. OVERVIEW OF THE COMMUNICATION BETWEEN HARDWARE AND SOFTWARE.

code (which we are working on improving), but also due to complicated dynamical features such as small hysteresis loops along the tracked curve.

Preliminary Tests for Stability Determination

Figure 7 shows another frequency response for the test-rig. Three different co-existing dynamical equilibria states are marked at a forcing frequency of 9 Hz: (1) Upper stable steady state, (2) Unstable steady state, (3) Lower stable steady state. Next we show how the system behaves when the control is turned off. This gives an indication of the usefulness of the different strategies proposed for determining stability. The tests relies on a newly implemented option to resume and correct a state from a previous continuation.

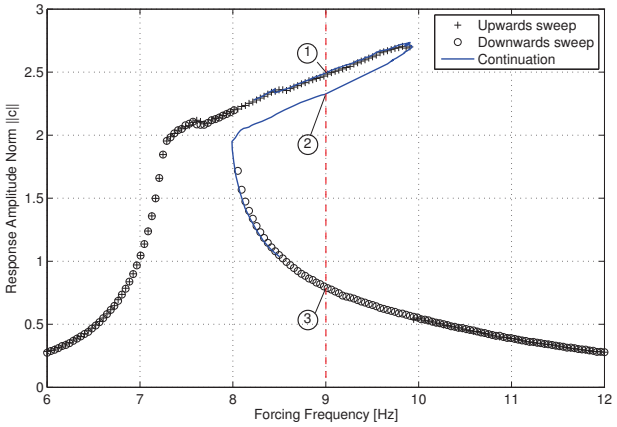

FIGURE 7. MULTIPLE CO-EXISTING STATES. (1) UPPER STABLE, (2) UNSTABLE, (3) LOWER STABLE.

Figure 8 shows a measured time-series with the system initiated on the unstable state (2) (cf. Fig. 7). After some time, the control is turned off, and the system diverges until it finally settles on the lower stable state (3). The *target trajectory* shown in the plot is the reference that the continuation requests from the control, when this is turned on. After the system has settled on the lower stable state (3), the control is turned back on, and the unstable state (2) is resumed.

Figure 9 shows a test similar to the previous. The system is initiated on the unstable state (2) and the control is turned off. In this case the system diverges until it settles onto the upper equilibrium (1), which is seen to have a slightly higher amplitude and is phase-shifted in comparison with the unstable state (2), and hence the target trajectory.

Figure 10 shows a test where the system is initiated on the upper stable state (1), and the control is switched off. As should be expected, the system does not diverge. Note that the control signal has approximately the same amplitude in all the three cases (Figs. 8 - 10), and that the stable state is maintained without any perturbation, when turning off the control (Fig. 10). This indicates that once the target trajectory is converged to a natural state for the system, the control power exerted is of noise level and our control is practically non-invasive.

DISCUSSION

The presented experimental results of applying control-based continuation (Figs. 6 and 7), show that the method works well to obtain bifurcation diagrams directly from an experiment. It can produce results similar to those of the parameter-sweeps and mathematical models. In addition to parameter-sweeps, the method is able to continue past folds and measure branches of unstable steady state dynamics. The refinement of details along the tracked curve is limited only by the quality of the measure-

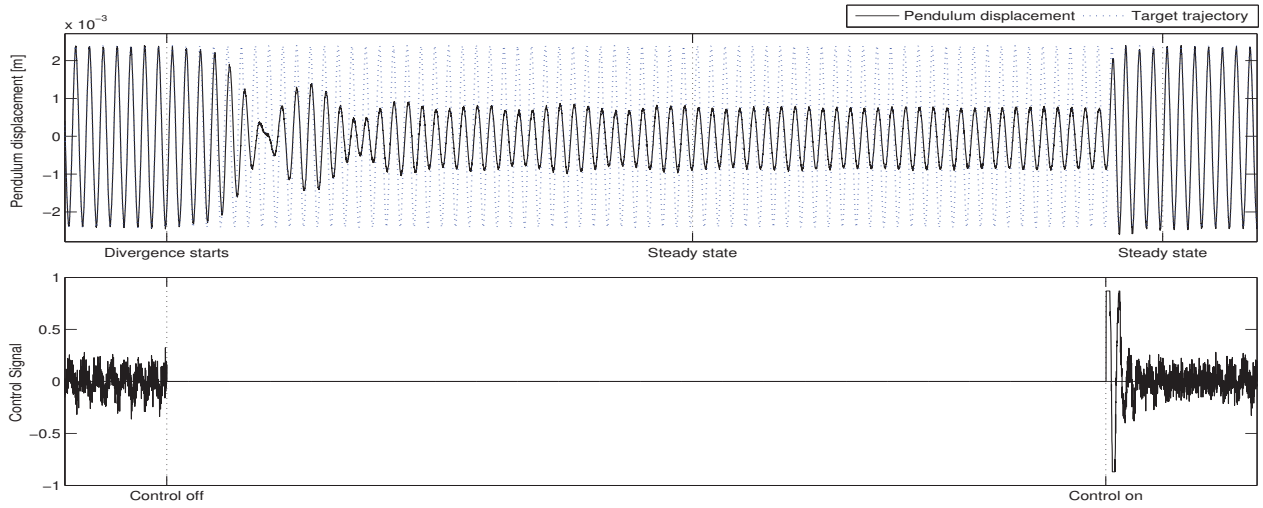

FIGURE 8. TIME SERIES: UNSTABLE STATE TO LOWER STABLE STATE.

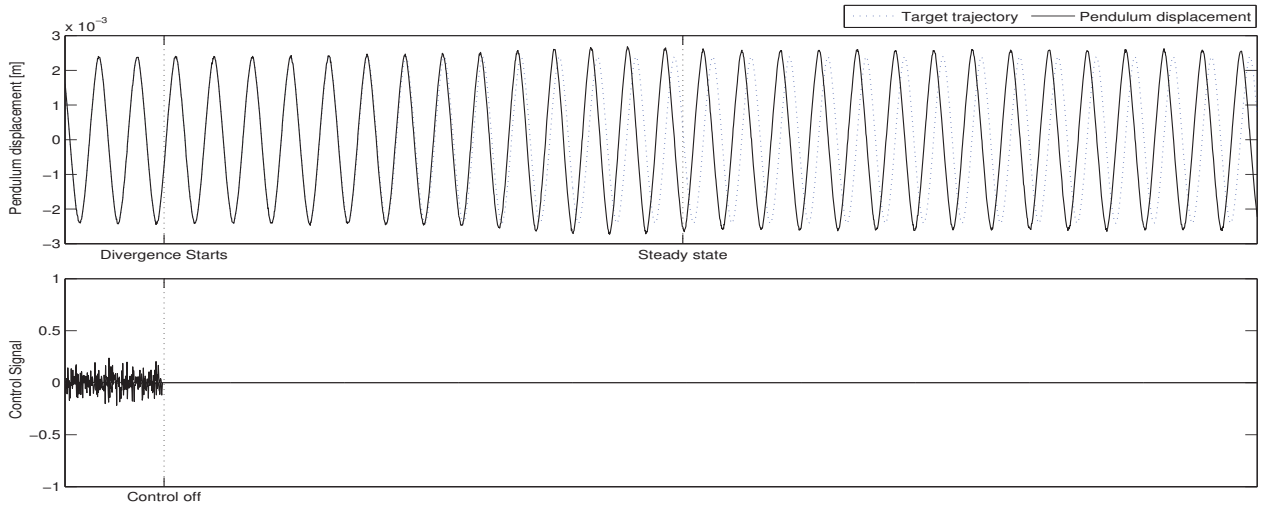

FIGURE 9. TIME SERIES: UNSTABLE STATE TO UPPER STABLE STATE.

ments and the control. In turn, forcing the continuation algorithm to use larger prediction-steps, it is to a certain extend possible to disregard small-scale dynamical features. For each step the continuation algorithm takes along the curve, it measures and interpolates many points. The interpolation-algorithm occasionally gives rise to undesirable artifacts. We are currently improving this.

The preliminary tests in Figs. 8, 9 and 10, show promising results for successful implementation of the different strategies for checking stability. The system diverges slowly from unstable equilibrium states, and can be resumed from any state, meaning that any of the proposed strategies for determining stability should be successful in future work. The stability check could be implemented for every step the continuation accepts as a natural state. Furthermore, the event-handling build into COCO [8, 9] should be able to locate the bifurcation point where stability changes. The aim is to produce experimental results resembling the theoretical curve of Fig. 1. That is, frequency response and similar bifurcation diagrams, with indication of stability along the traced branches.

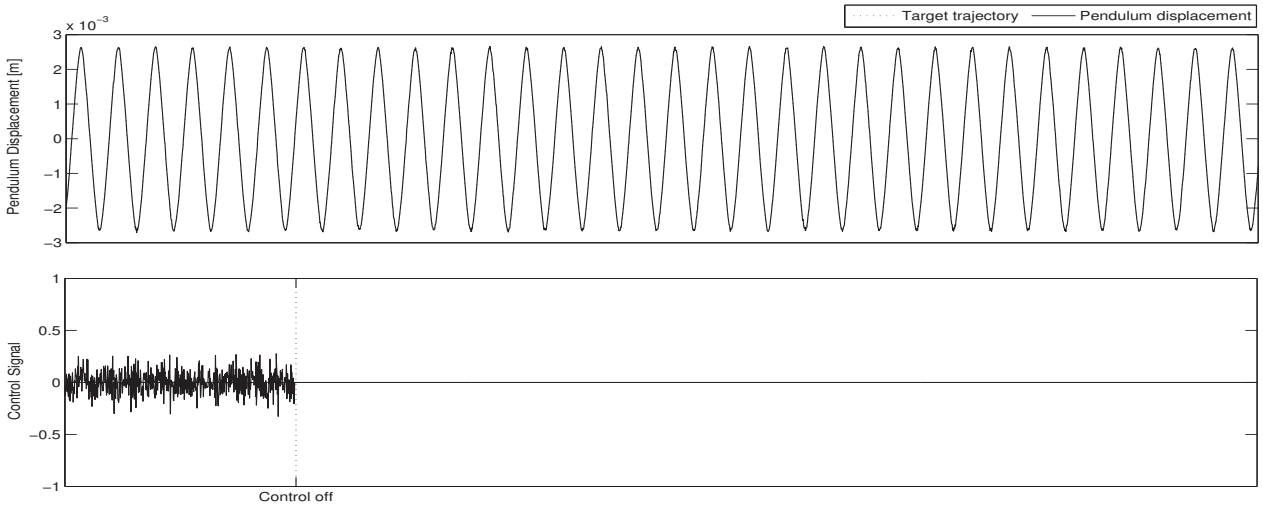

FIGURE 10. TIME SERIES: STABLE STATE.

ACKNOWLEDGMENT

This work is funded by the Danish Research Council FTP.

REFERENCES

[1] Sieber, J., and Krauskopf, B., 2008. "Control based bifurcation analysis for experiments". *Nonlinear Dynamics,* ***51***(3), pp. 365–377.

[2] Sieber, J., and Krauskopf, B., 2007. "Control-based continuation of periodic orbits with a time-delayed difference scheme". *International Journal of Bifurcation and Chaos,* ***17***(8), pp. 2579–2593.

[3] Sieber, J., Gonzalez-Buelga, A., Neild, S., Wagg, D., and Krauskopf, B., 2008. "Experimental Continuation of Periodic Orbits through a Fold". *Physical Review Letters,* ***100***, June, p. 244101.

[4] Sieber, J., and Krauskopf, B., 2009. "Using feedback control and Newton iterations to track dynamically unstable phenomena in experiments". *IFAC Proceedings Volumes (IFAC-PapersOnline),* ***2***(PART 1), pp. 211–216.

[5] Sieber, J., Krauskopf, B., Wagg, D., Neild, S., and Gonzalez-Buelga, A., 2011. "Control-Based Continuation of Unstable Periodic Orbits". *Journal of Computational and Nonlinear Dynamics,* ***6***(1), pp. –.

[6] Barton, D. A. W., and Burrow, S. G., 2011. "Numerical Continuation in a Physical Experiment: Investigation of a Nonlinear Energy Harvester". *Journal of Computational and Nonlinear Dynamics,* ***6***(1).

[7] Bureau, E., Schilder, F., Santos, I., Thomsen, J. J., and Starke, J., 2011. "Experimental bifurcation analysis for a driven nonlinear flexible pendulum using control-based continuation". In 7th European Nonlinear Dynamics Conference (Rome) Proceedings.

[8] Dankowicz, H., and Schilder, F., 2012. Coco - continuation core and toolboxes. On the WWW. URL `http://sourceforge.net/projects/cocotools/`.

[9] Dankowicz, H., and Schilder, F., 2011. "An extended continuation problem for bifurcation analysis in the presence of constraints". *Journal of Computational and Nonlinear Dynamics,* ***6***(3), p. 031003.

[10] Doedel, E. J., Champneys, A. R., Fairgrieve, T. F., Kuznetsov, Y. A., Sandstede, B., and Wang, X., 1997. Auto 97: Continuation and bifurcation software for ordinary differential equations (with homcont). Tech. rep., Concordia University. URL `http://cmvl.cs.concordia.ca/auto/`.

[11] Ing, Pavlovskaia, Wiercigroch, and Banerjee, 2008. "Experimental study of impact oscillator with one-sided elastic constraint". *Philosophical Transactions of the Royal Society London, Series A (Mathematical, Physical and Engineering Sciences),* ***366***(1866), pp. 679–704.

[12] Ing, J., Pavlovskaia, E., Wiercigroch, M., and Banerjee, S., 2010. "Bifurcation analysis of an impact oscillator with a one-sided elastic constraint near grazing". *Physica D: Nonlinear Phenomena,* ***239***(6), pp. 312–321.

P4 Publication 4

The following manuscript [P4] was submitted to Journal of Sound and Vibration in October 2013 and has been accepted for publication. It presents and successfully implements three different methods for determining the stability of equilibrium states during continuation.

Experimental Bifurcation Analysis of an Impact Oscillator - Determining Stability

Emil Bureau[a,*], Frank Schilder[b], Michael Elmegård[b], Ilmar F. Santos[a], Jon J. Thomsen[a], Jens Starke[b]

[a] *Department of Mechanical Engineering, Technical University of Denmark*
[b] *Department of Applied Mathematics and Computer Science, Technical University of Denmark*

Abstract

We propose and investigate three different methods for assessing stability of dynamical equilibrium states during experimental bifurcation analysis, using a control-based continuation method. The idea is to modify or turn off the control at an equilibrium state and study the resulting behavior. As a proof of concept the three methods are successfully implemented and tested for a harmonically forced impact oscillator with a hardening spring nonlinearity, and controlled by electromagnetic actuators. We show that under certain conditions it is possible to quantify the instability in terms of finite-time Lyapunov exponents. As a special case we study an isolated branch in the bifurcation diagram brought into existence by a 1:3 subharmonic resonance. On this isola it is only possible to determine stability using one of the three methods, which is due to the fact that only this method guarantees that the equilibrium state can be restored after measuring stability.

Keywords: Control-based Continuation, Experimental Bifurcation Analysis, Impact Oscillator, Electromagnetic Actuators, Determining Stability, Finite-Time Lyapunov Exponent (FTLE)

1. Introduction

We propose and test different strategies for experimentally determining the stability of dynamical equilibrium states (here periodic orbits with stationary amplitude) that can be applied when conducting experimental bifurcation analysis using a control-based continuation method. Control-based continuation [1, 2, 3, 4, 5, 6] is a technique that allows path following of stable as well as unstable dynamical equilibrium states under variation of system parameters, i.e. it enables investigations of the type shown in Figure 1. The method utilizes a non-invasive stabilizing control, which locally turns both stable and unstable equilibrium states into asymptotically stable ones. A consequence of adding control is that investigating the Jacobian or fitting a simple model to judge the stability of the system will yield information about the artificially stabilized system rather than the underlying uncontrolled system.

Following Lyapunov's idea of defining stability, we show how it is possible to assess the stability by modifying or turning off the control signal for a certain amount of time, and study the resulting behavior of the system. As a result it is possible to experimentally obtain bifurcation diagrams with indication of the stability of individual branches as well as locating the bifurcation points where the stability changes, cf. Figure 1. Under certain conditions it is possible to quantify the rate of divergence from an unstable state in terms of the finite-time Lyapunov exponent (FTLE). Depending on the type of system, it may be unacceptable to allow unbounded divergence from an unstable equilibrium: The divergence must not alter the system and the control must be able to restore the equilibrium state after the stability check. We show how it is possible to assess the stability of an equilibrium state while only allowing a limited divergence. Details on the experimental test rig (cf. Figure 2) and the implementation of the control-based continuation method are given in [6], while here we propose and test new methods for determining stability.

*Corresponding author. TEL: +45 2843 5906.
Email address: embu@mek.dtu.dk (Emil Bureau)

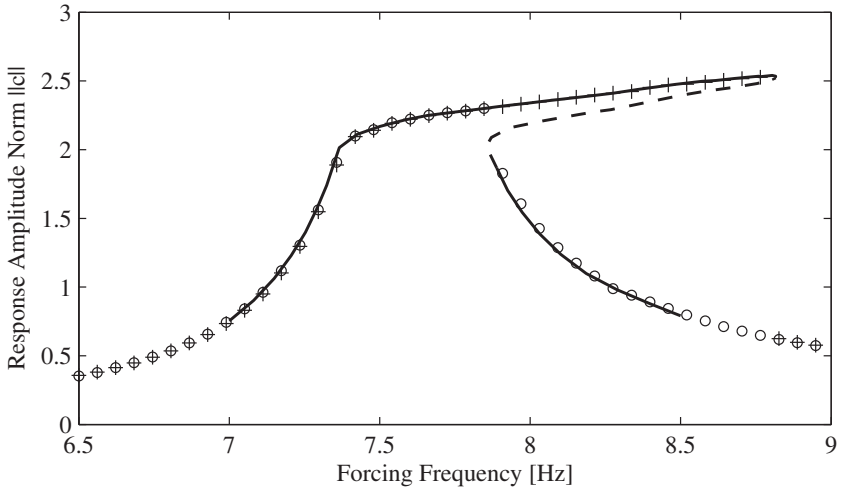

Figure 1: Experimental frequency response of a harmonically forced nonlinear impact oscillator obtained by parameter sweep and control-based continuation. Response from traditional frequency sweeps is denoted by (+) for increasing and (∘) for decreasing frequency. Response obtained by control-based continuation is denoted by (—) for stable part and (– – –) for unstable part.

2. Experimental Setup

The experimental test rig is shown in Figure 2; it comprises a harmonically forced impact oscillator with electromagnetic actuators. The impactor is a flexible beam with a tip mounted mass. The beam will impact the mechanical stops when the vibration amplitude exceeds the gap size. This impact causes an increased stiffness which results in highly nonlinear responses for certain ranges of forcing parameters, see Figure 1. Note that the electromagnetic shaker is not feedback controlled, causing a cross coupling between dynamics of the impactor and the shaker. Electromagnetic actuators mounted on each side of the impactor mass are used to generate a non-invasive control force u necessary for the control-based continuation. The direction of the generated force is dependent on the sign of the control signal. Two laser sensors are used to measure the relative displacement of the impactor mass, which is used for characterizing the current state of the experiment x. Note that several internal scalings are used in the continuation code, which means that the presented measured quantities are non-dimensionalized. The response amplitude of the impactor is measured using the norm:

$$\|c\| := \sqrt{\sum_{i=0}^{2Q} c_i^2}, \tag{1}$$

where the c_i are the Fourier components and Q denotes the number of Fourier modes used, in our experiment usually $Q = 5$. All results and plots presented throughout the paper are experimental measurements made using the test rig.

3. Suggestion of three methods for assessing stability in experiments

Control-based continuation employs a path following algorithm that tracks branches of stable and unstable equilibrium states under the variation of system parameters. It works by iterating a series of prediction and correction steps: First a prediction step is made in the tangent direction of the equilibrium branch, and then this prediction is corrected orthogonally back onto the branch using a root finding algorithm [7]. Since we are continuing dynamical equilibrium states, the predicted and current state are expressed in terms of a predicted reference trajectory $y(t)$ defined by the discrete points $y_j = y(t_j), t_j = t_0 + j\Delta t, j = 0, 1, \ldots, n$ and a measured state $x(t)$ defined by the sampled

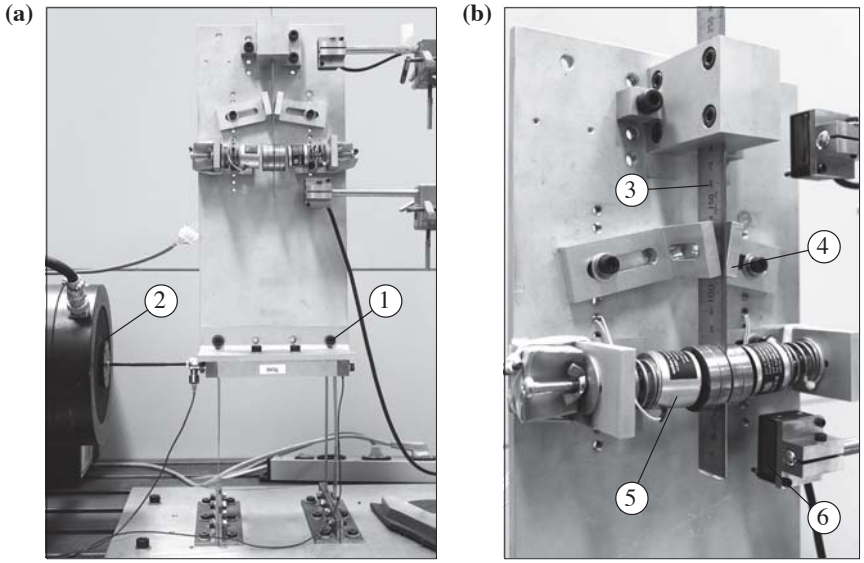

Figure 2: The experimental test rig: A harmonically forced impact oscillator with electromagnetic actuators. (a) Front view of the full test rig. (b) Impactor side view. The test rig consists of (1) a platform with flexible legs, which allows movement only in the direction of forcing; (2) an electromagnetic shaker to apply a harmonic excitation to the platform; (3) flexible beam with tip mass; (4) adjustable mechanical stops, which will cause impacts and increased stiffness when the vibration amplitude of the beam exceeds the gap size; (5) electromagnetic actuators which can exert a control force directly on the tip mass; (6) laser displacement sensors. Further details can be found in [6].

points $x_j = x(t_j)$, where $\Delta t = 1/f_s$ is the sampling interval and f_s the sampling frequency. The predicted state $y(t)$ is artificially created and stabilized by a non-invasive proportional derivative (PD) control:

$$u(t) = PD(x(t) - y(t)) := K_p(x(t) - y(t)) + K_d(\dot{x}(t) - \dot{y}(t)), \tag{2}$$

where K_p and K_d denote proportional and derivative gain, respectively.

The corrector keeps changing the reference state y until the predicted and measured state are close to identical $x - y \approx 0$, at which point the periodic contribution from control effectively vanishes ($u \approx 0$). The measured state x is accepted as a stable or unstable equilibrium state of the underlying uncontrolled system, and the control is only activated if the measured state x diverges from the reference state y. A bifurcation diagram (cf. Figure 3) consists of a number of such successful continuation steps. At each accepted state we wish to determine and possibly quantify the stability.

To determine stability information, we implement and test three simple ideas based on modifying or turning off the control, while observing the resulting behavior of the system. In theory nothing happens when turning off the control at a stable state, as long as turning off the control does not cause a perturbation to the system. Due to the fact that an experiment will have noise in both measurements and control, the continuation algorithm accepts a measured state x as an equilibrium state of the underlying uncontrolled system within some tolerance. Therefore, one must expect a small residual drift when turning off the control at a stable state. The stability tests presented here all require the tolerance with which the corrector accepts a state x as an equilibrium state to be sufficiently strict.

When turning off the control at an unstable equilibrium state, the current state x starts to diverge from the reference state y, cf. Figure 4. Branches of unstable equilibrium states act as seperatrices in the bifurcation diagram, so depending on the initial conditions given when turning off the control, the state will diverge and settle onto another stable state; in our system either a higher or a lower amplitude stable equilibrium state, cf. Figure 3. If the noise in the experiment is very low, it might be necessary to introduce a small in-phase perturbation in order to facilitate the divergence, but in our case the imperfections in the experiment make this unnecessary. In [6] it is explained how to implement such an in-phase perturbation and an in depth investigation of the effects of turning off the control at stable and unstable states is presented in [8].

Stability might also be assessed by locally identifying a linear model using grey- or black-box modelling on either the open- or closed-loop system; see [9, 10, 11] for reviews of these methods. The control-based continuation method is tailored towards experimental investigations of strongly non-linear dynamical systems, in some cases with unknown actuator dynamics, for which one might not want or might not be able to make model assumptions. Therefore, we restrict our attention here to methods that rely on observations only and, hence, allow for unconditional assessment of (in)stability.

3.1. Method 1: Free flight stability check

The first method is based on a simple heuristic idea: Turn off the control actuators and observe if the current state x diverges from the reference state y, implying that the equilibrium state is unstable. Figure 5 presents time series from such an experiment starting from different equilibrium states. A conclusion to draw from these time series is that it can be helpful to study the divergence of the difference $x - y$ rather than x. A state can diverge from an equilibrium both in amplitude and phase and the latter is more pronounced in the difference $x - y$ (compare Figure 5b and 5c). We define a normalized root mean square error

$$\varepsilon = \frac{\mathrm{RMS}(x - y)}{1 + \mathrm{RMS}(y)} \tag{3}$$

where RMS denotes the root mean square value of a sampled signal defined as

$$\mathrm{RMS}(x) = \sqrt{\frac{1}{n}\left(x_1^2 + x_2^2 + \cdots + x_n^2\right)}. \tag{4}$$

The error ε provides a combined measure of how fast and far a state x diverges from a reference state y upon disabling control, and it seems to be a robust measure of instability. A large error ε means that the state x has diverged from the reference state y, and we consider it to be unstable. Since ε is a continuous measure (it can assume any real

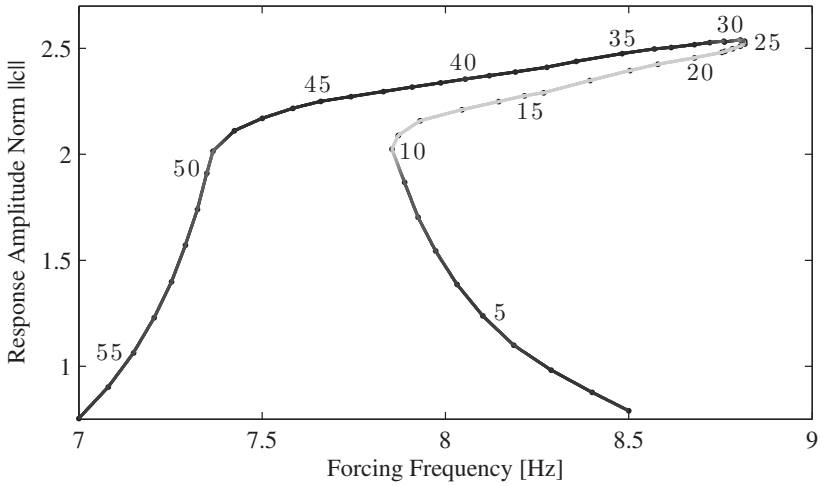

Figure 3: Bifurcation diagram with a continuous measure of stability plotted in grayscale (interpolated in between measurement points): Dark tones denote a small stability estimator and hence a stable state. Lighter tones denote a large stability estimator and hence an unstable state. All measurement points are marked with (·) and consecutively number labeled (shown for every fifth point). These labels will be used to identify different equilibrium states and will be referred to with # and label number throughout the paper.

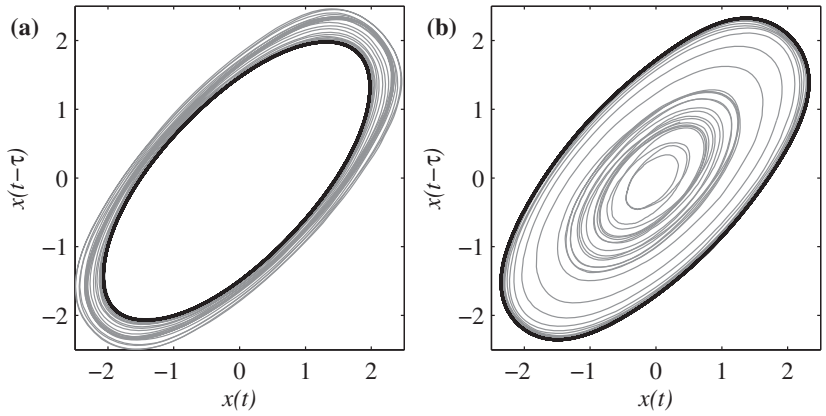

Figure 4: Reconstructed phase plane orbits using the current state $x(t)$ and a delayed coordinate $x(t-\tau)$, showing two examples of divergence from unstable equilibrium states. (a) System is initialized on the stabilized equilibrium state marked by #10 in Figure 3 corresponding to the initial orbit (▬). Once the control is disabled, the measured state x starts to diverge from this equilibrium state and settles onto the upper branch, at slightly larger amplitude. (b) Control is disabled from state #16 which results in x diverging and settling onto the lower branch, at a much smaller amplitude.

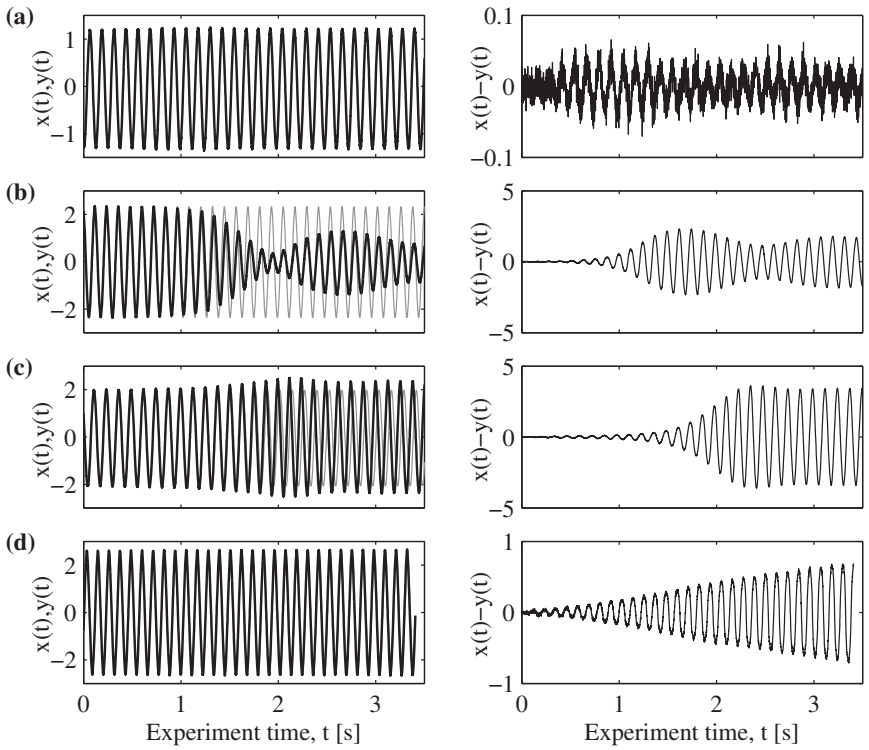

Figure 5: Time series for free flight stability tests. Left column: Time series of x (—) and y (—). Right column: Difference between current state and reference state ($x - y$). (a) Starting at a stable state (#5). (b) Divergence from unstable (#16) and settling onto lower amplitude stable state, the divergence predominantly changes the amplitude. (c) Divergence from unstable (#10) onto higher amplitude stable state, the divergence changes both phase and amplitude. (d) Stability test at a state very close to the upper fold point (#24), divergence is weakly exponential since the state is close to marginally stable. Note the different scales of the vertical axis in the right column.

number ≥ 0) it is required to select a threshold for instability. If the error exceeds this threshold, the equilibrium state is considered unstable and vice versa. Figure 6 shows the error ε for each point of the bifurcation diagram in Figure 3 along with the chosen threshold for stability. The grayscale used in Figure 3 reflects the value of ε and is interpolated between each measured point along the curve. It appears that the estimator predicts a region of instability that is in good agreement with theory.

There are some precautions to take when using the free flight stability test: Some systems can be allowed to have unbounded divergence, while others cannot. In order to resume the continuation after a stability check, the control must be able to restore the system to the reference state. This requires the divergence not to damage or alter the system, and requires more available control energy than is necessary for the continuation itself. Furthermore, stable and unstable states may lie close in phase space, and depending on precision of the test equipment it may be hard to distill a binary measure of stability, as the indicator for stability in some cases approaches the threshold for instability smoothly (cf. Figure 6).

Interpreting the time series for x or the difference $x - y$ (cf. Figure 5) is straightforward for some states but less obvious for others. Signals may look qualitatively different, depending on their location in the bifurcation diagram. Nevertheless the divergence seems to be close to exponential for most unstable states, which means that a one degree

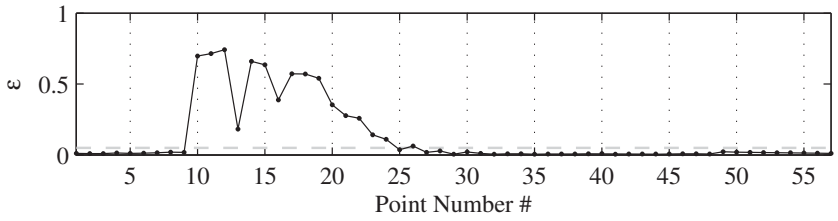

Figure 6: Stability indicator ε for the bifurcation diagram in Figure 3. Numbers on the x-axis correspond to label numbers along the bifurcation branch. The chosen threshold, which indicates the limit of instability $\varepsilon_t = 0.05$, is marked by (- - -).

of freedom linear harmonic oscillator solution of the form: $x - y = Ae^{\lambda t}\cos(\omega t + \phi) + d$ (with variable phase ϕ, variable amplitude A and DC-offset d) can be fitted. The finite-time Lyapunov exponent λ will give information about how fast the system diverges. A more simple strategy is to do a linear fit to the logarithm of the peaks (cf. Figure 7), which compares to looking at a Poincaré section. The slope of the linear fit will also yield the finite-time Lyapunov exponent λ.

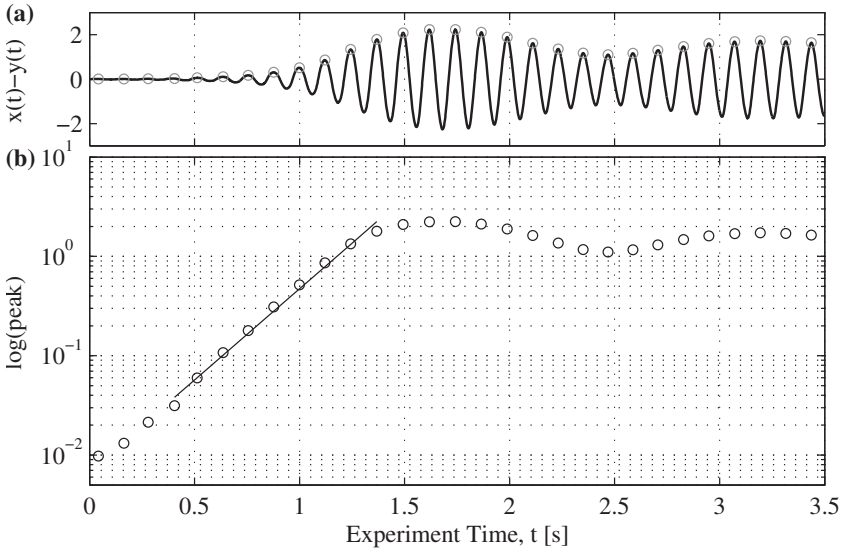

Figure 7: Retrieving stability information for an unstable state (#16) by using a linear fit to the logarithm of the peaks. (a) Smoothened difference $x - y$ with detected peaks (using the Matlab functions: Smooth (moving average filter from the Curve Fitting Toolbox) with a 20 points window and Findpeaks (Signal Processing Toolbox)). (b) Logarithmic plot of the detected peaks (∘) along with linear fit (—) in the time-interval $t \in [0.4; 1.2]$.

3.2. Method 2: Stability check using deadband control

We introduce a deadband Π in the non-invasive control signal (2)

$$u(t) = \begin{cases} 0 & \text{for } \|PD(x(t) - y(t))\| \leq \Pi \\ PD(x(t) - y(t)) & \text{for } \|PD(x(t) - y(t))\| > \Pi. \end{cases} \tag{5}$$

Now nonzero control will only be enabled when the requested control signal exceeds the deadband. Proper choice of this deadband will cause the control to enable only if the state x diverges from the reference state y. Stability is determined by noting if the control was enabled. The number of control bursts might also be used as a semi-continuous measure of stability for more noisy systems. Figure 8 shows time series for a deadband stability check for a stable and an unstable state. Note that the control is only enabled for the unstable state, and that the state x is not allowed to have unbounded divergence. The width of the deadband can be selected to be of the same order of magnitude as the noise in the control signal, but in Figure 8 it has been kept relatively wide for visualization purposes. For the deadband stability check to work, the deadband must be correctly adjusted (considering noise, closeness of nearby states and the controls' ability to restore the system) and the time window for the stability check must be long enough for the system to diverge noticeably at all unstable states.

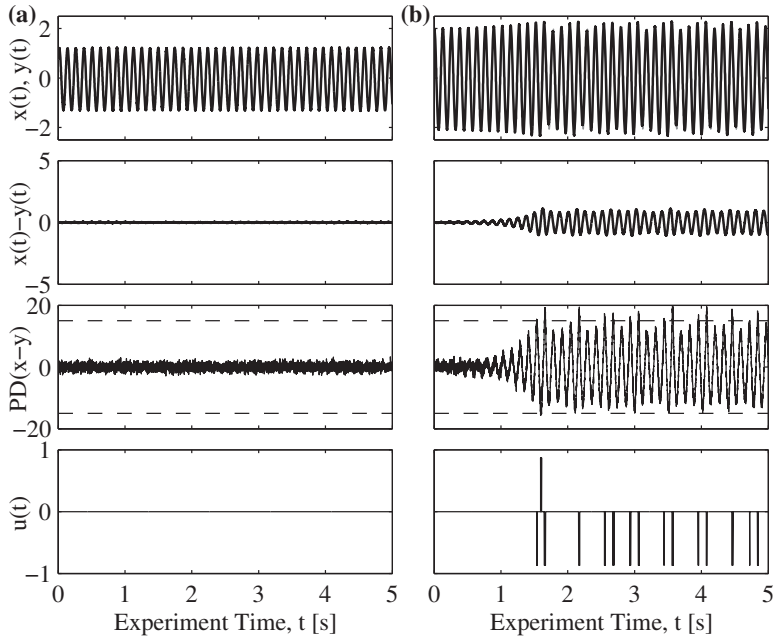

Figure 8: Time series for deadband control stability tests at (a) a stable state (#5) and (b) an unstable state (#10). Deadband limits (**- - -**) are shown together with controller output in the third panel and the deadbanded control signal which is sent to the actuators is shown in the fourth panel. Note that the control is only active for the unstable state (b) and that it manages to reduce the divergence amplitude of the system comparing with Figure 5c.

3.3. Method 3: Deadband-limited free flight

This method combines the advantages of Method 1 and 2 in order to measure finite-time Lyapunov exponents λ without allowing unbounded divergence. The trade-off is that the method requires conditions which cannot always be expected from an experiment: The measurements have to be relatively clean, and the divergence has to be approximately exponential. Furthermore, the measured states must be allowed to diverge inside the deadband, which requires the divergence to be completely reversible by the control. In other words, the divergence must not alter the system and the control must be able to restore the equilibrium state after measuring stability.

We modify the deadband control such that whenever the deadband is exceeded ($\|PD(x(t) - y(t))\| > \Pi$) the control signal $u(t)$ is held active for a certain time interval $T \in [t_{enable}; t_{enable+hold}]$. Consequently, the system is restored to the reference state meaning that $x - y \approx 0$. The result is a sequence with several periods of free flight limited to diverge only inside the deadband as it is shown in Figure 9. For a sufficiently narrow deadband the divergence will only include the local (linearized) behavior and not allow the system to settle onto a different stable equilibrium state. Our observations suggest that the estimated Lyapunov exponent is not dependent on which side of the branch of unstable equilibria the state diverges to, as long as we only study the local behavior. For each stability check (at every point of the bifurcation curve) the following postprocessing is performed:

1. Center the data set $x - y$ by subtracting its mean value.
2. Smoothen the time series using a moving average / lowpass filter. In Matlab this can be done by using the function 'Smooth' (Curve Fitting Toolbox).
3. Detect peaks of the absolute value of the smoothened signal to get both positive and negative peaks. It can be helpful to use a peak detection algorithm that can discard values smaller than a certain tolerance and require the peaks to be separated by a certain time span. In Matlab this can be done using the function 'Findpeaks' (Signal Processing Toolbox).
4. Divide the data set into separate segments of free flight. This can be done by checking the control signal, as this is zero when the system is in free flight, cf. Figure 9.
5. Evaluate the Cooks' distance [12] for each segment and use this information to remove statistical outliers from the data sets.
6. Perform linear interpolation on each set of peak data and average the slopes to get the finite-time Lyapunov exponent λ.

Near the fold points of the frequency response we experience a slow divergence (Figure 5d) but the exponential fit still seems to be robust, cf. Figure 10. Note also that the method only estimates the divergence rates for unstable states. For stable states the stability is not quantified and the value is set to zero for plotting purposes. For noisy experiments or experiments with low sampling rate, it can be helpful to consider intersections with a hyper plane in the phase space (e.g. zero velocity crossings) rather than detecting peaks of a time series, as the intersection can be located by linear interpolation [13].

4. Results

The following will present the results of applying the three suggested methods for determining stability during continuation using the test rig presented in Figure 2.

4.1. Continuation results

Figure 11 presents five consecutive continuation runs overlaid along with stability information obtained by the three different stability test methods. Note that Method 1 and 2 give very similar results, while Method 3 estimates the fold point amplitudes a bit higher and with less deviation than the other methods.

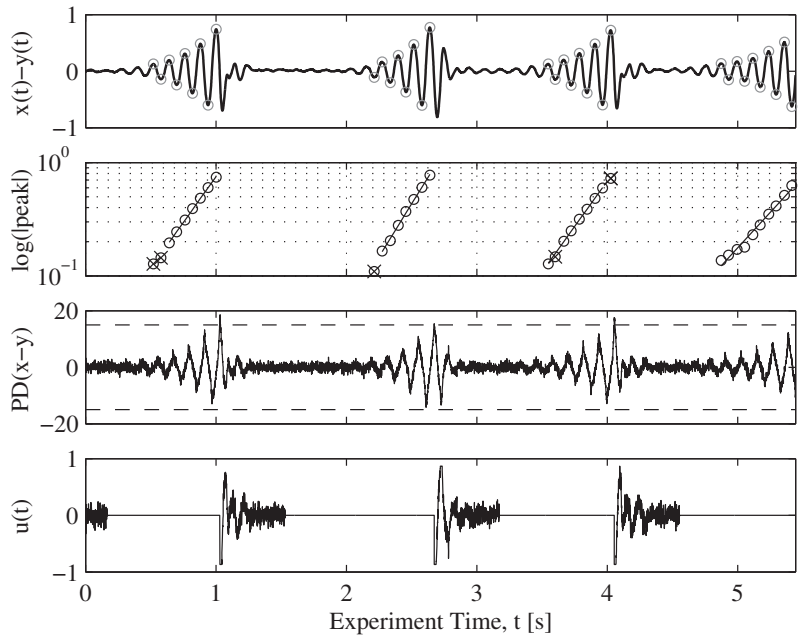

Figure 9: Deadband-limited free flight stability check at an unstable state (#16). Removed outliers are marked by (×) in fit. Average Lyapunov exponent: $\lambda = 3.65 \pm 0.58$.

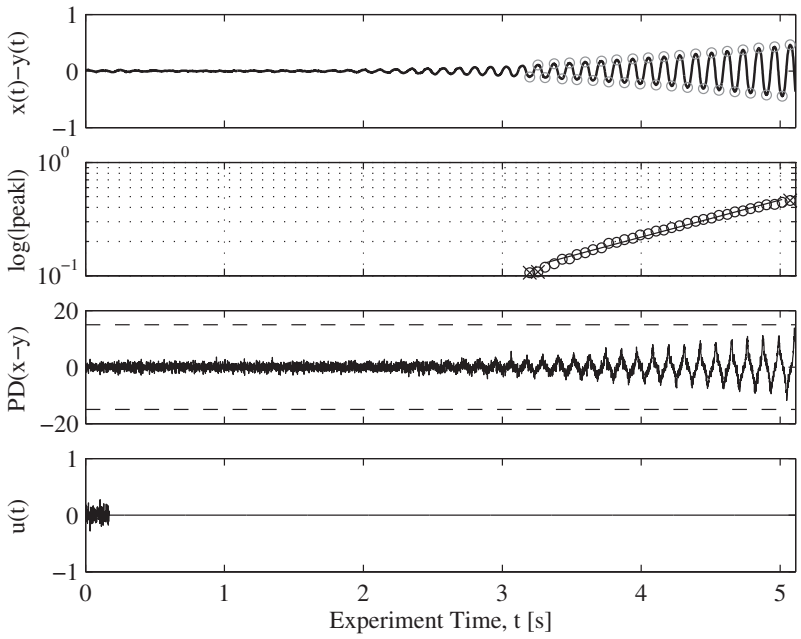

Figure 10: Deadband-limited free flight stability check near the upper fold point (#24). Average Lyapunov exponent: $\lambda = 0.76$. Note the slow divergence compared to the one in Figure 9.

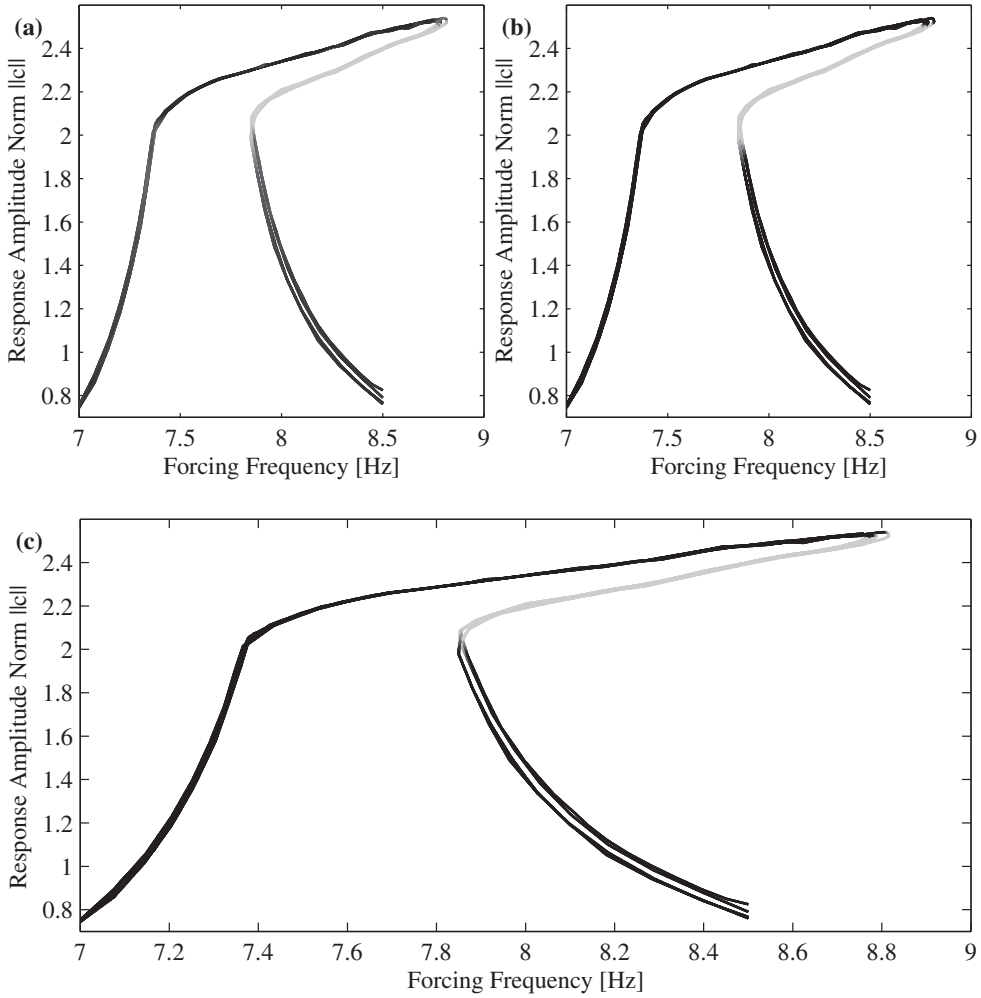

Figure 11: Five overlaid bifurcation diagrams for forcing strength $A = 0.5$ with stability estimator plotted in grayscale (dark for small values, light for larger values). Stability information retrieved using (a) the free flight method (Method 1), (b) the deadband control method (Method 2) and (c) the deadband-limited free flight method with Lyapunov exponent estimation (Method 3). Note that the grayscale has been scaled nonlinearly to visualize the change of stability at the fold points rather than the variation of the estimator along the unstable part of the branch.

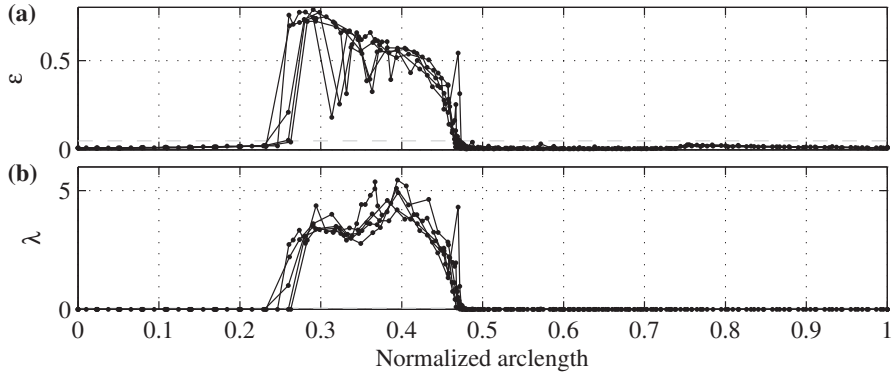

Figure 12: Stability estimator (normalized with respect to arclength of the branch in the bifurcation diagram) of multiple continuation runs. Chosen stability threshold $\varepsilon_t = 0.05$ is marked by (- - -). Top panel shows the normalized root mean square error ε for a free flight test (Method 1). Bottom panel shows the averaged Lyapunov exponent estimated by the deadband-limited free flight method (Method 3).

4.2. Stability near the fold points

Figure 12 shows the stability estimators for the five bifurcation diagrams depicted in Figure 11, calculated using methods 1 and 3. They are normalized with respect to the total arclength of the corresponding branch, e.g. applying this normalization to Figure 6 the first and last point would get values zero and one respectively. This is necessary since we use an adaptive continuation step length, causing the number of points along each branch to vary. The two methods are seen to give qualitatively similar results, but the free flight test (cf. Figure 12(a)) shows a large jump in estimator at the lower fold point and a smooth transition across the stability limit at the upper fold point. We ascribe this to the fact that the normalized root mean square error ε is a combined measure of how fast and far a state diverges, rather than an explicit divergence rate such as the finite-time Lyapunov exponent. At the lower fold point, the system diverges and settles onto a stable state quite far from the unstable state, whereas close to the upper fold the bifurcation branches lie very close (cf. Figure 13) causing a short divergence before settling onto a nearby stable state. In comparison, the divergence rate λ in Figure 12(b) changes smoothly with respect to the arclength at both fold points. Note that Method 3 detects the onset of instability by the control signal exceeding the deadband which means that an equilibrium state is considered unstable when $\lambda > 0$. Figure 13 shows a zoom of the upper fold point with stability information obtained using Method 3. It is interesting to note how the rate of divergence decreases smoothly when tracking around the fold point, meaning that the stability changes smoothly along the equilibrium branch.

4.3. Stability at a family of isolated equilibrium branches (isola)

Figure 14 presents the experimental finding of an isola, by which we mean a family of stable and unstable equilibrium branches that are detached from the primary resonance curve in the bifurcation diagram. This isola is created by a 1:3 subharmonic resonance, at which the impactor is forced at approximately three times its fundamental resonance frequency, but the response is approximately at its fundamental resonance frequency. The isola was found by parameter sweep and two consecutive continuation-runs. Its existence was suggested by simulation of a single-degree-of-freedom model of our test rig [14] and was initially found by systematic parameter sweeps. Several branches of stable as well as unstable equilibria seem to coexist in that parameter region and continuing of the unstable branches is a mean for mapping out a more complete picture of the possible dynamical responses. Near 26.6-26.8 Hz the branches cease to exist due to a shift in the phase between impactor and platform, i.e. the impactor and platform starts to vibrate in-phase, which causes the relative amplitude between impactor and mechanical stops to be insufficient for impact, which in turn effectively changes the response of the system. At this point, the sweep settles onto the non-impacting stable low-amplitude response, while the continuation reports non-convergence of the corrector and terminates. Our

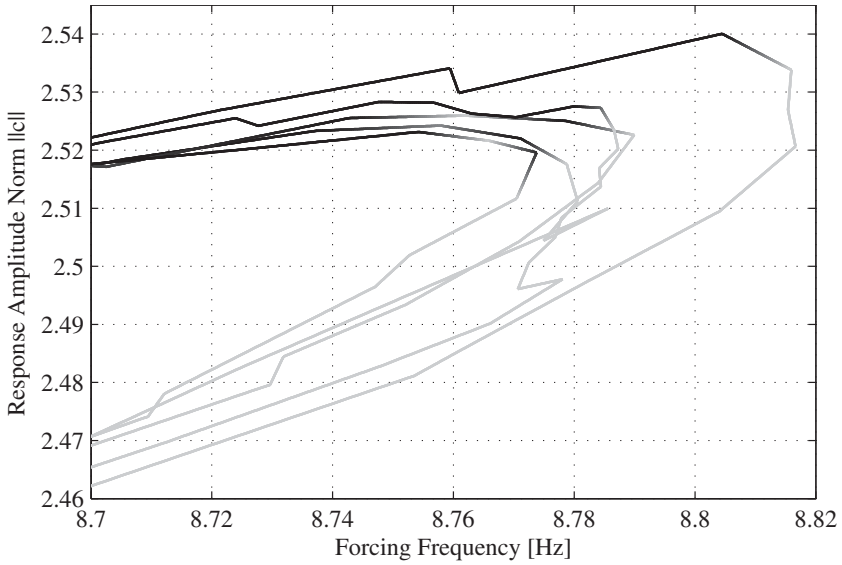

Figure 13: Zoom of the upper fold point in Figure 11(c).

observations indicate that the co-existing stable and unstable responses along the isola are so close to each other that it is very difficult to distinguish these in the experiment. Therefore, a more refined and systematic investigation of this isola seems to require an increased precision of measurements and actuation, as well as an implementation of means for systematic branch switching at bifurcation points.

For the case of the isola, it was only possible to successfully apply the deadband control stability test (Method 2), as it would otherwise not be possible for the control to restore the equilibrium states after stability check. The deadband had to be adjusted to only allow divergence just above the noise level (5 times tighter than the deadband in Figure 8). Due to noise, the control signal would exceed the deadband a few times at the stable states, causing a few control bursts, while unstable states were characterised by an effectively active control (an approximate factor of 100 more control bursts).

5. Conclusions

The experiments presented show that it is possible to assess stability during control-based continuation of bifurcation branches by momentarily modifying or turning off the control. Three different methods have been proposed: 1) Free flight stability check, 2) stability check using deadband control, and 3) deadband-limited free flight. All three methods have been successfully applied to determine stability during experimental continuation, and each of the methods is shown to be suitable in different situations:

The free flight stability test (Method 1) is robust and easy to implement but requires the divergence to be completely reversible by the control. The estimated normalized RMS error between reference and measured state is shown to give a good indication of the stability but does not provide direct information about the rate of divergence. Similarly, the deadband stability check (Method 2) does not provide information about the rate of divergence, but on the other hand has the advantage to be employable while only allowing minimal divergence. The isola presented in Section 4.3 is a good example of the usefulness of Method 2, since its ability to limit the divergence to a pre-defined maximum makes it the only of the three methods which allows stability assessment in this situation.

Finally the deadband-limited free flight method (Method 3) is able to provide an estimate of the rate of divergence while allowing only a limited divergence. In turn the method puts more requirements on the experiment, is more difficult to implement and has more parameters that need to be adjusted. The stability estimator is observed to approach

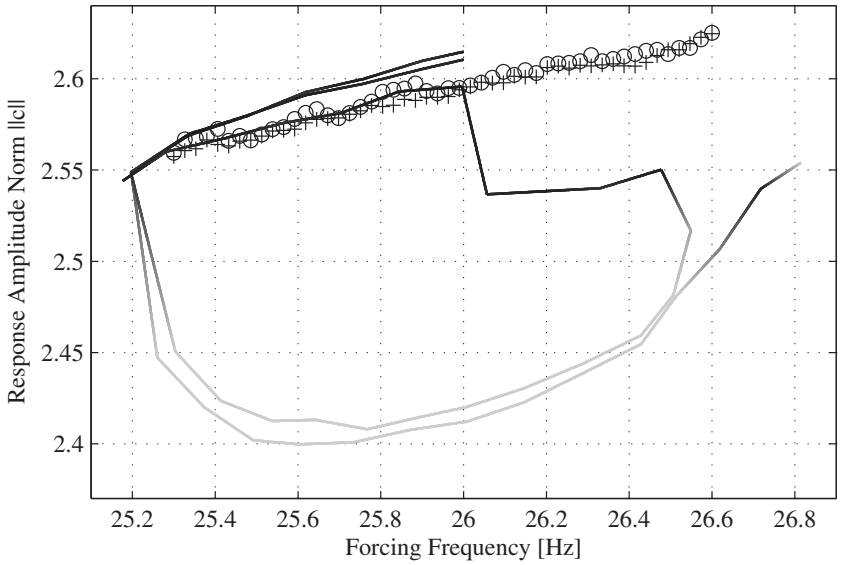

Figure 14: Isola composed of the stable and unstable equilibrium branches of a 1:3 subharmonic resonance found by a parameter sweep and two consecutive continuation-runs, using different settings for tolerances and step size. The sweep is denoted by (+) for increasing and (∘) for decreasing frequency. Stability information is assessed using Method 2.

the stability threshold smoothly at bifurcation points regardless of the stability test method. In other words, continuing a branch of equilibria, the stability is noted to change smoothly, e.g. from unstable to stable, especially at the upper fold point. A quantitative measure of stability is determined only at unstable states; to extend the capability to stable states, one could introduce an in-phase perturbation and measure the (exponential) decay of transients. Unfortunately, for the system that we investigate this is difficult because the transients are damped out within few oscillations at stable equilibrium states away from the fold points. To get just a few points for estimation the perturbation has to be so strong it effectively changes the response of the system. This could possibly be improved using a fitting method which fits the whole data set rather than just the peaks.

The isola presented in Figure 14 serves as a good example of the usefulness of control-based continuation method with additional stability investigations. It shows how the method can be used to obtain a more complete picture of the bifurcation diagram in regions where multiple stable and unstable equilibrium states coexist. Furthermore, it is seen that continuing branches of unstable equilibria can be the key in discovering seemingly unconnected stable equilibrium branches. It also points out room for improvement, by underlining the need for a method to switch between multiple branches at bifurcation points. Other possibilities for future research include fitting the time series obtained during free flight to a single-degree-of-freedom harmonic oscillator to get statistically more accurate estimates of the finite-time Lyapunov exponents. It might also be possible to determine the stability directly from the control signal. In our experiments the control signal appears to be uncorrelated noise once the correction step has converged, regardless of the stability of the equilibrium state. Perhaps superimposing the control with a noise signal or even introducing a locally destabilizing control can help to develop maybe a faster method to determine stability and to obtain further insights.

6. Acknowledgements

This work was supported by the Danish Research Council FTP under the project number 09-065890/FTP. The authors wish to thank Jan Sieber, David Barton, Harry Dankowicz and Bernd Krauskopf for helpful comments when setting up the experiments and Viktor Avrutin for his help with the model investigations of the isola.

References

[1] J. Sieber, B. Krauskopf, Control based bifurcation analysis for experiments, Nonlinear Dynamics 51 (3) (2008) 365–377. doi:10.1007/s11071-007-9217-2.

[2] J. Sieber, A. Gonzalez-Buelga, S. Neild, D. Wagg, B. Krauskopf, Experimental Continuation of Periodic Orbits through a Fold, Physical Review Letters 100 (2008) 244101. doi:10.1103/PhysRevLett.100.244101.

[3] J. Sieber, B. Krauskopf, D. Wagg, S. Neild, A. Gonzalez-Buelga, Control-Based Continuation of Unstable Periodic Orbits, Journal Of Computational And Nonlinear Dynamics 6 (1). doi:10.1115/1.4002101.

[4] D. A. W. Barton, S. G. Burrow, Numerical Continuation in a Physical Experiment: Investigation of a Nonlinear Energy Harvester, Journal Of Computational And Nonlinear Dynamics 6 (1). doi:10.1115/1.4002380.

[5] D. A. Barton, B. P. Mann, S. G. Burrow, Control-based continuation for investigating nonlinear experiments, Journal of Vibration and Control 18 (4) (2012) 509–520. doi:10.1177/1077546310384004.

[6] E. Bureau, I. Ferreira Santos, J. J. Thomsen, F. Schilder, J. Starke, Experimental bifurcation analysis of an impact oscillator - tuning a non-invasive control scheme, Journal of Sound and Vibration 332 (22) (2013) 5883–5897. doi:10.1016/j.jsv.2013.05.033.

[7] H. Dankowicz, F. Schilder, Recipes for continuation, Vol. 11 of Computational Science & Engineering, Society for Industrial and Applied Mathematics (SIAM), Philadelphia, PA, 2013. doi:10.1137/1.9781611972573.

[8] E. Bureau, I. Santos, J. J. Thomsen, F. Schilder, J. Starke, Experimental Bifurcation Analysis By Control-based Continuation - Determining Stability, in: Proceedings of the ASME 2012 International Design Engineering Technical Conferences & Computers and Information in Engineering Conference, 2012.

[9] J. Norton, An introduction to identification, Academic Press, 1986.

[10] L. Ljung, System identification : theory for the user, Prentice-Hall, 1987.

[11] J. R. Raol, N. K. Sinha, Advances in modelling, system identification and parameter estimation, Sadhana 25 (2) (2000) 71–73. doi:10.1007/BF02703749.

[12] R. Cook, Detection of influential observation in linear-regression, Technometrics 19 (1) (1977) 15–18.

[13] O. Corradi, P. Hjorth, J. Starke, Equation-free detection and continuation of a hopf bifurcation point in a particle model of pedestrian flow, SIAM Journal on Applied Dynamical Systems 11 (3) (2012) 1007–1032. doi:10.1137/110854072.

[14] M. Elmegård, B. Krauskopf, H. M. Osinga, J. Starke, J. J. Thomsen, Bifurcation analysis of a smoothed model of a forced impacting beam and comparison with an experiment, ArXiv e-printsarXiv:1308.3647.

P5 Publication 5

The following extended abstract [P5] is accepted for presentation at the 8th European Nonlinear Oscillations Conferences (ENOC) in Vienna, Austria 2014.

Experiments in nonlinear dynamics using control-based continuation: Tracking stable and unstable response curves

Emil Bureau*, Frank Schilder **, Ilmar F. Santos*, Jon Juel Thomsen* and Jens Starke **
*Department of Mechanical Engineering, Technical University of Denmark (embu@mek.dtu.dk)
**Department of Applied Mathematics and Computer Science, Technical University of Denmark

Summary. We show how to implement control-based continuation in an nonlinear experiment using existing and freely available software. We demonstrate that it is possible to track the complete frequency response, including the unstable branches, for a harmonically forced impact oscillator.

Introduction

We show how to perform experimental bifurcation analysis for nonlinear dynamical systems using control based continuation, in particular tracking complete frequency response curves including their unstable parts. Nonlinear dynamical systems are difficult deal with experimentally because of their ability to have multiple coexisting stable and unstable equilibrium states, super/sub harmonic resonances, quasi-periodic and chaotic behaviour. Many of the well established experimental methods use estimation and identification techniques that are based on the assumption that the system under test is linear or close to linear. Applying such techniques to strongly nonlinear systems can lead to wrong measurements and hence wrong model-assumptions, poor designs and failure of mechanical components. Experimental techniques for stabilizing unstable periodic orbits (UPOs) in chaotic systems, such as Delayed Feedback Control and OGY-control, are emerging (see [1] for an overview). For nonlinear mechanical systems with periodic or quasi-periodic behaviour, the parameter-sweep remains the only widely used counter-part to linear methods such as experimental modal analysis. Unfortunately, this method does not provide any information about unstable equilibrium states and can only handle co-existence of equilibrium states to a certain degree. The newly developed control-based continuation requires the constitution of a non-invasive real-time control and the use of a predictor-corrector type path following algorithm, but in turn the method can provide information about how both stable and unstable equilibrium states change when system parameters are varied. Furthermore, the stability can be determined and in some cases the instability can be quantified in terms of Finite Time Lyapunov Exponents [2]. The metod works for linear, weakly nonlinear and strongly nonlinear systems and can handle multiple co-existing equilibrium states, quasi-periodic behaviour and the occurrence of bifurcations. In the following we give an overview of how one can apply this method in experiments using freely available existing software.

Experimental test-rig

The experimental test-rig is shown in Figure 1a and b. It comprises a harmonically forced impact oscillator controlled by electromagnetic actuators. The harmonic excitation F_s is created by a electromagnetic shaker attached to the base and a control force F_m can be exerted directly on the impactor mass using the electromagnetic actuators. Data acquisition and the generation of control and forcing signals are done using a dSpace real-time control board.

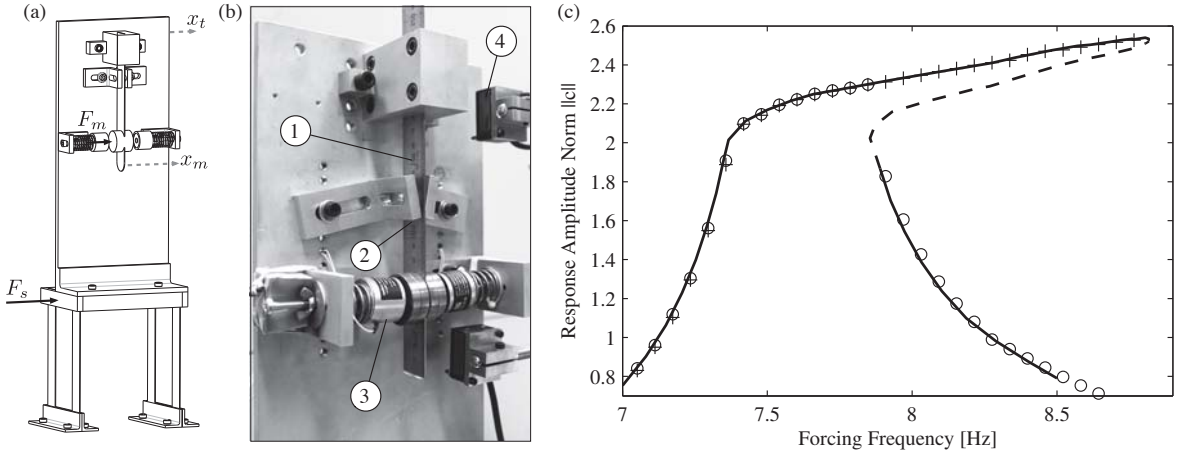

Figure 1: The experimental test-rig and results obtained by different experimental methods. (a) Illustration of the harmonically forced impact oscillator controlled by electromagnetic actuators. (b) Close-up picture of the impactor system: (1) Flexible impactor with tip mass; (2) mechanical stops causing impact and a hardening spring nonlinearity when vibration amplitudes exceeds the gap-size; (3) electromagnetic actuators used to create a non-invasive control force; (4) laser displacement sensors. (c) Comparison of an experimental frequency response obtained by frequency sweep and control-based continuation. Sweep is denoted by (+) for increasing frequency and (o) for decreasing. Continuation is denoted by (—) for stable and (- - -) for unstable equilibrium branch.

Implementing control-based continuation in an experiment

Control-based continuation was introduced in [3] and has been applied to different experiments in [4, 5, 6, 7, 8]. It employs a path following algorithm to track response curves, while the equilibrium states are stabilized by an non-invasive control. Some pre-requisites are necessary for control-based continuation: 1) It must be possible to vary the parameters of interest (i.e. forcing frequency and amplitude) smoothly. 2) A zero-problem and an appropriate interface must be set up, so that the continuation algorithm can evaluate the experiment. For time periodic equilibrium-states, such a zero-problem can be formulated as:

$$F(c, \mu; N) := \mathcal{F}_Q \left(Y(\mu, N, \mathcal{F}_\infty^{-1}(c)) \right) - c = 0, \tag{1}$$

where Y is the measurement of the controlled experiment, N is a number of sampled points, μ are parameters, Q is the number of modes used in the Fourier transformation and c is the predicted state expressed in terms of its Fourier modes. The continuation algorithm makes a predicted step in paramteres μ based on an experimentally estimated Jacobian, and a corrector algorithm (typically a Newton-method) corrects the predicted state c until the prediction and measurement match. 3) A non-invasive control must be realised. By non-invasive control we mean a control that is only active when the system is away from an equilibrium state of the underlying un-controlled system. This also means that if the control-actuators are not already a part of the system, they must not add any inertia, stiffness, damping or extra degrees of freedom. In some cases the control can be overlaid external excitation. A non-invasive control can be constituted as a PD control, G, with appropriately chosen gains K_p and K_d. The control signal $u_c(t)$ is thus expressed as

$$u_c(t) = G(x(t), y(t)) := K_p(x(t) - y(t)) + K_d(\dot{x}(t) - \dot{y}(t)), \tag{2}$$

where $y(t)$ is the measurement of the state of the controlled system at time t and $x(t) = \mathcal{F}_\infty^{-1}(c)$ is the reference trajectory produced by the continuation. When the correction converges $x(t) - y(t) \approx 0$ and $u_c \to 0$, meaning that one does in fact measure the local dynamics of the underlying un-controlled system. As presented in [8], the control gains K_p and K_d can be experimentally tuned by a performing a series of sweeps determining their ability to non-invasively stabilize stable and unstable periodic equilibrium states under influence of external perturbations. A Matlab/Simulink software toolbox by the name Continex (Continuation in experiments), which generates the non-invasive control signal, creates and evaluates a zero-problem and handles communication between an experiment and a numerical continuation code, has been developed and is freely available together with the continuation code COCO [9].

Conclusions

Figure 1c shows a frequency response obtained using both conventional parameter sweep and the control-based continuation method. The method is seen to be able to handle multiple co-existing equilibrium states, trace both the stable and unstable equilibrium states and determine their stability. The time needed for obtaining the experimental results is of the same order as the time needed for a parameter-sweep. Several measurements are made and statistically weighted for each accepted point along the response curve, and since the continuation algorithm only accepts a state as an equilibrium when the residuum (1) is sufficiently small, the quality of the measured data is ensured. A non-invasive control is necessary for the method to work, but in some cases the control force can be overlaid on the external excitation. Furthermore, many advanced electro-mechanical components, such as rotors supported by electromagnetic bearings, already include the necessary hardware. Control-based continuation is still under development, but it can be considered a suitable alternative to conventional parameter-sweeps. It will work in many situations where the parameter-sweep fails and it can provide valuable information about the unstable equilibrium states. The Matlab/Simulink Continex software toolbox which can be downloaded from [9] includes simulated examples that will run out of the box and makes it easy to set up experiments with control-based continuation.

References

[1] Marcelo A Savi, Francisco Heitor I Pereira-Pinto, and Armando M Ferreira. Chaos control in mechanical systems. *Shock and Vibration*, 13(4):301–314, 2006.

[2] Emil Bureau, Frank Schilder, Michael Elmegård, Ilmar Santos, Jon Juel Thomsen, and Jens Starke. Experimental bifurcation analysis of an impact oscillator - determining stability. *Manuscript under review for Journal of Sound and Vibration*, October 2013.

[3] Jan Sieber and Bernd Krauskopf. Control based bifurcation analysis for experiments. *Nonlinear Dynamics*, 51(3):365–377, 2008.

[4] Jan Sieber, Alicia Gonzalez-Buelga, Simon Neild, David Wagg, and Bernd Krauskopf. Experimental Continuation of Periodic Orbits through a Fold. *Physical Review Letters*, 100:244101, June 2008.

[5] Jan Sieber, Bernd Krauskopf, David Wagg, Simon Neild, and Alicia Gonzalez-Buelga. Control-Based Continuation of Unstable Periodic Orbits. *Journal Of Computational And Nonlinear Dynamics*, 6(1), 2011.

[6] David A. W. Barton and Stephen G. Burrow. Numerical Continuation in a Physical Experiment: Investigation of a Nonlinear Energy Harvester. *Journal Of Computational And Nonlinear Dynamics*, 6(1), 2011.

[7] David AW Barton, Brian P Mann, and Stephen G. Burrow. Control-based continuation for investigating nonlinear experiments. *Journal of Vibration and Control*, 18(4):509–520, 2012.

[8] Emil Bureau, Ilmar Ferreira Santos, Jon J. Thomsen, Frank Schilder, and Jens Starke. Experimental bifurcation analysis of an impact oscillator - tuning a non-invasive control scheme. *Journal of Sound and Vibration*, 332(22):5883–5897, 2013.

[9] Harry Dankowicz, Frank Schilder, and Emil Bureau. Coco - continuation core and toolboxes and continex - continuation in experiments. `http://sourceforge.net/projects/cocotools/`, 2013.

P6 Publication 6

The following (co-authored) extended abstract [P6] was submitted to and presented at the 7th European Nonlinear Oscillations Conferences (ENOC) in Rome, Italy 2011.

A Matlab Continuation Toolbox for Response Tracking in Experiments

Frank Schilder[*], Emil Bureau[†], Jens Starke[*], Harry Dankowicz[‡] and Jan Sieber[§]
[*]*Department of Mathematics, DTU, Kgs. Lyngby, Denmark*
[†]*Department of Mechanical Engineering, DTU, Kgs. Lyngby, Denmark*
[‡]*Department of Mechanical Science and Engineering, UIUC, Urbana, Illinois, USA*
[§]*Department of Mathematics, University of Portsmouth, Portsmouth, UK*

Summary. Control based continuation is a method that allows tracking of stable and unstable responses in experiments. We report on a development of a Matlab toolbox that implements this idea and allows for continuation guided experiments as well as simulations. This development is based on the recently released package COCO. As a forward-looking note we will illustrate how COCO's support for the task embedding paradigm together with our toolbox enables advanced applications such as dynamic sub-structuring.

Continuation Guided Experiments

Experiments, simulation and continuation are three established methods for response analysis of physical systems or models thereof, which we collectively refer to as *dynamical systems* (DSs). All three approaches can be used for producing a bifurcation diagram of a specific DS. However, each approach has distinctive advantages and disadvantages. While performing experiments is usually time- and resource intensive, it has the advantage that one investigates the actual system, which eliminates the possibility of modelling errors. Performing simulations on a computer implementation of a model of a DS, on the other hand, is considerably cheaper and it is much easier to change model parameters than in experiments. However, simulations of sophisticated models typically require substantial computational power. Furthermore, both methods share the drawback that they can only track stable responses, a restriction that is overcome by using continuation. The idea of continuation is to employ a path-following algorithm for specific types of states of a DS, for example, equilibrium states and periodic responses, and to monitor their stability, which allows to reproduce the global behaviour of a DS. While continuation can track stable as well as unstable responses, its application is most effective on carefully derived reduced models of relatively small dimension. A novel approach to overcome individual limitations of these methods is *control based continuation*, which aims at combining these methods in such a way that individual drawbacks are removed.

Control Based Continuation

The fundamental idea of control based continuation is to apply a control scheme that becomes non-invasive whenever the DS is in a natural state, which may be stable or unstable. The idea of non-invasive control was first introduced by Pyragas [1] and is today referred to as *Pyragas control*. Sieber et al. [2] and Barton et al. [3] later developed a non-invasive control for scheme continuation. To exemplify the principle, consider the Duffing oscillator with hardening spring

$$\ddot{x} + \lambda\dot{x} + \alpha x + \epsilon x^3 = A\cos(2\pi\omega t) + \delta u(t), \tag{1}$$

where $\lambda, \alpha > 0, \epsilon > 0$, A and ω are model parameters, u is an as yet unspecified control force and $\delta \in \{0, 1\}$ determines whether or not the control force is applied to (1). The bifurcation diagram of (1) for $\delta = 0$ is shown in Fig. 1(a). We clearly observe a hysteresis behaviour, which is a typical phenomenon of non-linear DSs. In experiments or with simulation we can only observe the stable responses, but not the unstable ones. However, as evidenced with this simple example, the unstable responses form an important part of the bifurcation diagram, which can only be revealed using continuation.

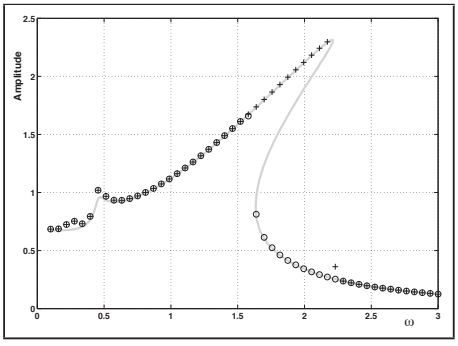

(a)

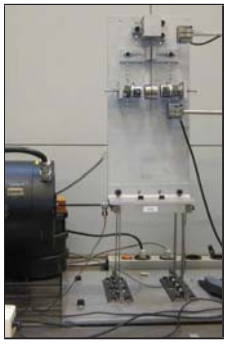

(b)

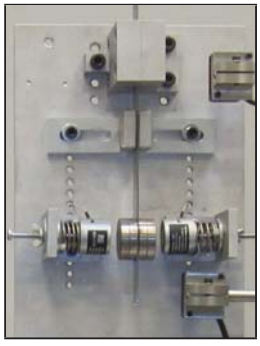

(c)

Figure 1: **(a)** Bifurcation diagram of the periodic responses of the Duffing oscillator (1) for $A = 1, \lambda = 1/5, \alpha = 1, \epsilon = 1$ and $\delta = 0$. Responses found in a forward sweep are marked with '+' and with a backward sweep are marked with '$\circ$'. The continuous curve was obtained using continuation guided simulation, which is able to trace the unstable part of the branch of responses. **(b)** Experimental set-up of an oscillator with hardening spring. The two-degree of freedom system consists of a shaker attached to a base structure, which in turn holds the pendulum. **(c)** The pendulum is a mass-spring-damper system, where the stiffening of the spring is caused by a mechanical stop. We use laser sensors to measure the position of the base structure and the pendulum mass. The feedback control is applied through two electromagnetic actuators mounted on opposite sides of the mass.

If one wants to observe the unstable responses in an experiment or a simulation, one needs to stabilise the unstable responses without actually affecting these responses, that is, the stabilisation must be non-invasive. In order to achieve this, we apply a control force that is proportional to the difference of the system's response and a target response. Obviously, if the target response is equal to a natural response, our control force will vanish, which means that our control is non-invasive. For our Duffing oscillator (1) we can achieve this with the proportional-derivative (PD) control scheme defined by

$$\left.\begin{array}{rcl} P &=& x - y(t), \\ D &=& (P - \sigma)/h, \\ u &=& K_1 P + K_2 D, \\ \dot{\sigma} &=& D, \end{array}\right\} \tag{2}$$

where P is the proportional, D the differential component of the control force u, h is a scaling factor larger than the sampling time of the state x and much smaller than the period of the response $x(t)$, $K_1 < 0$ and $K_2 < 0$ are the gains of the PD controller, and $y(t)$ is the as yet unknown control target. Evidently, $x(t) - y(t) \equiv 0 \Longrightarrow u(t) \equiv 0$.
Eqns. (1)-(2) form a system of *ordinary differential equations* (ODEs) for which the control target $y(t)$ can be considered as an external input. To transform this ODE into a continuation problem, we need to formulate a zero problem of the form $F(z, \mu) = 0$, where z is some representation of the control target and μ the vector of model parameters. One possibility is to set

$$F(z, \mu) := \Pi_N(P) = \Pi_N(x_{\mathrm{sample}}(t)) - z, \quad t \in [0, 1/\omega], \tag{3}$$

where Π_N is the projection onto the first N Fourier modes and $x_{\mathrm{sample}}(t)$ is a large enough sample of the state x over one period. In this case, we have $y = \Pi_N^{-1}(z)$ and the vector $z \in \mathbb{R}^{2N+1}$ contains a Fourier transform of the control target y. Obviously, Eqns. (2)-(3) are also well-defined if $x_{\mathrm{sample}}(t)$ is generated by measurements of an experiment, that is, this procedure applies to simulations as well as experiments. The final step now is to apply a continuation algorithm to the zero problem (3). In an actual implementation the function F will modify the control target and parameters as specified with z and μ, wait for some time until transients die out, sample the state x over at least one period and return the difference of the Fourier transform of this sample and z. Following this strategy we computed the full bifurcation diagram shown in Fig. 1(a), including the unstable responses.

Matlab Toolbox Implementation with COCO

We chose the continuation core toolbox COCO [4, 5] for implementing a Matlab toolbox for continuation guided simulation and experiments, because it is implemented in Matlab, which allows for easy use of Simulink and DSpace. Furthermore, the design of COCO is such that new continuation problems can be incorporated and the continuation algorithm can be exchanged by a user without modifying COCO itself. The latter was of particular importance, because one cannot simply employ traditional methods for problems that use noisy data, we have to use statistical methods instead. In a first step we implemented a continuation method based on a local least-squares approximation of a path of responses together with a basic toolbox that enables continuation guided simulation. In a second step we implemented an interface to DSpace and set-up an experiment with a non-linear mass-spring-damper system for testing the basic method with a real experiment; see Figs. 1 (b) and (c).
An interesting and advanced application of our toolbox is so-called *dynamic sub-structuring*, which is enabled by COCO's support for *task embedding*. Dynamic sub-structuring refers to the idea of splitting a large structure into a set of smaller sub-structures. Each of these sub-structures in now either simulated on a computer, or installed as a physical experiment in a lab. The connection between the physical and the virtual world is realised with, for example, DSpace controlled actuators. Task embedding, on the other hand, refers to the idea of splitting up a large continuation problem into a set of smaller problems, the connections being realised with *gluing conditions*. It is not hard to imagine that parts of such a decomposed continuation problem are instances of continuation guided experiments, where the gluing conditions are realisations of Pyragas control.
Challenges that we intend to tackle in the future are extracting stability information and branch-switching. In our set-up determining stability of a response is difficult, because the control makes every response locally asymptotically stable. For computer guided simulations one can, in principle, solve this problem by simultaneously integrating the controlled ODE together with the variational equation of the uncontrolled ODE, which allows to compute the Floquet multipliers and to detect bifurcations. However, this is not possible for experiments, where we also face the additional difficulty that we can only measure a small subset of the state variables.

References

[1] Pyragas, K. (1992) Continuous control of chaos by self-controlling feedback. *Physics Letters A,* **170(6)**:421-428.

[2] Sieber J. and Krauskopf B. (2008). Control based bifurcation analysis for experiments. *Nonlinear Dynamics,* **51(3)**:365377.

[3] Barton D.A., Mann B.P. and Burrow S.G. (2010). Control-based continuation for investigating nonlinear experiments. *Journal of Vibration and Control,* to appear.

[4] Dankowicz, H., Schilder, F. (2011) An Extended Continuation Problem for Bifurcation Analysis in the Presence of Constraints. *ASME J. Comput. Nonlin. Dyn,* **6(2)**, to appear.

[5] http://sourceforge.net/projects/cocotools/

P7 Publication 7

The following (co-authored) extended abstract [P7] is accepted for presentation at the 8th European Nonlinear Oscillations Conferences (ENOC) in Vienna, Austria 2014.

CONTINEX: A Toolbox for Continuation in Experiments

Frank Schilder*, Emil Bureau**, Ilmar Santos**, Jon Juel Thomsen**, Jens Starke*.
*Department of Applied Mathematics and Computer Science, DTU, Denmark.
**Department of Mechanical Engineering, DTU, Denmark.

Summary. CONTINEX is a MATLAB toolbox for bifurcation analysis based on the development platform COCO (computational continuation core). CONTINEX is specifically designed for coupling to experimental test specimen via DSPACE, but provides also interfaces to SIMULINK-, ODE-, and so-called equation-free models. The current version of the interface for experimental set-ups implements an algorithm for tuning control parameters, a robust noise-tolerant covering algorithm, and functions for monitoring (in)stability. In this talk we will report on experiments with an impact oscillator with magnetic actuators and algorithmic challenges we were facing during toolbox development.

Introduction

The goal of this development effort is a robust continuation toolbox that can be coupled to test specimen in a lab and runs without or with only minimal supervision, thus allowing unattended execution of sequences of continuation runs for extensive data acquisition. Furthermore, a well equipped toolbox will provide means for monitoring stability properties along the solution manifold, and for branch-switching at bifurcation points. The current version of the toolbox CONTINEX implements a fully functional covering algorithm as well as several monitor functions to detect instability of a solution. Hence, it provides basic means for the location of bifurcation points during continuation. The classification of such points and methods for branch-switching are subjects of ongoing research.

CONTINEX is based on the computational continuation core COCO, which implements a fully developed continuation toolbox and allows for easy overloading of specific parts of its continuation algorithms. For our development we only wish to overload a minimal amount of functionality, necessitated by particularities of continuation in experiments. One such particularity is the uncertainty of measurements, which implies that a solution manifold can only be defined in terms of expected values, if at all. Other significant particularities are addressed in the next section.

For developing and testing CONTINEX we set up a simple impact oscillator, which consists of a flexible vertical beam with a tip mass attached at the lower end. The beam is clamped and horizontally excited with an electromagnetic shaker at the upper end and impacts mechanical stops if the relative deviation of the tip mass exceeds a certain value. Such an impact causes an increase of stiffness, resulting in a non-linear mass-spring-damper system with stiffening spring. Although the oscillator was designed as a one degree of freedom system, the actual set up exhibits phenomena typical for two degree of freedom systems, that is, vibration suppression and resonances with the shaker.

Our experiment serves as a prototype for rotating machinery, where a periodic excitation is caused by unbalance forces. As a consequence, a control force cannot be added to the excitation directly. Instead, one typically uses active electromagnetic bearings (AEBs) that allow the application of forces to the shaft of a rotor. Our electromagnetic actuators mounted to both sides of the tip mass are a primitive realization of AEBs. While AEBs can apply large attracting and repelling forces over larger distances, our actuators can only excert attracting forces and have a rather small range of effect of approximately 2mm. Furthermore, the applied force depends non-linearly on the distance between tip mass and magnet, which makes our actuation system non-linear and state-dependent. An important question of interest was, if, and under which conditions, such an actuation system is suitable for constructing a non-invasive stabilizing control scheme required for applying control-based continuation.

Algorithmic challenges

Two obvious problems that need to be addressed by a toolbox for continuation in experiments are measurement noise and time. In the language of COCO [1], the presence of noise necessitates the implementation of suitable atlas and curve segment classes, while measurement times of the order of seconds per function evaluation call for update methods for derivatives instead of the application of finite difference methods used by default. Besides these two fundamental problems we observed a surprisingly large number of mostly unanticipated algorithmic challenges when coupling our algorithms to our impact oscillator:

Non-linearity of control system. Although expected, the non-linearity of the control system posed a serious problem, which was eventually solved by the development of a control tuning algorithm [2].

Resonances. Resonances of the pendulum with the shaker sub-system lead to a quite rich bifurcation structure, for example, small hysteresis loops with a size comparable to measurement noise. As consequences, we observed sudden and localized changes of variance in measurements, large jumps of the continuation method, double covering of the solution manifold, and failure of the default method of step-size control. Each of these problems was so severe that only about 10-20% of executed continuation runs were successful until we finally managed to find solutions to all of these issues.

Balancing of equations. To address phenomena caused by resonance we use non-linear arc-length conditions. The residuum of any such condition competes with the allowed residuum in the experiment, because both residues are combined in the stopping criterion of the corrector. This caused significant convergence problems in the correction method and was solved by using a pull-back algorithm that ensures zero residuum in the projection condition.

Drift of parameters. The least expected but highly relevant problem is the drift of environmental parameters during correction. Some parts of the bifurcation diagram of our test rig are so sensitive to changes in environmental parameters (we suspect temperature) that the solution manifold can slowly drift out of the trust region of our corrector during correction. When this happens, it is impossible to resume continuation. The solution to this problem was the implementation of statistical tests in the corrector algorithm, which will detect a likely failure of the correction step as fast as possible to allow restarting the correction step with changed settings while the drift is still small.

Once we discovered and addressed all these phenomena, the success rate of CONTINEX on our test rig was increased to above 95%. In addition, a parameter sweep with comparable accuracy will take approximately the same amount of time as a continuation run, which implies that continuation with CONTINEX does not only provide more information than, but is also competitive with the execution time of a sweep.

The toolbox CONTINEX

A generic algorithm for evaluating a zero problem $F(x, p)$ corresponding to an experiment, a simulation, or an equation-free model, where x represents a target solution and p are the problem parameters, is

1. Set problem parameters to p and reference solution to x.
2. Wait for results.
3. Read frame with data.
4. Compute and return residuum.

Since this algorithm is so general, CONTINEX provides a base class with four abstract methods corresponding to the steps above as an interface to an experiment or model. A user of CONTINEX is only required to to derive a problem specific sub-class from this base class and overload the four abstract methods. More specialized base classes with additional functionality are available for DSPACE, SIMULINK and ODE models. Once this sub-class is implemented, an instance of it together with initial values for the reference solution and parameters is passed to the toolbox constructor to initiate a continuation run. The CONTINEX specific atlas, curve segment and corrector algorithms are selected automatically.

Acknowledgements

This work was supported by the Danish research council (FTP).

References

[1] Dankowicz H., and Schilder, F. (2013) Recipes for continuation. *Computational Science & Engineering CS11*, Society for Industrial and Applied Mathematics (SIAM), Philadelphia, PA.

[2] Bureau E., Schilder F., Santos I., Thomsen JJ., Starke, J. (2013) Experimental bifurcation analysis of an impact oscillator - Tuning a non-invasive control scheme. *Journal of Sound and Vibration*, 332(22), 5883–5897.

[3] Bureau E., Schilder F., Elmegård M., Santos I., Thomsen JJ., Starke, J. (2013) Experimental bifurcation analysis of an impact oscillator - Determining Stability. *Under review.*

DTU Mechanical Engineering
Section of Solid Mechanics
Technical University of Denmark

Nils Koppels Allé, Bld. 404
DK- 2800 Kgs. Lyngby
Denmark
Phone (+45) 4525 4250
Fax (+45) 4593 1475
www.mek.dtu.dk
ISBN: 978-87-7475-377-3

DCAMM
Danish Center for Applied Mathematics and Mechanics

Nils Koppels Allé, Bld. 404
DK-2800 Kgs. Lyngby
Denmark
Phone (+45) 4525 4250
Fax (+45) 4593 1475
www.dcamm.dk
ISSN: 0903-1685